

REMARKS

The change in Examiner is noted.

Claims 23, 24 and 30 have been amended to more particularly point out and distinctly claim the subject matter that the applicants regard as the invention. No new matter has been added.

Turning first to the Examiner's rejection of claims 1-4, 6-27, 29, 33, 35-37, 39, and 64-71 under 35 USC § 112, Applicants note with thanks the Examiner's apparent recognition of the novelty of these pending claims. The Examiner has nonetheless rejected the claims as containing subject matter that was not described in the specification in such a way as to enable one skilled in the art to which it pertains, or with which it is most nearly connected, to make and/or use the invention. Specifically, the Examiner has concluded under *In re Wands* that the claimed invention could not be practiced by one having skill in the art without "undue experimentation." (Examiner's Rejection page 4). The Examiner states:

"The specification presents to utilize microfluidic devices and electrophoretic devices to move DNA molecules without providing guidance to be able to determine where an individual molecule is with the precision required to execute memory write and read operations on an individual molecule. The specification does not provide specific guidance regarding how data is to be processed for encoding into the sequences of DNA molecules, nor does the specification provide guidance regarding how DNA sequences of individual molecules are to be processed to regenerate stored data.

(Examiner's Rejection page 4). Applicants respectfully traverse the Examiner's rejection.

First, the Examiner has misconstrued the Applicants' invention. While methods are described that would allow for reading and writing of individual bases or components of a larger macromolecule, the claims are drawn to:

a write head that encodes strands of molecular material with sequences of binary data; a storage block for storing the strands; a read head for reading out a sequence of binary data from a selected strand; and a transport mechanism that

selectively moves the strands between the write head and the storage block, or in response to a read command, between the storage dock and the read head, and then to a dump or back to the storage block.”

These involve physical properties involving physical manipulations, not unpredictable or complicated reactions of living cells as in the case of In re Wands relied upon by the Examiner.

Moreover, Applicants are employing ~~well-known~~well-known physical manipulations as described in their specification, to practice their ~~invention~~.

invention. As the Applicants note in the specification, (Page 23) Gene chips were known in the art in early 2001 using thousands of unique DNA sequences on a single chip to make snapshots of gene activity. See e.g. W.W. Gibbs, “Biotechnology: Gene Chips,” *Scientific American* pp 33-34, February, 2001.

~~(Claim 1) Binary~~ Further, consistent with independent Claim 1, binary data may be stored on molecular material without that data being made up of a single base. The specification describes that the data may be “individual bases or collections of bases” depending on the precision of the instruments. (page 9). For example, an individual DNA base may be used and assigned a binary value (C=00, G=01, A=10 T=11 or some equivalent), or a string of bases may be used (CCCCCCCCC=00, GGGGGGGGGG=01 etc...). Reading and writing such sequences are well within the skill of those in the art.

The Examiner goes on to explain,

The specification provides guidance to synthesize the individual molecules to comprise a desired sequence on page 19-33. Write mechanism 1 requires in situ chemical synthesis. In situ synthesis is a time consuming and complicated procedure and the specification does not show how such a procedure is compatible with a read-write memory storage apparatus that functions with a practical time period.

(Page 4-5) The Examiner misapplies the standard of 35 USC § 112. While in situ synthesis may be time consuming, it is a practice that is well known in the art. Moreover, the fact that a synthesis may be “time consuming” per se is not a basis for rejecting a claim under 35 USC § 112. As pointed out by the Board in Appeal No. 1996-3409¹:

“The claims are indeed broad, and generating a frequency distribution data base for diseases and/or biological samples encompassed by the claims, but not demonstrated by working examples, would undoubtedly be time consuming. Nevertheless, the test for undue experimentation is not merely quantitative. As stated in PPG Indus., Inc. v. Guardian Indus. Corp., 75 F.3d 1558, 1564, 37 USPQ2d 1618, 1623 (Fed. Cir. 1996):

[T]he question of undue experimentation is a matter of degree. The fact that some experimentation is necessary does not preclude enablement; what is required is that the amount of experimentation “must not be unduly extensive.” Atlas Powder Co., v. E.I. DuPont De Nemours & Co., 750 F.2d 1569, 1576, 224 USPQ 409, 413 (Fed. Cir. 1984).

The Patent and Trademark Office Board of Appeals summarized this point in Ex parte Jackson, 217 USPQ 804, 807 (1982):

The test is not merely quantitative, since a considerable amount of experimentation is permissible, if it is merely routine or if the specification in question provides a reasonable amount of guidance with respect to the direction in which the experimentation should proceed to enable the determination of how to practice a desired embodiment of the invention claimed.

Moreover, it is well settled that the specification need not disclose what is well known in the art. Hybritech Inc. v. Monoclonal Antibodies, Inc., 802 F.2d 1367, 1385, 231 USPQ 81, 94 (Fed. Cir. 1986). The Examiner has not presented evidence that those skilled in the art would be unable to identify control and disease populations from which to generate frequency distribution data bases.

We have carefully reviewed the specification, including the working examples, in light of the Examiner’s commentary on pages 4 through 7 and 16 through 19 of the Answer, and appellant’s argument on pages 19 through 21 of the Brief and page 4 of the Reply Brief. We are persuaded that the specification provides adequate guidance enabling any person skilled in the art to generate frequency distribution databases and to diagnose disorders in addition to those

¹ While the Board’s decision in Appeal No. 1996-3409 was not published, the cases cited by the Board are citable precedent.

of the working examples; and that the experimentation necessary to practice the full scope of the claimed invention, while considerable, would not be undue. We hold that the Examiner has not set forth a reasonable basis for questioning the enablement of the claims on appeal; accordingly, the rejections of claims 1 through 20 under 35 U.S.C. § 112, first paragraph, is reversed.”

Applicants submit one being skilled in the art would be able to practice the claimed invention using in situ synthesis without undue experimentation. The time required to write a data source under this method is irrelevant. Furthermore, as the specification states, “a storage device can be configured with multiple read/write stations to access one or more blocks of parking lots to provide parallel read/write capability to reduce access time and increase throughput.” Using multiple, perhaps thousands, of parallel write stations, the synthesis of a macromolecule containing digital data may be achieved quickly and efficiently.

The Examiner goes on to state:

[In] Write mechanism 2 individual nucleotides are added to a chamber containing the growing chain and a polymerase, but the specification does not address how to prevent errors due to inlet of more than one nucleotide, or how a polymerase incorporates a single substrate molecule with perfect efficiency even though enzymes generally require minimum concentrations of substrates to function.

(Examiner’s Rejection page 5). This is inaccurate. ~~In fact,~~First, the specification describes error correction coding of the same type that is presently used in all data storage and communication systems. Namely, by adding error-correction bits to the data bits, one can always correct errors that arise either during the write process or during the read process (or both). (Page 14 lines 14-18). The specification also describes storing any information as a palindromic sequence or as a double strand to prevent transcription errors. (see pages 12-13).

Further, the specification states:

[T]he enzymes needed for the base insertion chemistry could be attached to the α -hemolysin proteins via a long tether, which would hold them in close

proximity to the pore while, at the same time, prevent the enzyme and the pore from interfering with each other's activity. The chemistry would then proceed more rapidly as the kinetics would no longer be limited by the diffusion rates of the enzymes and the DNA molecule. The chemistry would be further accelerated if the bases being added could be delivered in the vicinity of the localization site.

(Page 23). As stated, the tether allows more rapid kinetics of the enzyme and the base without interfering with activity. The tether would also allow enzymes to work at a lower concentration than those required by enzymes generally in a free fluid medium. Efficiency may also be improved by delivering the base in the vicinity of the site. Further, as stated above, the addition of bases need not be in single units. A series of bases may be used to encode a single binary datum. Accordingly, the specification is sufficiently clear to allow one having skill in the art to practice the described mechanism.

Next, the Examiner states: "Write mechanisms 3-5 require modification of individual DNA molecules or other polymers at precise positions, but the specification does not provide specific guidance for locating modifications at precise positions in an individual molecule." This is also not accurate. Write mechanism 3 employs excisable spacers to separate specific active molecules. The active molecules may be a single molecule or multiple molecules in a string and are positioned by "a micro-machine under the activator; for instance, optical tweezers may be used to drag the strand from right to left." (Specification page 25). The activator may be a laser beam, a localized electric field, a tunneling electrode, an anchored enzyme or any other activation method known in the art.

Writing mechanism 4 uses metal clusters, such as silver nanoclusters to encode binary or other data on a macromolecule. Specifically, the Specification describes:

Upon detection of a change in ion current signifying the initiation of translocation, the trans side of the channel will be irradiated with a short laser pulse ($< 1\mu\text{s}$ duration) corresponding approximately to the residence time of a

nucleotide in the channel. The laser pulse excites the photosensitizers on the surface and activates reduction of Ag^+ ions to Ag^0 atoms. The estimate is that (with reasonable coverage of the surface with sensitizers and excitation efficiency) on the order of thousands of atoms can be generated, and this can be controlled with the fluence of the light pulse. The generated atoms in solution will diffuse and some will encounter the translocating chain at the exit of the channel leading to the formation of small silver metal clusters **200** bound to the chain **202**. The generation of Ag atoms will be concentrated near the trans chamber wall because of the spatially fixed positions of the photosensitizers on the wall...

...[t]he concentration of the photogenerated atoms will be falling off cubically with distance away from the channel exit, so the reaction will be largely confined to a small length along the chain. Rough estimates suggest that the labeling of the chain with clusters would be limited to ~10 nm. After excitation and reduction of metal ions, a fraction of the surface attached sensitizers will become oxidized and these will be reduced to their original state with sacrificial electron donors **210**, sustained at moderately high concentration, in solution in the trans chamber. Given the estimate of the size of the bit, the shortest time interval between laser pulses will be ~10 μs . The system will be irradiated with light pulses **212** through a window **214** that are clocked in a sequence corresponding to the bit stream to be encoded while the chain, is being translocated, leading to a pattern of deposited silver nanocrystals along the chain. Additional agents may be needed to protect nanoclusters deposited on the oligonucleotide chain to prevent agglomeration of nanoclusters located at different positions along the chain.

This detailed description provides specific guidance for locating modifications at precise positions in an individual macromolecule. Such a process, then, could not be said to require undue experimentation.

Writing mechanism 5 uses ring-opening metathesis polymerization (ROMP), which was well described in the art at the time of the initial disclosure. (See examples page 31 of Specification).

Turning to the reading mechanisms, the Examiner states:

Read mechanisms 1 and 2 require use of a nanopore or atomic force microscopy without providing specific guidance as to the nanopore or the parameters that can be measured to sequence through a nanopore or atomic force device. The specification provides guidance to use optical tweezers to move individual molecules from one part of the apparatus to another.

HAYES SOLOWAY P.C.
3450 E. SUNRISE DRIVE,
SUITE 140
TUCSON, AZ 85718
TEL. 520.882.7623
FAX. 520.882.7643

175 CANAL STREET
MANCHESTER, NH 03101
TEL. 603.668.1400
FAX. 603.668.8567

Rhee et al., published 4 years after the effective filing date of the instant application, shows that nanopore sequencing is a promising idea that has not yet been reduced to practice. Among the practical problems to nanopore sequencing that Rhee et al. notes are that alphahemolysin pores and other nanopores used allow for discrimination of some sized of single stranded DNA, but do not allow for sequencing.

(Rejection page 5-6) As the Examiner notes, Rhee et al. describe that alpha-hemolysin nanopores allow for discrimination of some DNA but do not allow for sequencing. Rhee et al. state that none of the alpha-hemolysin pore technologies have achieved "single base resolution." (Rhee et al. abstract) The current specification addresses this concern in two ways. First, multiple bases may be used to encode a single binary datum making single base resolution unnecessary. Second, the specification describes manufacturing solid-state synthetic nanotubes using, for example, Argon ions. This nanopore may be significantly thinner than an alpha-hemolysin nanopore, improving signal to noise ratio. The specification thus allows one having skill in the art to practice the claimed invention.

In the Action, the Examiner raises the question of accuracy of the read/write process, seemingly believing that every single base must be written and read correctly for the entire process to work. This is not necessary, however, as the macro-molecular storage system allows for error correction coding of the same type that is presently used in all data storage and communication systems. By adding error-correction bits to the data bits, one can always correct errors that arise either during the write process or during the read process (or both).

Enclosed as Exhibit A "ODSpaper.pdf," is a manuscript of a paper presented by one of the Inventors at the Data Storage Conference in April 2001. In this paper is described the Gene Chip technology (see page 5) as an example of the existing technology (back in 2001) for writing DNA sequences, precisely as described in our patent application. The Examiner's objection that methods of "writing" were not known at the time is therefore incorrect.

HAYES SOLOWAY P.C.
3450 E. SUNRISE DRIVE,
SUITE 140
TUCSON, AZ 85718
TEL. 520.882.7623
FAX. 520.882.7643

175 CANAL STREET
MANCHESTER, NH 03101
TEL. 603.668.1400
FAX. 603.668.8567

Also enclosed as Exhibit B is a paper by Thorsen et al. published in 2002 (Microfluidic Integration...pdf), describing methods of creating micro-fluidic devices on a large scale.

Several other journal articles and conference proceeding papers are attached as Exhibits C-F which clarify the points that show how parallelism, for example, can increase the data rates (both reading and writing), or how a single-strand of DNA can be directed through a single nano-pore (JAP_Paper.pdf) simply by applying a voltage across the "read chamber," thus guiding the negatively-charged DNA strand toward (and eventually through) the nano-pore.

In summary, each of the methods used to practice the claimed invention is described sufficiently to allow one having skill in the art to practice the invention without undue experimentation. Since the claimed invention is described in the specification and in the art in existence at the time of the initial disclosure, the rejection based on 35 USC § 112 is improper.

Turning to the art rejections, and considering the rejection of claims 30-32, 34, and 38 under 35 USC § 102(b) as being anticipated by Lagally et al., the reference does not describe, teach, or suggest strands of molecular material encoded with a sequence of coherent binary data in liquid-filled canals and selectively movable therein between different locations on a substrate in response to an external command as required by independent claim 30. DNA is composed of 4 distinct base pairs. It cannot be said that the DNA is encoded with binary data unless the base pairs have been assigned a binary value. Lagally et al. does nothing to describe a molecular material that is encoded with a sequence of binary data. Because Lagally et al. does not teach all of the restrictions of the amended claims, the rejection is improper.

In view of the foregoing amendment and comments, it is believed that all of the presently pending claims are allowable over the art.

HAYES SOLOWAY P.C.
3450 E. SUNRISE DRIVE,
SUITE 140
TUCSON, AZ 85718
TEL. 520.882.7623
FAX. 520.882.7643

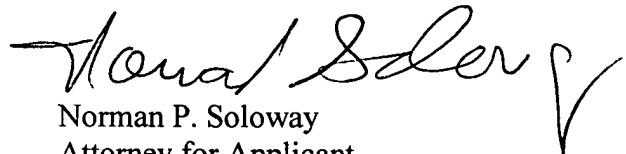
175 CANAL STREET
MANCHESTER, NH 03101
TEL. 603.668.1400
FAX. 603.668.8567

Form PTO-2038 authorizing credit card payment in the amount of \$60.00 to cover the cost of the Petition for One Month Extension accompanies this Amendment.

Having dealt with all the objections raised by the Examiner, the Application is believed to be in order for allowance. Early and favorable action is respectfully requested.

In the event there are any fee deficiencies or additional fees are payable, please charge them (or credit any overpayment) to our Deposit Account Number 08-1391.

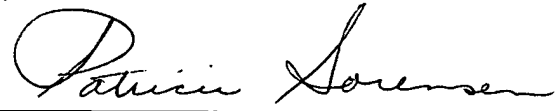
Respectfully submitted,



Norman P. Soloway
Attorney for Applicant
Reg. No. 24,315

CERTIFICATE OF MAILING

I hereby certify that this correspondence is being deposited with the United States Postal Service as First Class Mail in an envelope addressed to: MAIL STOP AMENDMENT, Commissioner for Patents, P.O. Box 1450, Alexandria, VA 22313-1450 on October 1, 2008, at Tucson, Arizona.

By 

NPS:CEP:ru:ps

HAYES SOLOWAY P.C.
3450 E. SUNRISE DRIVE,
SUITE 140
TUCSON, AZ 85718
TEL. 520.882.7623
FAX. 520.882.7643

175 CANAL STREET
MANCHESTER, NH 03101
TEL. 603.668.1400
FAX. 603.668.8567

EXHIBIT A

DNA, Human Memory, and the Storage Technology of the 21st Century

Masud Mansuripur

Optical Sciences Center, The University of Arizona, Tucson, Arizona 85721
e-mail: <masud@u.arizona.edu>

Abstract. The sophisticated tools and techniques employed by Nature for purposeful storage of information stand in stark contrast to the primitive and relatively inefficient means used by man. We describe some impressive features of biological data storage, and speculate on approaches to research and development that could benefit the storage industry in the coming decades.

Introduction. The storage of information is ubiquitous in our technological society: paper, film, semiconductor memories, audio/video-tapes, magnetic/optical disks, etc., collectively contain many petabytes of information. In contrast, Nature has been frugal in its use of information storage techniques. Blueprints of life, both of plant and of animal, are stored in the DNA molecules.¹⁻³ Pre-programmed (i.e., instinctive) as well as learned information reside in the nervous systems of higher animals.^{4,5} The human immune system stores information about past pathogens in the form of primed lymphocytes (e.g., T-cells and B-cells), using this information to mass-produce and rapidly deploy antibodies and specialized immune cells when an old pathogen reappears.^{6,7} These instances aside, it is hard to find purposeful employment of data storage in Nature.

Despite their rarity, the natural mechanisms of information storage are extremely powerful and versatile. A complement of chromosomes not only contains the entire description of a plant or an animal, but it also carries the step-by-step instructions for building the individual from a single initial cell. The human brain can store vast amounts of information embodied in images, sounds, scents, event sequences, and abstract concepts to which an individual may be exposed through a lifetime. The brain forms automatic links among the stored data, recalls by association, and responds to external events by exploiting its reservoir of pre-programmed and learned data-bases.

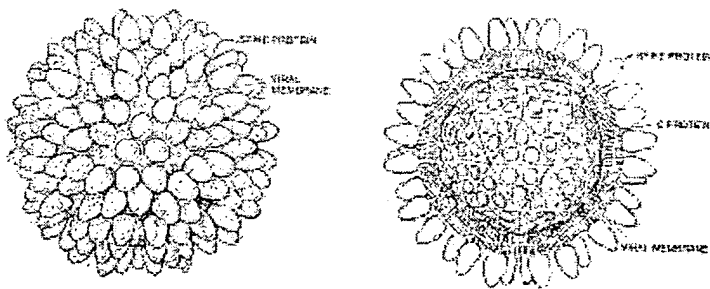


Figure 1. The SFV particle is 65 nm in diameter. The RNA inside the capsid is a chain of 12,700 nucleotides, the order of which provides the information needed for making the viral proteins. The capsid consists of 180 molecules of a protein, forming a regular polygon with 60 triangular faces. The outer viral membrane is composed of two layers of lipid molecules, with their hydrophobic heads facing outward and their hydrophilic tails facing inward. Inserted into this membrane are 180 spikes, each made up of three linked proteins.⁸

(Copyright © 1982, estate of Bunji Tagawa)

To cite just one example of efficient data storage by Nature, consider the Semliki Forest Virus (SFV) depicted in Fig. 1. The virus consists of a 12,700 nucleotide-long strand of RNA, wrapped in a coat of exquisitely arranged protein molecules and surrounded by a spike-protein studded lipid membrane. The entire virus is 65 nm in diameter, smaller than the tiniest pit on a Digital Versatile Disk (DVD), yet the information content of its RNA molecule is 25.4 kbits (2 bits per

nucleotide). When this virus enters a host cell, it sheds its membrane and protein coat, and takes over the machinery of the host cell to make copies of its own RNA and proteins. The host cell eventually assembles the mass-produced components of the SFV, and sends them out at the rate of several thousand per hour to infect other cells within the host organism.⁸

This paper reviews some of the fundamental aspects of cellular processes and neuronal behavior in biological systems, with an eye toward the mechanisms responsible for information storage and retrieval. Recent years have witnessed a steady convergence of digital electronic storage and computation or information processing. It should not come as a surprise, therefore, to find convergence, even seamless merger, of storage and processing in biological systems as well. Admittedly, we are far from the ultimate goal of employing biomaterials and our knowledge of biological processes in the service of building better information storage devices. It is our modest intention, however, to point out the power and flexibility of biological information processing, and to encourage the reader to explore this path in search of alternative modes and means for future technologies. For the reader unfamiliar with the language of the biologist, a glossary of relevant terms and concepts is included at the end of the paper.

Information Stored in Chromosomes. A typical bacterial chromosome consists of a double-helix ring of deoxyribonucleic acid (DNA), making up tens or hundreds of genes;⁹ see Fig. 2. (Bacteria are prokaryotes, that is, cells without nuclei. The bacterial chromosome floats in the cell's cytoplasm, surrounded by the cell membrane and a protective shell.) All the proteins and enzymes needed by the bacterium are encoded by these genes, and are made by the protein-fabricating machinery of the cell.¹⁰⁻¹² The DNA molecule, therefore, contains the blueprint for the construction of the entire organism. The basic operating principle is the same in fungi, plants, and animals – all of which belong to the class of eukaryotes and consist of nucleated cells;⁹ see Fig. 3. Eukaryotes, however, have more chromosomes (for example, 4 pairs in fruit flies, 23 pairs in human beings), and each chromosome is longer and may contain more genes (on average, a few thousand genes per human chromosome).¹⁰

In sexually-reproducing organisms there are pairs of each chromosome (i.e., the homologous chromosome pair), each member of the pair containing the same gene – or different alleles of the same gene – at identical loci. Of the two members of a given pair of chromosomes, one is contributed by the mother, the other by the father. Different alleles of a given gene (residing at a specific locus along a given chromosome) encode for the same protein or enzyme, but the alleles are biochemically different, and could therefore give rise to structurally and functionally different proteins/enzymes. In some cases only one of the two alleles (either maternal or paternal) is expressed, while the other copy of the gene remains dormant (recessive). In other cases both genes (residing, as they are, at identical loci of a homologous pair) are expressed. In a sexually-reproducing organism, each of the two copies of a given gene has a 50% chance of being transmitted to the offspring in a gamete (i.e., sperm or egg cell).^{1,10}

At any given time during the life of a cell, some of the genes are copied onto messenger ribonucleic acid or mRNA (see Fig. 4) and transported to the cytoplasm, outside the cell nucleus.¹⁰ There they line up the amino-acids (the same 20 amino-acids are used in all living organisms) with help from ribosomes, transfer RNA, and specific enzymes, and create the proteins encoded in the genes. At the same time, some of the products of the genes (enzymes,

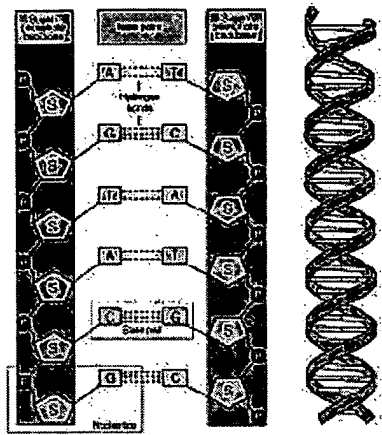


Figure 2. Deoxyribonucleic acid (DNA). Built from nucleic acid bases, sugars, and phosphates, the double-stranded molecule is twisted into a helix. Each spiraling strand, comprised of a sugar-phosphate backbone and attached bases, is connected to a complementary strand by non-covalent hydrogen bonding between paired bases. The bases are adenine (A), thymine (T), cytosine (C) and guanine (G). A and T are connected by two, and G and C by three hydrogen bonds. The right-handed double helix has ~10 nucleotide pairs per helical turn. The double-helix structure of DNA was discovered in 1953 by James Watson and Francis Crick. (Reproduced with permission from: <http://www.nhgri.nih.gov/>)

Figure 3 In eukaryotes the chromosomes reside in the nucleus of the cell. In sexually-reproducing organisms every chromosome comes in a pair, one member of the pair from the mother, the other from the father. During normal cell division (mitosis), each chromosome is copied, and the daughter cells receive a copy of each and every chromosome, thus receiving a full complement of all chromosomal pairs. During germ cell (gamete) production (meiosis) the homologous chromosome pairs within the nucleus come together and recombine (i.e., shuffle their genes), before the cell splits to form individual gametes. The gametes receive only half of the total number of chromosomes, one from each pair.¹⁰ (Reproduced with permission from: <http://www.nhgri.nih.gov/>)

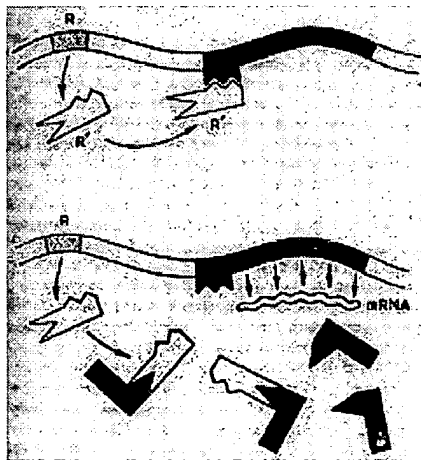
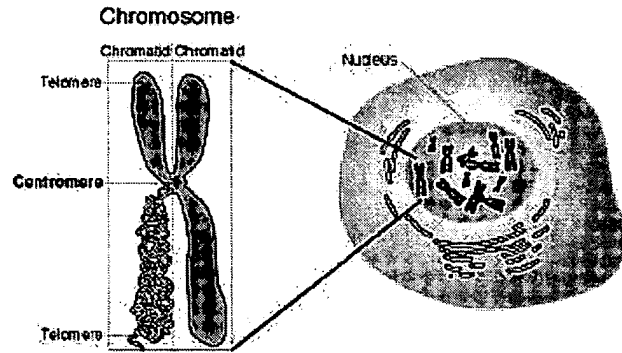


Figure 5. Gene-activating mechanism. A gene, shown in black, is prevented from acting by a repressor substance R' produced by the gene R. Below, 'inducing' molecules, also shown in black, have entered the cell from outside, and by combining with the repressor substance prevent the repressor from switching the gene off. The gene is therefore producing mRNA.¹⁰

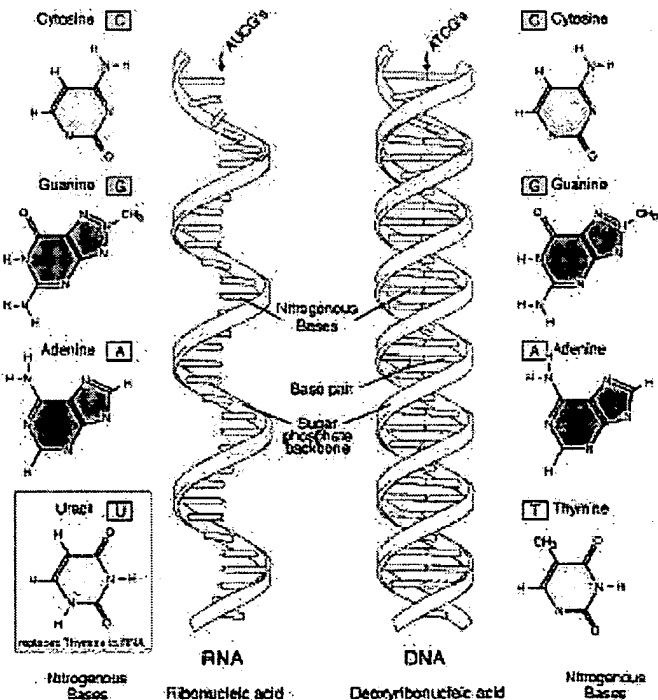


Figure 4. Ribonucleic acid (RNA). A chemical similar to a single strand of DNA. In RNA the letter U (for uracil) is substituted for T in the genetic code. Messenger RNA delivers DNA's genetic message to the cytoplasm of a cell where proteins are made. Three-letter sequences of messenger RNA, known as codons, code for specific amino acids. (Reproduced with permission from: <http://www.nhgri.nih.gov/>)

proteins) return to the nucleus, and prevent other genes from expression, say, by blocking their pairing with mRNA molecules; see Fig. 5. The information stored in the genes, therefore, not only encodes for specific proteins, but it also enables some of these proteins to return to the nucleus to act on other genes, thereby modifying their behavior. The chemistry of the environment also plays a significant role in determining which genes are expressed in a given cell during a given phase of development of the organism.^{13,14}

The bottom line is that the information stored in chromosomes, like a giant software package, has many subroutines that can be invoked under various circumstances, and the next subroutine to be invoked is determined by the results of previous “computations” in a particular environment. (The data fed to the computer program plays the role of the electrochemical environment within which a cell performs its functions). Like a jumbo-jet factory, the body of a complex organism consists of many divisions and subdivisions. A complete copy of the instruction manual for building the jumbo-jet may be present in each and every subdivision, but workers at each location use only the instructions in one or perhaps a few sections of the manual for constructing the part(s) assigned to their subdivision.

Natural versus Man-made Data Storage. There are similarities but also significant differences between man-made and natural memories. For example, DNA is a one-dimensional molecule that uses a quaternary base of nucleic acids (Adenine, Cytosine, Guanine, and Thymine) to store a sequence of information along its length. Similarly, information on a CD is recorded along a spiral track using a sequence of 9 symbols (pit lengths = 3T–11T). In both cases special symbols are employed to mark the beginning and the end of a single block of information (a gene, a sector). Error correction coding is employed to ensure the integrity of the information-content against random errors. In a CD various sectors are linked through a file allocation table (FAT) that specifies the logical sequence of these sectors, even though they may not be stored sequentially along the track. Similarly, links exist among various genes, not only on the same chromosome but also on different chromosomes, that specify the sequence of their activation, or prohibit the expression of one gene based on the expression or non-expression of others.

Both the DNA molecule and the spiral track on a CD are one-dimensional although, in principle, there are no reasons why DNA should not be two-dimensional (i.e., sheets containing A, C, G, T or similar molecules connected to their neighbors on all sides). In our 3D world, a 2D sheet can easily replicate itself by acting as the template for constructing a complementary sheet, then separating from its copy, much the same as a single strand of DNA replicates itself. 3D replication based on the same principle, however, is impossible, because of the need for the molecules to interpenetrate, link, and then separate. Nature has chosen 1D strands of DNA over 2D sheets, presumably because the sheets are either difficult to make or because they provide no additional advantages.

The differences between DNA and CD data storage are staggering. The chromosomes are copied in their entirety during each cell division, so that a new cell will have a complete set of chromosomes of the entire individual (except for the gametes, i.e., the egg and sperm cells, which carry only one copy of each chromosome, and also the red blood cells, which have no chromosomes at all). A given cell obviously does not need all the genes, because only a few genes are expressed in each cell; the rest remain dormant. Most of the genes in a given cell are

never used; those that are needed are not used all the time, but are typically expressed at certain stages of development of the organism. In contrast, when a file from a CD is copied to another medium, only those sectors that constitute the desired file are transferred; there is no need to copy an entire CD if all one needs is a specific piece of information. Each chromosome consists of a complementary pair of DNA strands, the double helix; although the useful information is only recorded on one of the two strands, both are needed to ensure the success of the reproduction process during cell division. In contrast, data along a CD track is single-stranded, because the copying mechanism does not rely on the existence of a complementary strand.

In sexually-reproducing organisms, the chromosomes come in pairs, with the same gene appearing on two homologous chromosomes (one maternal, the other paternal). Both genes are capable of expression, although in certain cases the end product of one gene may be dominant over that of its counterpart. When one of the genes is dysfunctional (either by inheritance, or because of copying errors during cell division, or because of mutation) the other “allele” of the same gene is usually used by the cell’s protein-building machinery, thus avoiding malfunction. A serious problem usually arises when both genes are dysfunctional (e.g., a protein is not produced, or a modified version of it is produced). In contrast, the stored information on a CD typically comes in a single copy, and there are no (functionally similar but physically different) duplicates that could be used if and when the necessity arises.

Example of Existing Technology: The DNA Chip (adapted from [15]). By adapting methods of microprocessor manufacturing, Affymetrix, a California-based company, has created microchips that contain thousands of distinct DNA probes on a glass substrate; see Fig. 6. The glass is coated with a grid of tiny spots, $\sim 20\mu\text{m}$ in diameter, each spot containing millions of copies of a short sequence of DNA. A computer keeps track of the location of each DNA sequence.



Figure 6. DNA chip can sense the state of up to 400,000 genes in a tissue sample. The number of probes on a single glass wafer may soon exceed 60 million, in which case the entire human genome will fit on 200-300 wafers.¹⁵ (Copyright © 2001, Affymetrix, Inc.)

To make snapshots of gene activity, the workers extract mRNA from sample cells. Using enzymes, they make millions of copies of these mRNA molecules, tag them with fluorescent dyes, and break them up into short fragments. The tagged fragments are spread over the chip and, overnight, perform a remarkable feat of pattern matching, randomly bumping into the DNA probes fixed to the chip until they stick to one that contains a perfect genetic match. Although

there are occasional mismatches, the millions of probes in each spot ensure that it lights up only if complementary mRNA is present. The brighter the spot fluoresces when scanned by a laser, the more mRNA of the kind exists in the cell.

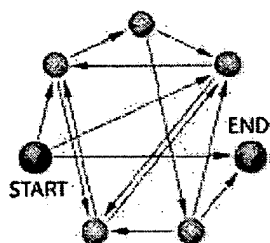
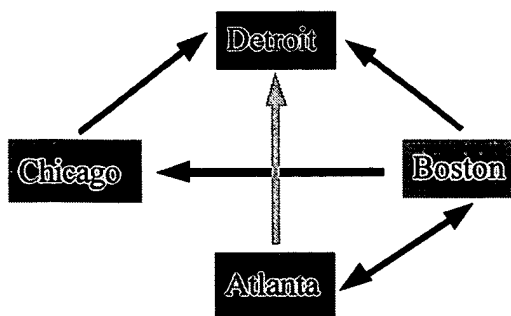
Affymetrix currently makes over 100,000 chips a year, using photosensitive chemicals to build DNA probes one nucleotide at a time. Agilent, Hitachi, and Protogene Laboratories, among others, use modified ink jet printers whose heads squirt A, T, G, and C nucleotides instead of cyan, magenta, yellow, and black inks. Canon is reportedly working with bubble jets to deposit DNA sequences, whereas Corning, Motorola, and Incyte Genomics employ precision robots that place microdroplets of presynthesized sequences onto prepared slides.

The Gene Chip technology clearly demonstrates the feasibility of recording and readout of information using DNA molecules and biochemical principles; the speed and efficiency of the process, however, leave something to be desired.

Biochemical and DNA-based Nanocomputers (adapted from [16]). A chemical computer is one that processes information by making and breaking chemical bonds, storing logic states in the resulting molecular structures. A chemical nanocomputer would perform such operations selectively among molecules taken a few at a time, in volumes only a few cubic nanometers. Proponents of biochemical nanocomputers point to an "existence proof" in the commonplace activities of humans and other animals with multicellular nervous systems. Presently, the possibility of artificial fabrication of biochemical computers seems remote because the operating mechanisms of animal nervous systems are poorly understood. In the absence of a deeper understanding, research has proceeded in alternative directions. One line of investigation has sought to adapt naturally occurring biochemicals for use in computing processes that do not have parallels in Nature. Another approach has been to culture and employ living tissues for computational purposes.

In 1994 Leonard Adleman, then at MIT, took a giant step towards fulfilling the promise of artificial biochemical computers.^{17,18} He used fragments of DNA to compute the solution to a complex graph theory problem (a version of the traveling salesman problem). As shown in Fig. 7, Adleman utilized DNA base-sequences to represent vertices of a network or graph. Combinations of these sequences, formed randomly by the massively parallel biochemical reactions in test tubes, described random paths through the graph. Using the tools of biochemistry, Adleman extracted the correct answer to the posed problem out of the many random paths represented by the product DNA strands. Like a multiprocessor computer, this type of DNA computer is able to consider many solutions to a problem simultaneously. Moreover, the approximately 10^{23} DNA strands employed in such a calculation are orders-of-magnitude greater in number (and more densely packed) than the processors in today's massively parallel electronic computers.

It seemed at first that Adleman's method would be limited to the solution of combinatoric problems. Recent work by R. Lipton at Princeton University has shown, however, that the approach may be applied to a much wider class of digital computations. The problems of fast and efficient input/output, as well as numerous other obstacles, must be overcome before this promising new approach can be broadly applied.^{19,20}



CITY	DNA NAME	COMPLEMENT
Atlanta	ACTTGCAG	TGAACGTC
Boston	TCGGACTG	AGCCTGAC
Chicago	GGCTATGT	CCGATACA
Detroit	CCGAGCAA	GGCTCGTT
FLIGHT		DNA FLIGHT NUMBER
Atlanta-Boston		GCAGTCGG
Atlanta-Detroit		GCAGCCGA
Boston-Chicago		ACTGGGCT
Boston-Detroit		ACTGCCGA
Boston-Atlanta		ACTGACTT
Chicago-Detroit		ATGTCCGA

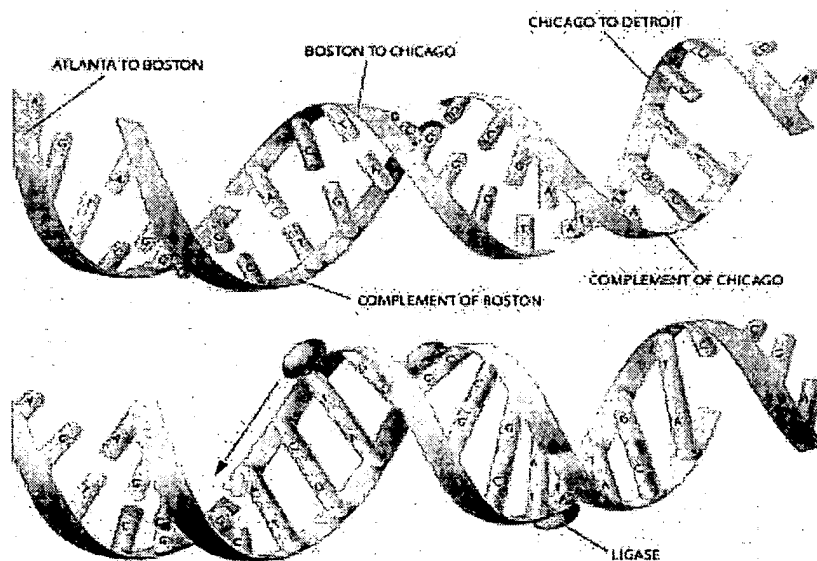


Figure 7 (Adapted from L. M. Adleman, "Computing with DNA," *Scientific American* 279, August 1998). The Hamiltonian path problem is exemplified by a map of cities connected by certain nonstop flights. In this example, for instance, one can fly directly from Boston to Chicago but not vice versa. The goal is to determine whether a path exists from the start city of Atlanta to the finish city of Detroit, passing through each of the remaining cities exactly once. In Adleman's scheme each city is assigned a DNA sequence (TCGGACTG for Boston) consisting of a first name (TCGG) and a last name (ACTG). Also shown in the Table are the Watson-Crick complementary city names in which every C is replaced by a G, every A by a T, etc. DNA flight numbers are assigned by concatenating the last name of the city of origin with the first name of the city of destination. For this particular problem only one Hamiltonian path exists, Atlanta→Boston→Chicago→Detroit, represented by the 24-base-long sequence GCAGTCGGACTGGGCTATGTCCGA. (Also shown in this figure is the diagram of seven cities and 14 connecting flights used in the original Adleman's experiment.) Watson-Crick annealing, in which Cs pair withGs and As join with Ts, results in DNA flight-number strands being held end-to-end by strands encoding the complementary DNA city names. Ligases connect the splinted molecules; wherever the protein finds two strands of DNA in proximity, it will covalently bond them into a single strand. (Copyright © 1995, Tomo Narashima.)

Bacteriorhodopsin-based Memories. Robert Birge of Syracuse University has suggested to use the light-sensitive protein dye bacteriorhodopsin, produced by some bacteria, for memory and logic device applications (see Figs. 8, 9). According to Birge and his collaborators, bacteriorhodopsin can provide a high-density optical memory that can be integrated into an electronic computer to yield a hybrid device of superior performance compared to conventional, purely electronic computers.²¹⁻²³

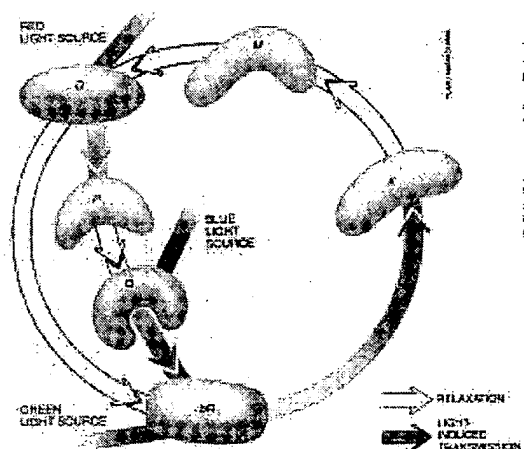


Figure 8. Salty waters of Owens Lake, California, shown in an aerial view, have a purple hue caused by the presence of bacteria (inset) containing the colorful protein bacteriorhodopsin. The protein, depicted here as a ribbon, includes a light-absorbing chromophore segment (shown as balls and sticks). When the chromophore is excited by light, its structure changes and thereby alters the conformation of the rest of the protein. Because bacteriorhodopsin adopts different, readily detectable states in response to light, it can serve as logic gates, or switches, in protein-based optical computers.²²

Copyrights ©: Barrie Rokeach, 1995 (left), Rick Gross and Deshan Govender, 1995 (inset), and Tomo Narashima, 1995 (right).

Figure 9. Sequence of structural changes induced by light allows for the storage of data in bacteriorhodopsin molecules. Green light transforms the initial resting state, bR, to the intermediate K, which then relaxes and forms M followed by O. If the O intermediate is exposed to red light, a so-called branching reaction occurs. Structure O converts to P, which quickly relaxes to the Q state, a form that remains stable almost indefinitely. Blue light, however, converts Q back to bR. Any two long-lasting states can be assigned the binary value 0 or 1, making it possible to store information as a series of bacteriorhodopsin molecules in one state or the other.²²

(Copyright © 1995, Tomo Narashima)



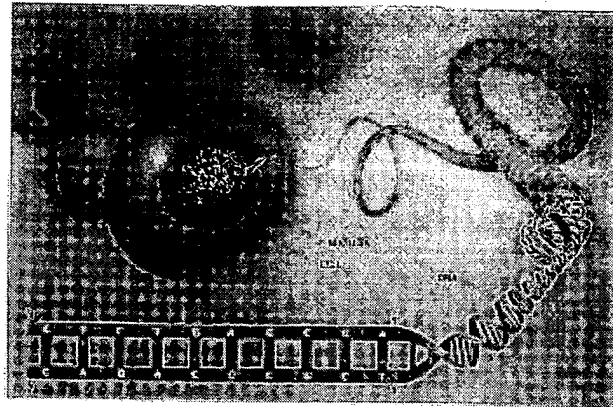
Polymerase Chain Reaction. The simple and elegant method of polymerase chain reaction (PCR) for amplifying small amounts of DNA fragments was discovered in 1983 by K. B. Mullis, then at Cetus Corporation.²⁴ The fragments may come from a human tissue, they may be isolated from a sample of hair or blood recovered from a crime scene, from a woolly mammoth that has been frozen in a glacier for forty thousand years, or from an insect trapped within 80 million year-old amber (fossilized pine resin). The PCR amplification of a single fragment of DNA into billions of identical pieces can be accomplished in just a few hours in a test tube that contains at least one piece of the original DNA (the template), mixed with some simple chemicals and reagents. Figure 10 shows a section of DNA molecule from a chromosome residing inside the nucleus of a cell. By chemical convention, one end of a given strand of DNA is denoted 3' and the other end 5'. Since the two complementary strands are antiparallel, the 3' end of one strand is always paired with the 5' end of the other strand.

One must add a sufficient number of “primer” molecules to the PCR test tube to satisfy the growing needs of the rapidly multiplying DNA throughout the process. A primer molecule (also known as an oligonucleotide probe) is typically made by the techniques of organic chemistry, and contains 20-30 nucleotide bases (A, T, G, C). Each primer must be complementary to an a priori known segment on one strand of the original DNA molecule (the template), which enables

the primer to bind to that segment under proper conditions. A separate primer must be furnished in the test tube for each strand of the original template; in other words, two different types of primer are needed for a given template.

Figure 10. DNA consists of two strands of linked nucleotides, the sequence in one strand being complementary to that in the other (i.e., A's are always opposite T's, and G's are opposite C's). Complementarity binds the strands together. Each strand has a 3' and a 5' end. Because their orientations oppose one another, the strands are said to be antiparallel.²⁴

(Copyright © 1990, George V. Kelvin)



Each primer must be designed to bind to a location near the 3' end of its corresponding DNA strand, as shown in Fig. 11. A primer molecule, when attached to a single strand of template DNA, begins to grow at its own 3' end in accordance with the complementary base sequence specified by the attached template. (Of course the solution must contain plenty of A, T, C, G nucleic acids to satisfy the needs of the growing molecules. In addition, there must be present in the solution an abundant supply of DNA polymerase, a natural enzyme that facilitates the duplication of DNA strands.) After a few minutes in the test tube, each primer grows all the way to the 5' end of its associated strand, thus completing the duplication of the original template.

The first step in a polymerase chain reaction is to heat up the test tube containing nucleic acid molecules, an appropriate DNA polymerase, two types of primer for the intended DNA target, and, of course, the original fragment of DNA. (The essential criterion for any DNA sample is that it contain at least one intact DNA strand encompassing the region to be amplified, and that any impurities are sufficiently diluted so as not to inhibit the polymerization step of the PCR.) When heated to $\sim 95^{\circ}\text{C}$ for 30 seconds, the two strands of the template separate from each other; the DNA molecule is said to be denatured at this point. The temperature is subsequently lowered to $\sim 55^{\circ}\text{C}$, where two primer molecules bind (or "anneal") to specific locations on the two (separated) strands from the template; this binding may take about 20 seconds. Once the primers are bound, the temperature of the solution is raised to $\sim 75^{\circ}\text{C}$, at which point the DNA polymerase goes to work, adding bases (complementary to those on the corresponding DNA strands) at the 3' end of each primer molecule. The copying of the two strands will be completed in approximately one minute, and the original DNA molecule (the

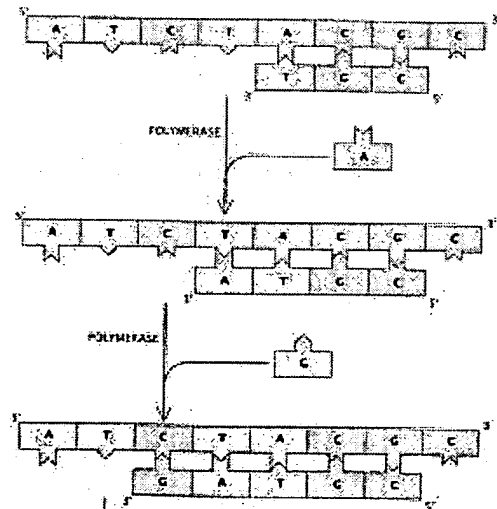


Figure 11. The enzyme DNA polymerase can lengthen a short strand of DNA, called an oligonucleotide primer, if the strand is bound to a longer "template" strand of DNA. The polymerase does this by adding the appropriate complementary nucleotide to the 3' end of the bound primer.²⁴

(Copyright © 1990, Michael Goodman)

template) will be reproduced in duplicate. The process can be repeated by cycling the temperature, thus doubling the number of DNA molecules at the end of each cycle. The total number of double-stranded DNA molecules in the test tube thus grows exponentially, reaching a billion in just 30 steps.

If the DNA polymerase is obtained from aquatic bacteria residing in thermal vents or hot springs (bacteria that can withstand high temperatures), there will be no need to replenish the supply of polymerase at the end of each heating cycle, because it will not degrade by heating. The DNA polymerase extracted from *Thermus aquaticus*, the sultry bacterium from the Yellowstone National Park, is now universally favored for PCR.

DNA polymerases, whether from humans, bacteria, or viruses, cannot copy a chain of DNA without a short sequence of nucleotides to "prime" the process, or get it started. (Cells have an enzyme called a "primase" that actually makes the first few nucleotides of the copy.) This stretch of DNA is called a primer. Once the primer is made, the polymerase can take over making the rest of the new chain.

Primers are annealed to the denatured DNA template to provide an initiation site for the elongation of the new DNA molecule. Primers can be specific to a particular DNA sequence or they can be "universal." The latter are complementary to nucleotide sequences that are common in a particular set of DNA molecules. Thus, universal primers bind to a wide variety of DNA templates. Bacterial ribosomal DNA genes, for example, contain nucleotide sequences common to all bacteria. Thus, universal primers for bacterial DNA can be made by creating primers which are complementary to these sequences. Examples of universal primers for bacteria are:

Forward 5' GAT CCT GGC TCA GGA TGA AC 3' (20 mer)
Reverse 5' GGA CTA CCA GGG TAT CTA ATC 3' (21 mer)

Animal cell-lines contain a particular sequence known as the ALU gene. (Approximately 900,000 copies of the ALU gene are distributed throughout the human genome, and multiple copies of the same can be found in the genome of other animals.) The ALU gene thus provides a universal primer for animal cell-lines; this primer is especially useful because it binds in both forward and reverse directions.

ALU universal primer: 5' GTG GAT CAC CTG AGG TCA GGA GTT TC 3' (26mer)

When using universal primers, the annealing temperature should be lowered to 40-55°C.

Memory and the Nervous System. There are an estimated 10^{10} – 10^{11} neurons in the central nervous system of a human being. Although there are many types of neurons of differing sizes and shapes, the principles of operation of these neurons are remarkably similar.^{4,25} Figure 12 shows the structure of a typical neuron. The neuron is a specialized cell, consisting of a cell body (soma), where the nucleus resides, a relatively long cable, axon, along which the output signal travels to reach other neurons (or muscle cells, or glands), and many short branches, dendrites, which are in contact with the axonal terminals of other neurons, acting as receiving terminals for their own neuron;²⁵ see Fig. 13. A typical cell may have hundreds or thousands of dendrites, each

no more than a millimeter long. The axon, on the other hand, could be quite long, reaching in length to several feet in some cases. Each axon branches off and makes contact with dendrites of several other neurons.^{5,25} The contact between the end-point of an axonal branch and another cell's dendrite or cell body is called a synapse (see Fig. 14). Electrical signals travel down an axon in the form of spikes (pulses) of ~ 100 mV magnitude and ~ 1 ms duration, reaching the dendrites unattenuated, as shown in Fig. 15. The travelling speed of these signals is typically of the order of several meters per second (in some cases reaching 100 m/s or even faster).²⁶

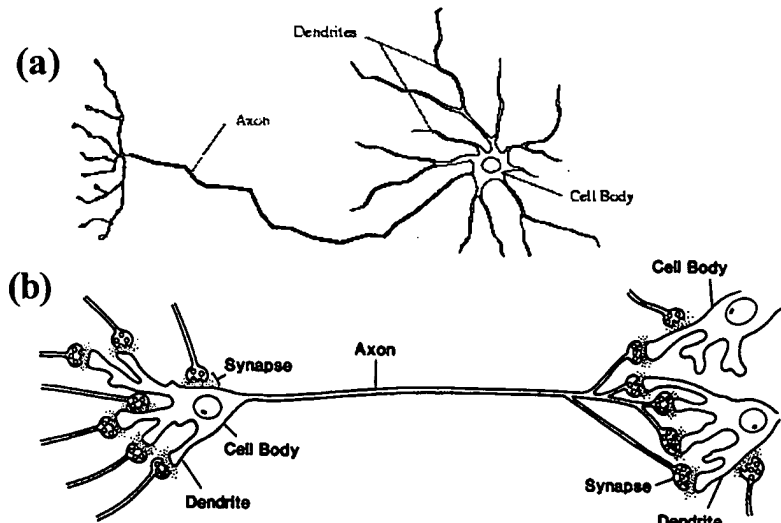


Figure 12. (a) The structural unit of the nervous system, a neuron contains a nucleus and cell body from which has grown a tree of many branches and twigs spreading in various directions. A neuron typically has many dendrites and one axon. The dendrites branch and terminate in the vicinity of the cell body. In contrast, axons can extend to distant targets, more than a meter away in some instances. Dendrites are rarely more than about a millimeter long and often much shorter. (From: Synapse Web, Boston University, <http://synapses.bu.edu/>)

(b) The electrical signals flow into the dendrites and out through the axon. Thus in this diagram the information flows from left to right. (Copyright © 1994, Francis H. C. Crick.)

At the synapse, the arriving electrical pulse causes the release of certain chemicals (neurotransmitters) into the region between the two terminals (the synaptic cleft). These chemicals are picked up by receptors on the postsynaptic neuron and cause the transmission of an electrical signal from the dendrite to the postsynaptic cell. Communication between the connected cells may therefore be characterized as electrical \rightarrow chemical \rightarrow electrical.⁵



Figure 13. Spiny dendrites from hippocampal pyramidal neuron. Left: Light microscope image. Right: Reconstruction from serial electron microscopy.

(From: Synapse Web, Boston University, <http://synapses.bu.edu/>)

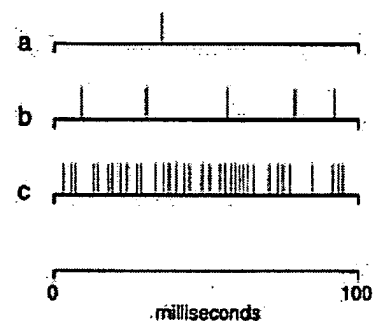


Figure 15. The firing of a single neuron. Each short vertical line represents a spike. In (a) the neuron is firing at its background rate. In (b) it is responding to some relevant input by firing at an average rate. In (c) it is responding about as fast as it can.⁵ (Copyright © 1994, Francis H. C. Crick)



Figure 14. (a) Schematic of a synapse. (b) Presynaptic axon and postsynaptic dendritic spine. (c) The synaptic cleft, into which neuro-transmitter is released, is the narrow gap that separates the axonal bouton (PRE) from the postsynaptic cell (POST). (From: Synapse Web, Boston University, <http://synapses.bu.edu/>)

Broadly speaking, there exist two kinds of neurons: excitatory and inhibitory; see Fig. 16. They have different neuro-transmitters (e.g., the amino acid glutamate in excitatory nerve cells, GABA in inhibitory cells). In the human brain roughly 20% of all neurons are of the inhibitory type. The receiving neuron will make a decision as to whether or not to fire a signal down its axon, based on the collection of signals it receives at its input (dendritic) terminals. The signals coming into a neuron from excitatory cells tend to enhance the possibility of its firing, while the inhibitory signals hamper such chances. The final decision as to whether or not to fire is based on the overall pattern of the inputs; this involves a nonlinear process, which polls the multitude of input signals, performs a complex weighted averaging on them (positive coefficients for excitatory inputs, negative for the inhibitory ones), and if the weighted average exceeds a certain threshold the nerve cell will fire, otherwise it remains in its resting state.^{27,28}

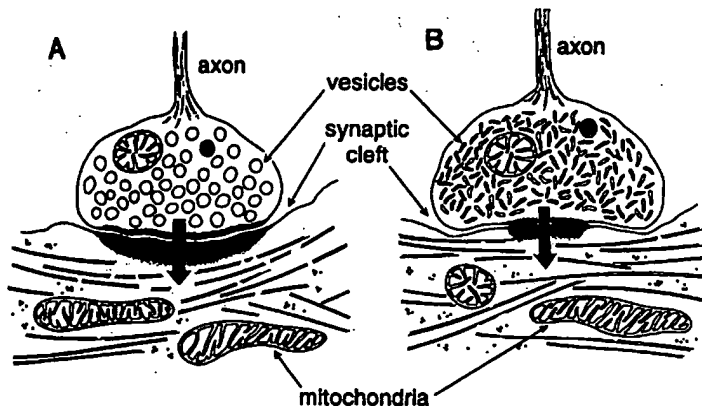


Figure 16. The two main types of synapses found in the cortex. A, Type I (excitatory); B, Type 2 (inhibitory). In each figure the axon is at the top, the dendrite at the bottom, with the synaptic cleft in between. The arrows show the direction of the main flow of information. From the (presynaptic) axon to the (postsynaptic) dendrite.⁵ (Copyright © 1994, Francis H. C. Crick)

The workings of a neuron in terms of the physical processes of generating an electrical signal, releasing neuro-transmitters, etc., are fairly well understood. As for the mechanism of memory, a model suggested as early as 1945 by the Canadian psychologist Donald Hebb²⁹ postulates that the synaptic connection between two neurons is strengthened as a result of a successful firing. In other words, if neuron A sends a signal to neuron B, and B decided to fire after polling its inputs, somehow the coincident firings of A and B will affect the strength of the synaptic coupling between the two, making it stronger if A happens to be an excitatory neuron, and reducing the synaptic strength if A happens to be inhibitory. Presumably, the reverse happens if B does not

fire in response to A. Human memory, therefore, seems to be formed in the rich pattern of interconnections among billions of neurons in the cortex, by the adjustment of the synaptic strengths.

The Olfactory System (Adapted from [28]). The complex interaction among interconnected neurons extending from an external sensory organ to the deepest recesses of the brain is exemplified by the olfactory system. When an animal sniffs an odorant, molecules carrying the scent are captured by a few of the immense number of receptor neurons in the nasal passages; the receptors are somewhat specialized in the kinds of odorants to which they respond. Cells that become excited fire pulses, which propagate through axons to the olfactory bulb (see Fig. 17). The number of activated receptors indicates the intensity of the stimulus, and their location in the nose conveys the nature of the scent. Each scent is expressed by a spatial pattern of receptor activity, which in turn is transmitted to the bulb.

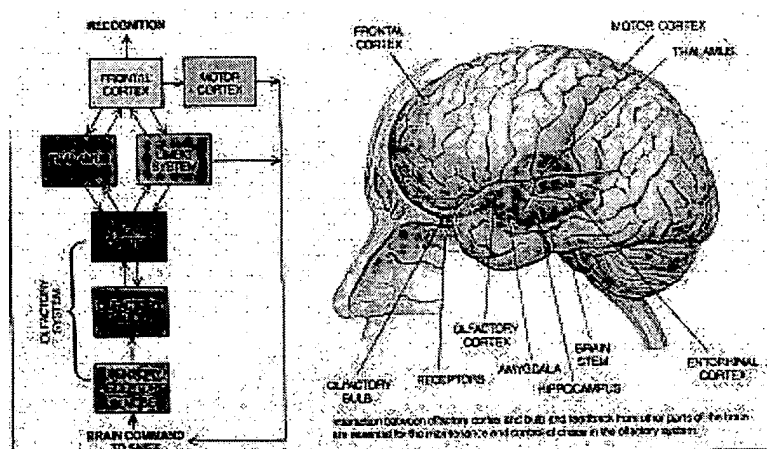


Figure 17. Basic flow of olfactory information in the brain.²⁸ (Copyright © 1991, Carol Donner.)

The bulb analyzes each input pattern and transmits its own message to the olfactory cortex. From there, new signals are sent to many parts of the brain, including the entorhinal cortex, which combines the signals with those from other sensory systems. The result is a perception that is unique to each individual; a perception that cannot be understood solely by examining individual neurons, but depends on the global activity of millions of neurons throughout the cortex.

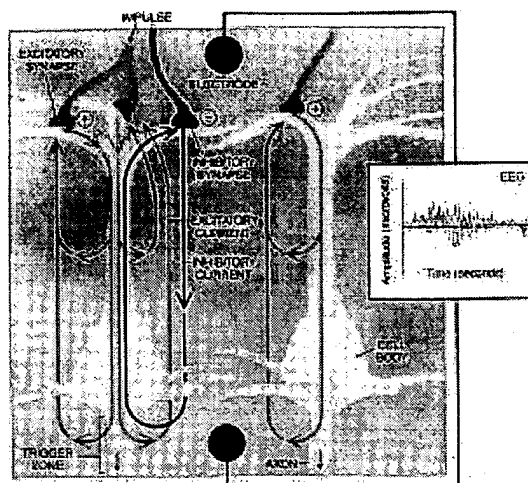
Cortical neurons continuously receive pulses from thousands of other neurons. Certain incoming pulses generate excitatory waves of electric current in the recipients; others generate inhibitory waves, as shown in Fig. 18. These dendritic currents are fed through the cell body to the “trigger zone” at the start of the axon. There the currents cross the cell membrane into the extracellular space. As they do, the cell calculates the overall strength of the currents by adding excitatory currents and subtracting inhibitory ones. If the sum is above a threshold level, the neuron fires.

By attaching electrodes to an area of the bulbar surface, researchers can collect sets of simultaneously recorded electroencephalogram (EEG) as the animal breathes in and out. Each tracing reflects the mean excitatory state of local pools of neurons lying in a layer beneath the electrodes. Rises in the EEG amplitude indicate increasing excitement; dips represent diminished excitement caused by inhibition. Each EEG is related to the firing pattern of neurons in a neighborhood of the cerebral cortex. The tracings detect essentially the same information that

neurons assess when they "decide" whether or not to fire impulses, but an EEG records that information for thousands of cells at once.

Figure 18. EEG waves reflect the mean excitation of pools of neurons. Excitatory inputs at synapses generate electric currents that flow in closed loops within the recipient neuron toward its axon, across the cell membrane into the extracellular space and, in that space, back to the synapse (*red arrows*). Inhibitory inputs generate loops moving in the opposite direction (*black arrows*). In cells the trigger zone adds current strengths (reflected in changes in voltage across the membrane), and it fires impulses if the sum is sufficiently positive. Electrodes on the brain tap those same currents after they leave the cell. The resulting EEGs indicate the excitation of whole groups of cells, not individuals, because the extracellular avenues from which the EEGs arise carry currents contributed by thousands of cells.²⁸

(Copyright © 1991, Dana Burns-Pizer)

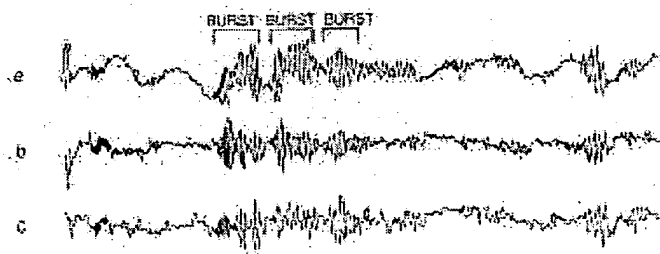


As shown in Fig. 18, the mechanism producing each EEG tracing sums the currents initiated at the dendrites, but it taps the currents after they leave the cell. The tracings reflect the excitatory state of groups of neurons rather than of individual ones, because the extracellular space is traversed by currents from thousands of cells.

In living individuals, EEGs always oscillate to some extent, but the oscillations are usually quite irregular. When an animal inhales a familiar scent, a burst can be seen in each EEG tracing. All the waves from the array of electrodes suddenly become more regular for a few cycles – until the animal exhales (see Fig. 19). The waves often have a higher amplitude and frequency than they do at other times. (The bursts are often called 40 Hz waves, although the frequency can actually range from 20 to 90 Hz.)

Figure 19. Simultaneous recordings from the olfactory bulb (a) and front (b) and rear (c) parts of a cat's olfactory cortex show low-frequency waves interrupted by bursts – high-amplitude, high-frequency oscillations that are generated when odors are perceived. The average amplitude of a burst is $\sim 100 \mu\text{V}$. Each lasts a fraction of a second, for the interval between inhalation and exhalation.²⁸

(Copyright © 1991, Walter J. Freeman)



Curiously, it is not the shape of the carrier wave that reveals the identity of an odor. Indeed, the wave changes every time an animal inhales, even when the same odorant is repeatedly sniffed. The identity of an odorant is discernible only in the bulbwide spatial pattern of the carrier-wave amplitude. It is believed that something called "the nerve cell assembly" is both a crucial repository of past associations and an essential participant in the formation of the collective bulbar burst. The hypothetical assembly consists of neurons that have simultaneously been excited by other neurons during learning.

When animals are trained to discriminate among olfactory stimuli, certain synapses that connect neurons within the bulb and within the olfactory cortex become selectively strengthened during training. That is, the sensitivity of the postsynaptic cells to excitatory input is increased at the synapse, so that an input generates a greater dendritic current than it would have generated in the absence of special training.

The strengthening occurs not in the synapse between an input axon (e.g., a nasal receptor) and the neuron it excites (e.g., a bulbar neuron), but in the connection between neurons that are simultaneously excited during learning. Neurons in the bulb and in the olfactory cortex are connected to many others in those regions. Such strengthening is predicted by the Hebb rule, which holds that synapses between neurons that fire together become stronger, as long as such synchronous firing is rewarded. (Strengthening involves modulator chemicals released by the brain stem during reinforcement.)

Thus a nerve cell assembly, consisting of neurons joined by Hebbian synapses, forms for a particular scent as the individual learns to identify that odorant. Subsequently, when any subset of neurons in the assembly receives the familiar input, the entire assembly is stimulated, as excitatory signals race across the favored Hebbian synapses. The assembly, in turn, directs the rest of the bulb into a distinct pattern of activity.

If the odorant is familiar and the bulb has been primed by arousal, the information spreads like a flash fire through the nerve cell assembly. First, excitatory input to one part of the assembly during a sniff excites the other parts, via the Hebbian synapses. Then those parts reexcite the first, increasing the gain, and so forth, so that the input rapidly ignites an explosion of collective activity throughout the assembly. The activity of the assembly, in turn, spreads to the entire bulb, igniting a full-blown burst. The bulb then sends a "consensus statement" simultaneously along parallel axons to the olfactory cortex (see Fig. 20).

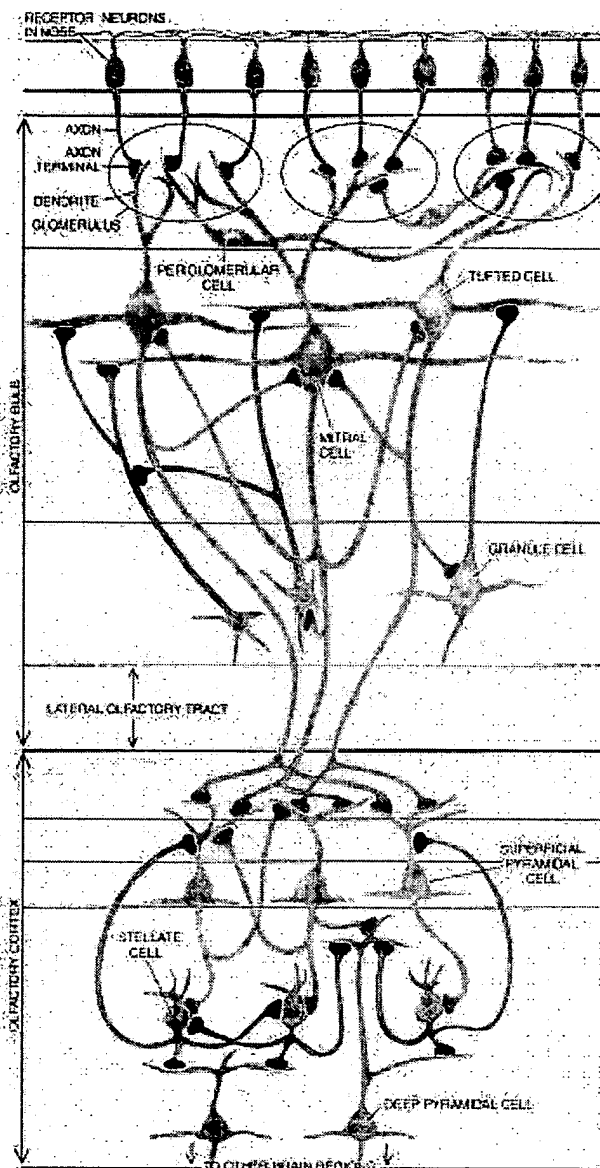


Figure 20. Neurons of the olfactory system share information through a rich web of synapses, junctions where signals flow from neuron to neuron. Usually signals pass from projections called axons to projections called dendrites, but sometimes they pass from dendrite to dendrite or axon to axon. The widespread sharing leads to collective activity. In this highly schematic diagram, red shading signifies that a neuron is exciting another cell, black shading that a neuron is inhibiting another.²⁸ (Copyright © 1991, Dana Burns-Pizer.)

How does that cortical area distinguish the consensus statement from the background of other stimuli? The answer has to do with the wiring that joins the bulb to the cortex. The bulb generates trains of impulses that run simultaneously along the parallel axons leading from the bulb to the cortex. Each axon branches extensively and transmits pulses to many thousands of neurons across the olfactory cortex, and each cortical target cell receives input from thousands of bulbar cells. The carrier activity of the incoming lines, synchronized by cooperation, probably stands out for the simple reason that such signals add together. Nonsynchronous inputs, which are not at the carrier frequency and phase, effectively cancel one another.

Thus, every recipient neuron in the olfactory cortex picks up a share of the cooperative bulbar signal and transmits the summed signals to thousands of its neighbors simultaneously. In response, the cortical neurons, which have formed nerve-cell assemblies, promptly generate their own collective burst, albeit one having a spatial pattern that differs from those in the bulb. Just as a burst in the bulb guarantees the delivery of a coherent message to the cortex, the global burst in the cortex enables outgoing messages from that region to stand above the din when they reach other regions of the brain.

The Hierarchy of Cell Assemblies (adapted from [26]). Donald Hebb first entertained the cell assembly theory in the mid-1940s after reading Marius von Senden's *Space and Sight*, originally published in 1932. In this work von Senden assembled existing records on 65 patients from the eleventh century up to the year 1912 who had been born blind due to cataracts. At ages varying from 3 to 46, the cataracts were removed, and a variety of reporters observed them as they went about handling the sudden and often maddeningly novel influx of light.

One of the few uniformities in these cases was that the process of learning to see "is an enterprise fraught with innumerable difficulties, and that the common idea that the patient must necessarily be delighted with the gifts of light and color bequeathed to him by the operation is wholly remote from the facts." Not every patient rejoiced upon being forced to make sense of light that was all but incomprehensible, and many found the effort of learning to see so difficult that they simply gave up. The doctor of a 21 year-old woman reported:

Even before the operation she was dull and spiritless. Whenever I visited her afterwards, the bandages having been long since discarded, I found her with her eyes closed, though not forced to do so by any aversion to the light. Laborious persuasion was needed before she would even come to look at the things immediately about her, and at last to become acquainted with them. Some years ago, her father wrote that she carefully shuts her eyes whenever she wishes to go about the house, especially when she comes to a staircase, and that she is never happier or more at ease than when, by closing her eyelids, she relapses into her former state of total blindness.

If seeing were a simple reflex, the restoration of vision should have completed a circuit, allowing a patient to view the world as lucidly as if he or she had done so all along. Instead von Senden's accounts suggest that seeing was not at all automatic. The friend of one 15 year-old patient, in an attempt to encourage him to learn to see, tried the following experiment:

One day, during the vine-harvest, she picked a bunch of grapes and showed it to him from a distance. "What is that?" she asked. "It is dark and shiny," he replied. "Anything else?" "It isn't smooth, it has bumps and hollows." "Can one eat it?" she asked. "I don't know." As soon as he touched the bunch, he cried: "But they're grapes!"

The reports indicated that patients who had been completely dependent on tactile impressions before the operation, had an awareness of space that was totally different from a normal visual awareness. At first, von Senden discovered, "the patient feels visual impressions to be something alien, intruding on his mind without action on his own part." Later, he reported, "the stimuli impinging on the visual organ from an objective shape merely occasion the act of perception as such, but do not determine its outcome." A 9 year-old boy, for example, spent days trying to learn how to tell a sphere from a cube. From his record:

He gradually became more correct in his perception, but it was only after several days that he could tell by his eyes alone, which was the sphere and which the cube. When asked, he always, before answering, wished to take both into his hands. Even when this was allowed, when immediately afterwards the objects were placed before the eyes, he was not certain of the figure.

That such observations are not artifacts of the surgery or uniquely human was established through observations on a pair of chimpanzees that had been reared in the dark by a colleague of Hebb. After being brought out into the light, these animals showed no emotional reactions to their new experiences. They seemed unaware of the stimulation of light and did not try to explore visual objects by touch. Hebb concluded that the chimps showed no visual response because they had not formed the neural assemblies that are necessary for visual perception.

"How," Hebb asked, "can it be possible for a man to have an IQ of 160 or higher, after a prefrontal lobe has been removed?" If a particular memory is stored in a certain neuron, its continued existence depends on the life of the cell. Cell death, in this model, means total loss of the memory. Assembly storage, on the other hand, is robust because physical damage – leading to the death of a few cells – will not necessarily destroy specific assemblies but instead degrade many by roughly equal degrees. This loss could then be restored through recruitment of additional cells into the assembly.

If one accepts the concept of cell assemblies, it is interesting to ask how many might be able to form. This is a difficult question, but Charles Legéndy has obtained some results from a simple model. He assumes that the brain is already organized into subassemblies and discusses their organization into larger assemblies. The assembly and one of its subassemblies variously represent "a setting and a person who is part of it, a word and one of its letters, an object and one of its details."

In Legéndy's model, interconnections are assumed to be evenly distributed over the neocortex to avoid the complications of spatial organization. His subassemblies are formed through weak contacts, and assemblies emerge from subassemblies through the development of latent into strong contacts between neurons. From statistical arguments, Legéndy estimates the maximum number of assemblies in a brain to be about $(N/ny)^2$, where N is the number of neurons in the

brain, n is the number of neurons in a subassembly, and y is the number of subassemblies in an assembly. Taking $N = 10^{10}$, $n = 10^4$, and $y = 30$, he finds $\sim 10^9$ assemblies, as a conservative estimate for "the number of elementary things the brain can know." The number of neurons in the neocortex may be an order of magnitude greater than 10^{10} , and the real neuron is much more complex than the simple model assumed by Legédy, but 10^9 is approximately the number of seconds in 30 years. Thus a model of the brain based on simple neurons provides sufficient storage for the complex memories of a normal lifetime.³⁰

Cortical Stimulation (adapted from [26]). The Canadian neurosurgeon W. Penfield and his colleagues induced hallucinations in several patients through electrical stimulation of the neocortex.³¹ The purpose of such stimulation was to locate the origin of epileptic activity in order to remove the offending portion of the cortex. Gentle electrical stimulation was applied to the temporal lobes of 520 patients, of whom 40 reported experiential responses. Stimulating currents between 50 and 500 μA were used in pulses of 2 to 5 ms at frequencies of 40 to 100 Hz.

M.M. was a typical case. A woman of 26, she had her first epileptic seizure at the age of 5. When she was in college, the pattern included visual and auditory hallucinations, coming in flashes that she felt she had experienced before. One of these

had to do with her cousin's house or the trip there – a trip she had not made for ten to fifteen years but used to make often as a child. She is in a motor car which had stopped before a railway crossing. The details are vivid. She can see the swinging light at the crossing. The train is going by – it is pulled by a locomotive passing from the left to right and she sees coal smoke coming out of the engine and flowing back over the train. On her right there is a big chemical plant and she remembers smelling the odor of the chemical plant.

During the operation, her skull was opened and her right temporal region explored to locate the epileptic region. Figure 21 shows the exposed lobe with numbered tickets that mark the sites at which positive responses were evoked. Penfield termed the responses *experiential* because the patient felt that she was reliving the experience – not merely remembering it – even as she remained aware that she was lying in the operating room and talking to the doctor. The following experiential responses were recorded upon electrical stimulation at the numbered locations:

11. She said, "I heard something familiar, I do not know what it was."

11. Repeated without warning. "Yes, sir, I think I heard a mother calling her little boy somewhere. It seemed to be something that happened years ago." When asked if she knew who it was she said, "Somebody in the neighborhood where I live." When asked she said it seemed as though she was somewhere close enough to hear.

11. Repeated 18 minutes later. "Yes, I heard the same familiar sounds, it seems to be a woman calling. The same lady. That was not in the neighborhood. It seemed to be at the lumber yard."

13. "Yes, I heard voices down along the river somewhere – a man's voice and a woman's voice calling." When asked how she could tell it was down along the river, she said, "I think I saw the river." When asked what river, she said, "I do not know, it seems to be one I visited as a child."

13. Repeated without warning. "Yes, I hear voices, it is late at night, around the carnival somewhere – some sort of a travelling circus. When asked what she saw, she said, "I just saw lots of big wagons that they use to haul animals in."

12. Stimulation without warning. She said, "I seemed to hear little voices then. The voices of people calling from building to building somewhere. I do not know where it is but it seems very familiar to me. I cannot see the buildings now, but they seemed to be run-down buildings."

14. "I heard voices. My whole body seemed to be moving back and forth, particularly my head."

14. Repeated. "I heard voices."

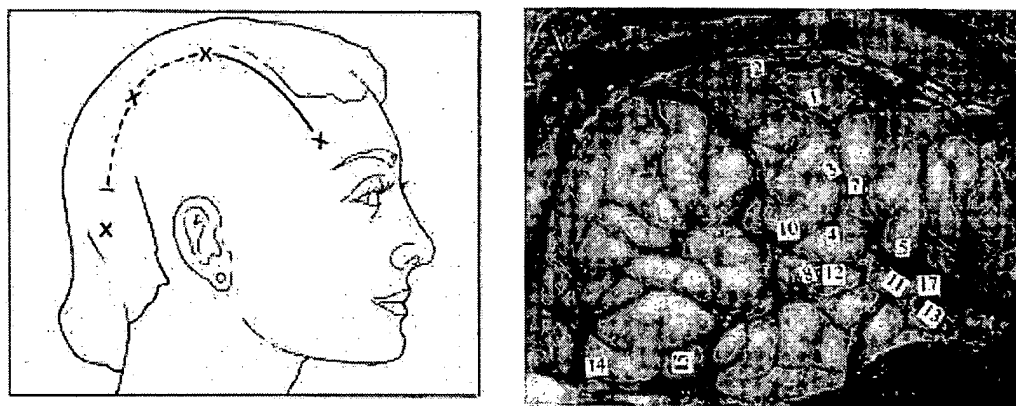


Figure 21. The right temporal lobe of M.M. with numbers that indicate points of positive stimulation.³¹

The forty cases surveyed by Penfield and his colleagues show that this particular example of experiential response is not at all unique. They conclude that, in the human brain, there is a remarkable record of the stream of each individual's consciousness, and that stimulation of certain areas of the neocortex – lying on the temporal lobe between the auditory and visual sensory areas – causes previous experience to return to the mind of a conscious person.²⁶

Information in Human Societies. The information used by humans is of several kinds. We write down recipes and instruction sets for making things such as high-rise buildings, apple pies, DVD-players, clothing items, chemicals, movies, etc. Musicians compose new music, playwrights write original plays, painters create new paintings, mathematicians discover new theorems, scientists uncover facts about Nature, and legislators create new laws. These ideas and expressions (rendered in various media) need to be stored and protected for use by other members of the society, or for transmission to future generations. Daily events, stock prices, sports news, and weather information are likewise useful and often worthy of short-term or long-term storage. A culture is shaped by the collection of all such information learned, created, applied, imitated, modified, improved upon, and transmitted within a population and from one generation to the next.

Within the human brain, a piece of information is more than just a rigid set of connections among certain neurons. The sounds, images, scents, events, ideas and intuitions residing within the confines of a given skull are interconnected. In some instances they help to reinforce one another, in others they give rise to logical inconsistencies and absurdities that the conscious mind

attempts to resolve. Once resolution occurs some of the memories gain prominence at the expense of others. Mental activity of this kind often results in the creation of new concepts and ideas, which themselves explore the content of the brain and attempt to form new connections. This is a dynamic, self-propelled environment, which is constantly gaining knowledge, combining and restructuring the existing memories, discounting or forgetting some previously-held beliefs, and initiating actions that result in new explorations, further acquisition of information, and so forth.

Compare the above situation with the passive nature of the information stored in a book or on a hard drive. By and large the various pieces of information are ignorant of each other, their interactions are either non-existent, or mediated by the mind of a user or by the CPU of a computer. Our data storage technology is divorced from the processing technology that operates on the stored information. Our stored information cannot initiate a search for other pieces of related data, cannot resolve its internal inconsistencies, cannot form alliances with other pieces of data sitting on the same medium that might bolster its effectiveness, cannot create new pieces of information or improve its own content. Such are the shortcomings of the storage technology at the end of the 20th century. Although the search for denser, faster, and cheaper memories is a worthy goal for now and for many years to come, it is far more challenging (and proportionately more rewarding) to search for alternative modes of storage that would overcome the passive nature of the present-day technology in the broad sense just described.

To the lively and evolving environment within a human brain, now add the interactions among billions of similar brains on the planet. An idea formed in one head moves to several other heads, undergoes modifications, forms new alliances, then propagates further to others. Spoken language was perhaps the first extensive means of inter-brain communication, followed by the written word. Then came the printing press in the 1440's and revolutionized human lives and cultures. Electronic communication (radio, TV, phone, fax, copy machines) has had a profound effect on our lives over the past century, but perhaps all these revolutions will be dwarfed by the promise of the internet and what it will do for the inter-brain connectivity.

The internet is not just allowing us human beings to access all the knowledge of the past and the present, and to explore each other's minds. The internet is also allowing computers and other electronic means of information processing and storage to communicate among themselves. At the moment this communication is mediated by humans: All inter-computer communication is under the control of software written by engineers and enthusiasts. But imagine the day when all the computers of the world, connected via the internet, can exchange their information and form data structures above and beyond those imposed upon them by their human masters. Imagine the day when control programs, recipes, musical scores, movie scripts, mathematical theorems, etc., can mutate, mate, replicate, propagate through the internet, and survive or perish in the competition with their kin or with other denizens of the net. In their constant struggle for survival, only those memes³² that are best adapted to their natural environment will emerge and flourish. (Meme is the unit of cultural inheritance; see the glossary for further details.)

Does Nature Follow any Principles of Organization? Darwin's principles of evolutionary biology³³ are quite simple, yet they have provided a powerful framework for the study of life processes and their historical development. First there is the inheritance of biological

characteristics by the offspring from parent(s). Second, genetic mutation can change some of these transmitted characteristics in apparently random ways. Third, there is natural selection based on the survival of the fittest individuals.² The genetic code, while transmitted from one generation to the next, remains largely intact, although paternal and maternal chromosomes are shuffled rather extensively, and a few genes here and there are modified in the course of transmission to the next generation.¹⁰ If these modified genes endow the offspring with useful qualities – qualities that help survival and reproduction – then they remain in the gene pool and spread throughout the population, otherwise the individual will die or will fail to reproduce, causing the disappearance of those (harmful) mutated genes.

The Darwinian principles do not explain the hierarchical organization and the “sense of purpose” that seem to guide the processes of evolution. Are there additional rules that Nature follows in directing the evolution of species? The complex pattern of interconnection among the brain cells, to pick but one example, is not likely to have resulted from random trial and error;^{34,35} there are just too many possibilities for interconnection and too little time (~ 600 million years since the appearance of multicellular organisms) for these connections to have been tried in all their varieties before being adopted. What rules does Nature follow in allowing collective mutations, for example? To what extent and under what circumstances is repetition (e.g., gene duplication) used by Nature? What kind of mutations in duplicated genes are most beneficial? We do not know the answers to these questions; in fact, we probably have not even begun to ask the right questions. Perhaps the time is now ripe to begin to focus on such issues, as the underlying structure and functioning of the cells and the electrochemical basis of intercellular communication have already been worked out in great detail during the past century. Our understanding of the molecular basis of life has reached a point that one can now ask questions about higher-level principles of organization with regard to the architecture of complex biological systems. It is in asking and attempting to answer such questions that humanity faces one of its greatest challenges today.

Observations Concerning Higher-level Principles of Organization Here is one set of principles that the Nature seems to have consistently used throughout the biosphere.

(i) There exist simple functional or operational units (hereinafter referred to as action units), that appear over and over again within an organism, or even cross the boundaries of individual organisms to appear across large groups of individuals and species. Examples include:

- Expansion or contraction of a muscle cell in response to a command from a motor neuron.²⁵
- Splitting into two parts and forming new functional units similar in constitution to the parent (i.e., cell division, DNA duplication).
- Random shuffling (e.g., chromosome recombination during meiosis to endow one’s offspring with a mixture of traits from one’s own parents;¹⁰ gene shuffling in the immune cells for producing a large number of receptor molecules to match a multitude of foreign antigens⁶).

These “fundamental” units of biological action are activated in response to a set of input signals, and result in specific outputs or actions. The input signals may vary over a limited range without affecting the output, or they may affect the output quantitatively but not qualitatively. In other

words, the basic action units have some degree of flexibility, tolerating variations in the level of the electrical/chemical input signal(s), relative timing of these signals, etc.

(ii) The various action units communicate and interact with each other. One action can trigger another, and in turn be affected by the result of the action it triggers. In other words, inputs to each unit could be the outputs from other units. Biological means of communication include:

- Cell-to-cell communication by chemical means, e.g., via neurotransmitters and hormones.
- Cell-to-cell communication by electrical signaling, e.g., from neuron to neuron, from neuron to muscle cell and vice versa, and from neuron to glandular cell.
- Migration of individual cells through the blood circulation system, through the lymphatic system, or by crawling over other cells.
- Directional growth and branching of individual cells to establish contact with distant cells.³⁴

The interaction between two units may occur simultaneously, or it may occur sequentially in the sense that the response of one unit will follow the action of another. Some actions are triggered by external causes (e.g., variations in temperature or pressure, influx of light, arrival of chemicals from the outside world), while others are initiated by internal signals produced by some other action unit(s).

(iii) Individual action units have the potential to switch from one mode of operation to another, depending on their internal state and the nature of the incoming signals. For example,

- Motor neurons can grow additional branches from their axons and make new contacts to the muscle cells if some of their neighbors die (e.g., in polio survivors), or if they are stimulated to do so by exercise.
- The fertilized eggs of many reptiles (e.g., turtles, various lizards) grow into males or females depending on their ambient temperature.
- Various stem cells can grow into different types of cell, depending on their mode of stimulation and chemical environment. The stem cells of the immune system, for instance, originate in the bone marrow and, after several divisions, are transformed into erythrocytes (red blood cells) or lymphocytes (white blood cells, such as T-cells, B-cells, phagocytes, etc.) depending on whether they mature in thymus or bone marrow, and also depending on the chemical signals they receive prior to differentiation and maturation.⁶

This degree of flexibility is supported by the fact that each cell within the organism carries the entire genetic code of that organism, making it possible to switch from one instruction set to another when prompted by the circumstances in which the cell might find itself.

(iv) The strength of interaction between two action units could be modified depending on the outcome of their direct interaction (e.g., the Hebbian model for adjustment of the synaptic strength), or as a result of internal modifications to individual units (i.e., an increase or decrease in the amount of available neurotransmitter molecules), or as a result of a change in the environment. Moreover, two disjoint units could develop interactions (for example, by growth and connection of new axonal branches), or two interacting units may lose their connections over time.

We do not yet know how Nature decides to establish connections among various action units. Does the Nature follow any specific rules in deciding whether two units should or should not interact? Since the underlying network of interactions (or the propensity of individual units to grow towards others, make contact with them, regulate the strength of their interactions, etc.) are controlled by the genes, one should ask whether there are any features of chromosomal recombination during meiosis, gene duplication, and gene transfer, etc., that could be responsible for promotion of such behavior among the individual action units. Once this underlying network, and the guiding principles for its growth and connectivity are established, each individual organism responds to its unique environment (and its unique upbringing) by developing special connections among its constituent action units. The individual thus forms its own memories, talents, personality, etc.³⁰ None of these acquired features, of course, are heritable and, therefore, they do not induce changes in the genome of the species.¹⁰ But they help the individual to prosper and to survive long enough to transfer to its offspring the same genes that endowed him/her with those advantageous traits.³³

For the technologist seeking to imitate Nature, the task ahead may thus be summarized as follows: Identify the genetic mutation rules and patterns that enable the formation, growth, and development of individual action units, which tend to seek and establish “beneficial” interactions with other (similar or dissimilar) units. Needless to say, deciding what constitutes a beneficial interaction may, in itself, be a formidable task.

Conclusion. Nature has evolved certain biological systems that are capable of processing and storage of information far more efficiently than any man-made device produced to date can accomplish. Progress in molecular biology and fundamental understanding of embryology, immune system function, the genetic basis of inheritance, etc., have created an impressive knowledge-base pertaining to the functioning of individual cells and many of their interactions.³⁶⁻³⁹ What seems to be lacking is an understanding of the principles of development of interaction among various units, and the organizational principles that allow useful interactions to develop, while providing flexibility for interconnections to modify themselves according to the environmental conditions.⁴⁰ These underlying principles are believed to be simple and elegant. Just as the Darwinian principles of evolutionary biology have provided a framework and a guiding light for biologists, the heretofore undiscovered principles of organization among the fundamental biological action units will enable information technologists to create new methods of information storage/processing that promise to be far more powerful than any method that is predicated on existing technologies.

Glossary

Allele. One of the variant forms of a gene at a particular locus, or location, on a chromosome. Different alleles produce variation in inherited characteristics such as hair color or blood type. In an individual, one form of the allele (the dominant one) may be expressed more frequently than another form (the recessive one).

Axon. The output cable of a neuron. A neuron usually has only one axon, although it often branches extensively.

Basket cell. In the cerebral cortex, a type of inhibitory nerve cell, often with a rather long axon, that extends to make multiple contacts on or near the cell bodies of other neurons.

Cerebral cortex. Often called simply “the cortex.” A pair of large folded sheets of nervous tissue, one on either side of the top of the head. It is sometimes divided into three main regions, called the neocortex (the largest part in primates), the paleocortex, and the archicortex.⁵

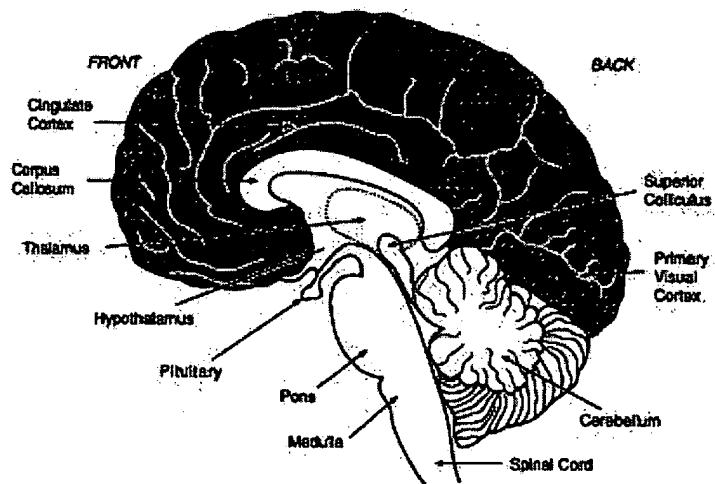
Corpus callosum. A very large tract of nerve fibers (axons), connecting the two halves of the cerebral cortex.⁵

Chromosome. One of the threadlike packages of genes and other DNA in the nucleus of a cell. Different organisms

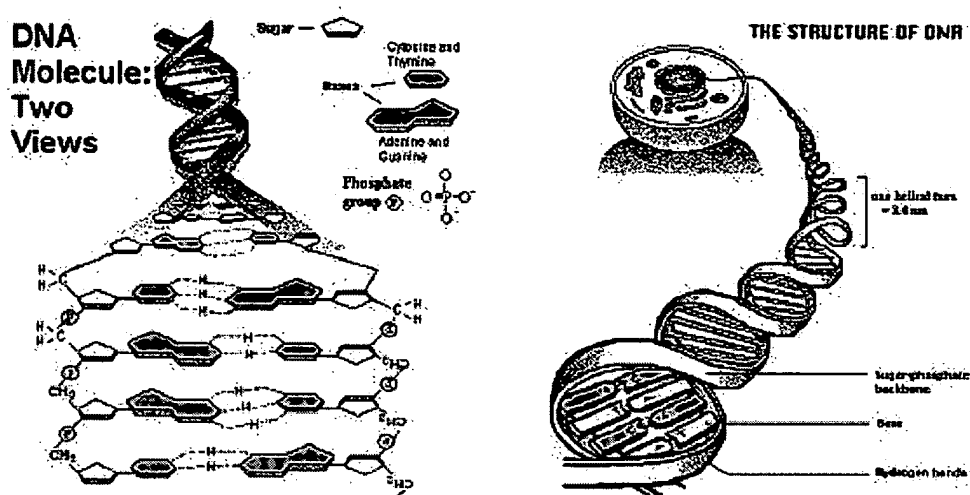
have different numbers of chromosomes. Humans have 23 pairs of chromosomes, 46 in all: 44 autosomes and two sex chromosomes (XX in females, XY in males). Each parent contributes one chromosome to each pair, so children get half of their chromosomes from their mothers and half from their fathers. Human beings have ~3.2 billion base pairs and ~34,000 genes in their 23 chromosome pairs. These genes are estimated to give rise to between 500,000 and 1,000,000 different proteins. The fruit-fly genome has 185 million base pairs and 13,601 genes. The genome of the roundworm has 97 million base pairs and 19,099 genes.

Dendrite. A treelike part of a nerve cell, dendrites receive signals from other nerve cells.

DNA (deoxyribonucleic acid). Built from nucleic acid bases, sugars, and phosphates, the double-stranded molecule is twisted into a helix. Each spiraling strand, comprised of a sugar-phosphate backbone and attached bases, is connected to a complementary strand by non-covalent hydrogen bonding between paired bases. The bases are adenine (A), thymine (T), cytosine (C) and guanine (G). A and T are connected by two, and G and C by three hydrogen bonds. The right-handed double helix has ~10 nucleotide pairs per helical turn. The double-helix structure of DNA was discovered in 1953 by James Watson and Francis Crick.



Major parts of the human brain, viewed from the inside. The cortex is shaded gray.⁵ (Copyright © 1994, Francis H. C. Crick.)



(Reproduced with permission from: <http://www.accessexcellence.org/>)

Enzyme. A protein, made from amino acids, acting as a catalyst in the intracellular chemical processes. In almost all cases enzymes are very large protein molecules, although some have smaller organic molecules attached to them. Enzymes help break down external molecules that are useful to the cells, and increase the chemical rates of interaction between various organic molecules. For example, the attachment of amino acids to transfer RNA (tRNA) is mediated by certain enzymes. (A catalyst accelerates a chemical reaction, but is unchanged at the end of it.)

Eukaryote. Eukaryotes include protozoa, green algae, yeasts, fungi, and all higher plants and animals. Eukaryotic cells have a nucleus and nuclear membrane. Their chromosomal DNA is permanently associated with a variety of proteins. The cells contain mitochondria and, in algae and higher plants, chloroplasts.^{9,10}

GABA. A small chemical whose proper name is gamma-amino-butyric acid. It is the major inhibitory neurotransmitter in the forebrain.⁵

Glutamate. A small organic chemical, the major excitatory neurotransmitter in the forebrain.⁵

Hebb's rule. Named after Canadian psychologist Donald O. Hebb. A type of alteration to the strength of a synapse that depends on both the presynaptic activity coming into the synapse and the activity (of some sort) of the receiving neuron on the postsynaptic side. It is important because the alteration to the synapse requires the association in time of two distinct forms of neural activity.⁵

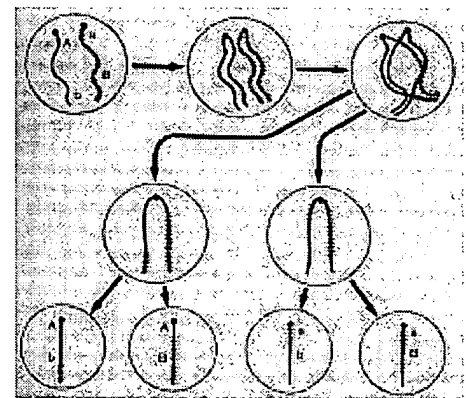
Lipid. A general descriptive term for certain organic molecules that have one water-loving end and one fat-loving end. A double layer of lipid makes up the lipid bilayer that forms the basis of most biological membranes, such as that which surrounds each cell.⁵

Meiosis. The process of cell division that results in the production of sperm or egg cells (gametes). During meiosis (lessening) each cell splits twice, but the chromosomes split only once, resulting in sperm or egg cells that contain only one chromosome from each pair of

chromosomes present in the original cell. The rules of Mendelian inheritance, however, cannot explain the behavior of linked genes (i.e., genes at different loci on the same chromosome). The relevant facts are illustrated in the figure below (only a single pair of homologous chromosomes is shown). The important events are as follows:

- (a) Each chromosome is replicated, so that it consists of two identical threads.
- (b) Pairs of homologous chromosomes come to lie side by side, forming bivalents. Each bivalent then consists of four similar threads.
- (c) The two members of a pair repel one another, but are held together at a few points, called chiasmata; there are two such chiasmata in the bivalent depicted in the figure.
- (d) There are two successive divisions of the nucleus, without further chromosome replication, giving rise to four nuclei (the gametic nuclei), each containing a single set of chromosomes.

In the figure, the chromosome derived from the father (paternal) is shown cross-hatched, to distinguish it from the maternal chromosome. In the four-strand and later stages, sections of chromosome which are copies of the original paternal chromosome are likewise shown cross-hatched, although it is not normally possible to distinguish maternal and paternal chromosomes under the microscope. The genetic consequence of all this is that if two genes are inherited from the same parent, they tend to be transmitted together, but if a recombination takes place between them, one is transmitted without the other.¹⁰



Recombination of a pair of 'homologous' chromosomes during meiosis.¹⁰

Meme. A word coined by Richard Dawkins in his best-selling book, *The Selfish Gene*.² Meme is the unit of cultural inheritance; it copies itself from brain to brain via any available means of copying. Memes can be good ideas, good tunes, memorable jokes, religious beliefs, popular poems, brilliant insights in mathematics, clever techniques for tying knots, etc. Those memes that spread do so because they are good at spreading; they don't have to be good or bad in any practical or utilitarian sense. Memes spread in a population because of the biologically valuable tendency of individuals to imitate. Memes not only leap from mind to mind by imitation in culture, but also they thrive, multiply, and compete within our minds. Whereas genes build the hardware, memes are the software; the coevolution of genes and memes is what may have driven the inflation of the human brain. (Adapted from R. Dawkins, *Unweaving The Rainbow*, Mariner Books, 1998.)

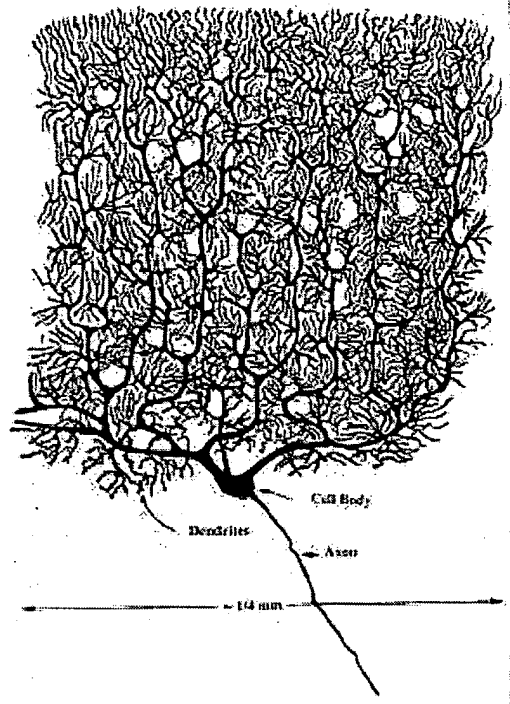
Mitosis. The process of cell division. In mitosis both pairs of chromosomes are duplicated, and each daughter cell receives a complete complement of chromosomes from its progenitor.

Neuron. The structural unit of the nervous system, contains a nucleus and cell body from which has grown a tree of many branches and twigs spreading in various directions.²⁵ A neuron typically has many dendrites and one axon. The dendrites branch and terminate in the vicinity of the cell body. In contrast, axons can extend to distant targets, more than a meter away in some

cases. Dendrites are rarely more than a millimeter long and often much shorter. The drawing on the right (after Ramón y Cajal, 1952) shows a purkinje cell of the human cerebellum, which receives about 80,000 synaptic inputs.²⁶

Prokaryote. A cellular organism (as a bacterium or a blue-green alga) that does not have a distinct nucleus or nuclear membrane. The DNA is arranged in a single ring-shaped chromosome with few associated proteins. There are no separate chloroplasts or mitochondria. Prokaryotes are the most primitive (and the most successful) form of life, dating back about 3.2 billion years.⁹

Protein. A molecule formed as a linear sequence of amino acids. Although there are many amino acids in nature, only 20 of them are used as the building blocks of proteins. These amino acids are the same in all living organisms. The basic end of one amino acid typically combines with the acidic end of another to form a lasting connection, and in the process releasing a molecule of water. Unlike DNA molecules, all proteins are single stranded. They usually fold on themselves under the influence of electrostatic forces to assume various geometrical shapes. Examples of amino acids used as building blocks of proteins are leucine, valine, proline, tryptophan, methionine, arginine, and phenylalanine.



A purkinje cell of the human cerebellum.²⁶

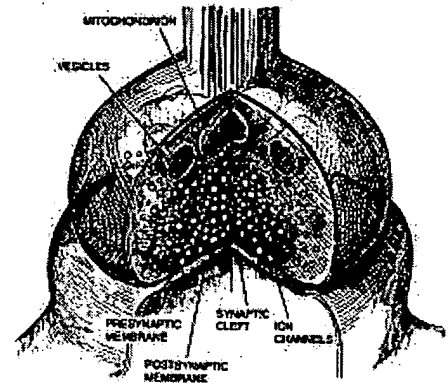
Hair and skin are made of a protein called keratin, which is also the crucial ingredient in biological materials like feathers and fingernails, hooves and horns. Another protein, collagen, is the stuff of connective tissues such as tendons, bones, and cartilage. Fibroin is the silk of cocoons and spider webs. Sclerolin forms the external skeletons of insects such as the firefly. Such proteins are *structural*, lending shape and form to life. Still other proteins are more *functional*, taking crucial roles in other processes within cells. Insulin is a well-known protein that regulates the metabolism of glucose, a natural sugar. Rhodopsin, in the retina of the eye, converts incoming light to ionic signals in the optic nerve. Myosin and actin provide the forces in vertebrate muscle cells. Dynein is an energy-inducing component of the cytoskeleton. Hemoglobin carries oxygen in the blood, and myoglobin (a close cousin) carries oxygen in muscle. Myoglobin has the chemical formula $C_{738}H_{1166}FeN_{203}O_{208}S_2$; the iron atom forms part of an active site, the heme group, that binds oxygen deep inside the molecule. Almost all enzymes – catalysts that speed biochemical reactions but are not consumed by them – are functional proteins. So are the transmembrane sodium-, potassium-, and calcium-channels in nerve membranes, which support the basic electrochemical activity of the brain.²⁶

Protozoan Any of a phylum or subkingdom (Protozoa) of minute protoplasmic acellular or unicellular animals which have varied morphology and physiology and often complex life cycles which are represented in almost every kind of habitat, and some of which are serious parasites of man and domestic animals (Webster's new dictionary). Protozoa are single-celled eukaryotes.

RNA (Ribonucleic acid). A chemical similar to a single strand of DNA. In RNA, the letter U, which stands for uracil, is substituted for T in the genetic code. Messenger RNA delivers DNA's genetic message to the cytoplasm of a cell where proteins are made. Three-letter sequences of messenger RNA, known as codons, code for specific amino acids. For example, UUU and UUC both code for phenylalanine, AUG codes for methionine, and UGG codes for tryptophan. Some amino acids have only one codon, others have more than one (for example, leucine has six). Three codons (UAA, UAG, and UGA) operate as “stops,” marking the end of a gene.

For each kind of coded triplet on mRNA, there exists a special transfer RNA molecule (tRNA), which will pair with just that triplet, and also a special activating enzyme, which will attach one kind of amino acid, and only one kind, to that transfer molecule. It is the function of the transfer molecules and activating enzymes to line up the amino acids opposite their appropriate triplets in the messenger molecule. The amino acids are then joined up end to end to form the completed protein. The triplet of bases on a transfer molecule which pairs with a codon on mRNA is called an anticodon.¹⁰

Synapse. The connection between one nerve cell and another. Most of these have a minute gap (between the terminal of the incoming axon and the recipient neuron) across which neurotransmitter molecules can diffuse. In some parts of the brain the dendrites of one cell can form a synapse on the dendrites of another, but such synapses are rare or absent in the cerebral cortex.⁵



Copyright © 1994, Francis H. C. Crick.

References

1. E. Schrödinger, *What is Life?* Cambridge University Press, London, 1944.
2. R. Dawkins, *The Selfish Gene*, Oxford University Press, London, 1976.
3. R. Dawkins, *The Blind Watchmaker*, W. W. Norton, New York, 1986.
4. D. E. Wooldridge, *The Machinery of the Brain*, McGraw-Hill, New York, 1963.
5. F. Crick, *The Astonishing Hypothesis*, Simon & Schuster, New York, 1994.
6. Special Issue of *Scientific American*, “Life, Death, and the Immune System,” September 1993.
7. T. Boon, “Teaching the Immune System to Fight Cancer,” *Scientific American*, pp82-89, March 1993.
8. K. Simons, H. Garoff, and A. Helenius, “How an animal virus gets into and out of its host cell,” *Scientific American*, February 1982.
9. C. de Duve, “The Birth of Complex Cells,” *Scientific American*, pp50-57, (April 1996).
10. John Maynard Smith, *The Theory of Evolution*, 3rd edition, Cambridge University Press, London, 1975.
11. S. L. McKnight, “Molecular Zippers in Gene Regulation,” *Scientific American*, pp54-64, April 1991.

12. R. Tjian, "Molecular Machines that Control Genes," *Scientific American*, pp54-61, February 1995.
13. J. Rennie, "DNA's New Twists," *Scientific American*, pp122-132, (March 1993).
14. F. S. Collins and K. G. Jegalian, "Deciphering the Code of Life," *Scientific American*, pp86-91, December 1999.
15. W. W. Gibbs, "Biotechnology: Gene Chips," *Scientific American*, pp33-34, February 2001.
16. J. C. Love and J. C. Ellenbogen, "Biochemical and DNA-based Nano-computers," MITRE Nanosystems Group, www.mitre.org/research/nanotech/biocomputers.html.
17. L. M. Adleman, "Molecular Computation of Solutions to Combinatorial Problems," *Science* **266**, 1021-1023, 11 November 1994.
18. L. M. Adleman, "Computing with DNA," *Scientific American* **279**, 54-61, August 1998.
19. T. A. Bass, "Gene Genie," *Wired Magazine*, p. 114, August 1995.
20. G. Kolata, "A Vat of DNA May Become a Vast Computer of the Future," *The New York Times*, p. C1, 11 April 1995.
21. R. R. Birge, "Protein-Based Three-Dimensional Memory," *American Scientist*, pp.348-355, July-August 1994.
22. R. R. Birge, "Protein-Based Computers," *Scientific American*, pp90-95, March 1995.
23. M. Hampp and D. Ziesel, "Mutated Bacteriorhodopsins," *IEEE Engrg. in Medicine and Biology* **13**, pp.67-74, and references therein.
24. K. B. Mullis, "The Unusual Origin of the Polymerase Chain Reaction," *Scientific American*, pp44-51, April 1990.
25. B. Katz, *Nerve, Muscle, and Synapse*, McGraw-Hill, New York, 1966.
26. A. Scott, *Stairway to the Mind*, Copernicus, An Imprint of Springer-Verlag, New York, 1995.
27. J-P. Changeux, "Chemical Signaling in the Brain," *Scientific American*, pp58-62, (November 1993).
28. W. J. Freeman, "The Physiology of Perception," *Scientific American*, pp.78-85, February 1991.
29. P. M. Milner, "The Mind and Donald O. Hebb," *Scientific American*, pp124-129, January 1993.
30. R. J. Greenspan, "Understanding the Genetic Construction of Behavior," *Scientific American*, pp72-77, April 1995.
31. W. Penfield and P. Perot, "The brain's record of auditory and visual experience – A final summary and discussion," *Brain* **86**, 595-696 (1963).
32. S. Blackmore, "The Power of Memes," *Scientific American*, pp64-73, October 2000.
33. Charles Darwin, *The Origin of Species*, Penguin books, 1968.
34. C. S. Goodman and M. J. Bastiani, "How Embryonic Nerve Cells Recognize One Another," *Scientific American*, pp49-57, December 1984.
35. T. Beardsley, "Getting Wired: New observations may show how neurons form connections," *Scientific American*, pp24-25, June 1999.
36. R. V. Miller, "Bacterial Gene Swapping in Nature," *Scientific American*, pp66-71, January 1998.
37. W. A. Haseltine, "Discovering Genes for New Medicines," *Scientific American*, pp92-97, March 1997.
38. W. French Anderson, "Gene Therapy," *Scientific American*, pp124-128, September 1995.
39. M. R. Capecchi, "Targeted Gene Replacement," *Scientific American*, pp52-59, March 1994.
40. J. E. LeDoux, "Emotion, Memory, and the Brain," *Scientific American*, pp50-57, June 1994.

EXHIBIT B

REPORTS

3. A. Hubert, R. Schäfer, *Magnetic Domains* (Springer, Berlin, 1998).
4. J. Raabe et al., *J. Appl. Phys.* **88**, 4437 (2000).
5. T. Shinjo, T. Okuno, R. Hassdorf, K. Shigeto, T. Ono, *Science* **289**, 930 (2000).
6. M. Pratzner et al., *Phys. Rev. Lett.* **87**, 127201 (2001).
7. S. Heinze et al., *Science* **288**, 1805 (2000).
8. A. Kubetzka, M. Bode, O. Pietzsch, R. Wiesendanger, *Phys. Rev. Lett.* **88**, 057201 (2002).
9. The Cr film thickness dependent reorientation transition may be caused by the surface anisotropy that dominates at small thickness.
10. M. Bode, M. Getzlaff, R. Wiesendanger, *Phys. Rev. Lett.* **81**, 4256 (1998).
11. O. Pietzsch, A. Kubetzka, M. Bode, R. Wiesendanger, *Phys. Rev. Lett.* **84**, 5212 (2000).
12. D. Wortmann, S. Heinze, Ph. Kurz, G. Bihlmayer, S. Blügel, *Phys. Rev. Lett.* **86**, 4132 (2001).
13. The spin polarizations of the tip and the sample are defined as $P_{s,T}(E) = (n_{s,T}^{\uparrow}(E) - n_{s,T}^{\downarrow}(E)) / (n_{s,T}^{\uparrow}(E) + n_{s,T}^{\downarrow}(E))$ with $n_{s,T}^{\uparrow}(E)$ and $n_{s,T}^{\downarrow}(E)$ being the density of states of majority and minority electrons.
14. O. Pietzsch, A. Kubetzka, D. Haude, M. Bode, R. Wiesendanger, *Rev. Sci. Instr.* **71**, 424 (2000).
15. U. Gradmann, G. Liu, H. J. Elmers, M. Przybylski, *Hyperfine Interactions* **57**, 1845 (1990).
16. The tiny bright spots randomly distributed in both images are caused by adsorbates that appear as dips in the topograph (Fig. 2A) and locally change the value of C in Eq. 1; i.e., the signals are not of magnetic origin.
17. The simulations were performed with the OOMMF program, release 1.2 alpha 2 (<http://math.nist.gov/oommf/>) using a lateral grid with a cell size of 1 nm². The shape as well as the averaged island height of 8 nm was taken into account. Because the height of the Fe islands of about 8 nm is only 2.5 to 3 times larger than $\sqrt{A/K_d}$, the magnetization was assumed to be independent of the z coordinate [3, 18].
18. U. Gradmann, J. Korecki, G. Waller, *Appl. Phys. A* **39**, 101 (1986).
19. The small deviation between experimental and simulated data at $d_{vc} = 10$ to 15 nm in the presence of external fields is caused by the lateral movement of the vortex core (Fig. 4B), which has not been considered in the simulations. At the rim of the Fe island, the magnetization tilts stronger into the direction of H_{ext} than in the island center.
20. Financial support from the BMBF (grant no. 13N7647) and SFB 508 is gratefully acknowledged.

20 June 2002; accepted 4 September 2002

Microfluidic Large-Scale Integration

Todd Thorsen,¹ Sebastian J. Maerkl,¹ Stephen R. Quake^{2*}

We developed high-density microfluidic chips that contain plumbing networks with thousands of micromechanical valves and hundreds of individually addressable chambers. These fluidic devices are analogous to electronic integrated circuits fabricated using large-scale integration. A key component of these networks is the fluidic multiplexor, which is a combinatorial array of binary valve patterns that exponentially increases the processing power of a network by allowing complex fluid manipulations with a minimal number of inputs. We used these integrated microfluidic networks to construct the microfluidic analog of a comparator array and a microfluidic memory storage device whose behavior resembles random-access memory.

In the first part of the 20th century, engineers faced a problem commonly called the “tyranny of numbers”: there is a practical limit to the complexity of macroscopically assembled systems (*1*). Using discrete components such as vacuum tubes, complex circuits quickly became very expensive to build and operate. The ENIAC I, created at the University of Pennsylvania in 1946, consisted of 19,000 vacuum tubes, weighed 30 tons, and used 200 kW of power. The transistor was invented at Bell Laboratories in 1947 and went on to replace the bulky vacuum tubes in circuits, but connectivity remained a problem. Although engineers could in principle design increasingly complex circuits consisting of hundreds of thousands of transistors, each component within the circuit had to be hand-soldered—an expensive, labor-intensive process. Adding more components to the circuit decreased its reliability, as even a single cold solder joint rendered the circuit useless.

In the late 1950s, Kilby and Noyce solved the “tyranny of numbers” problem for electronics by inventing the integrated circuit. By fab-

ricating all of the components out of a single semiconductor—initially germanium, then silicon—Kilby and Noyce created circuits consisting of transistors, capacitors, resistors, and their corresponding interconnects in situ, eliminating the need for manual assembly. By the mid-1970s, improved technology led to the development of large-scale integration (LSI): complex integrated circuits containing hundreds to thousands of individual components.

Microfluidics offers the possibility of solving similar system integration issues for biology and chemistry. However, devices to date have lacked a method for a high degree of integration, other than simple repetition. Microfluidic systems have been shown to have potential in a diverse array of biological applications, including biomolecular separations (*2–4*), enzymatic assays (*5, 6*), the polymerase chain reaction (*6, 7*), and immunohybridization reactions (*8, 9*). These are excellent individual examples of scaled-down processes of laboratory techniques, but they are also stand-alone functionalities, comparable to a single component within an integrated circuit. The current industrial approach to addressing true biological integration has come in the form of enormous robotic fluidic workstations that take up entire laboratories and require considerable expense, space, and labor, reminiscent of the macroscopic approach to circuits consisting of massive vacuum

tube-based arrays in the early 20th century.

There are two basic requirements for a microfluidic LSI technology: monolithic microvalves that are leakproof and scalable, and a method of multiplexed addressing and control of these valves. We previously presented a candidate plumbing technology that allows fabrication of chips with monolithic valves made from the silicone elastomer polydimethylsiloxane (PDMS) (*10*). Here, we describe a microfluidic multiplexing technology and show how it can be used to fabricate silicone devices with thousands of valves and hundreds of individually addressable reaction chambers. As possible applications of fluidic LSI technology, we describe a chip that contains a high-density array of 1000 individually addressable picoliter-scale chambers that serves as a microfluidic memory storage device, and a second chip analogous to an array of 256 comparators.

Our microfluidic multiplexors are combinatorial arrays of binary valve patterns that increase the processing power of a network by allowing complex fluid manipulations with a minimal number of controlled inputs. Although simple microfluidic arrays can be designed in which each fluid channel is controlled by its own individual valve control channel, this non-integrated strategy cannot be efficiently scaled up and thus faces problems similar to those encountered in pre-LSI electronic circuits. In contrast, multiplexors work as a binary tree (Fig. 1) and allow control of n fluid channels with only $2 \log_2 n$ control channels. We fabricated the devices with established multilayer soft lithography techniques (*11*), using two distinct layers. The “control” layer, which harbors all channels required to actuate the valves, is situated on top of the “flow” layer, which contains the network of channels being controlled. All biological assays and fluid manipulations are performed on the flow layer. A valve is created where a control channel crosses a flow channel. The resulting thin membrane in the junction between the two channels can be deflected by hydraulic actuation. Simultaneous addressing of multiple noncontiguous flow channels is accomplished by fabricating control

¹Biochemistry and Molecular Biophysics Option, ²Department of Applied Physics, California Institute of Technology, Pasadena, CA 91125, USA.

*To whom correspondence should be addressed. E-mail: quake@caltech.edu

channels of varying width while keeping the dimension of the flow channel fixed ($100\ \mu\text{m}$ wide and $9\ \mu\text{m}$ high). The pneumatic pressure in the control channels required to close the flow channels scales with the width of the control channel, making it simple to actuate $100\ \mu\text{m} \times 100\ \mu\text{m}$ valves at relatively low pressures ($\sim 40\ \text{kPa}$) without closing off the $50\ \mu\text{m} \times 100\ \mu\text{m}$ crossover regions, which have a higher actuation threshold.

By using multiplexed valve systems, the power of the binary system becomes evident: Only 20 control channels are required to specifically address 1024 flow channels. This allows a large number of elastomeric microvalves to perform complex fluidic manipulations within these devices, and the interface between the device and the external environment is simple and robust. Introduction of fluid into these devices is accomplished through steel pins inserted into holes punched through the silicone. Unlike micromachined devices made out of hard materials with a high Young's modulus (12), silicone is soft and forms a tight seal around the input pins, readily accepting pressures of up to $300\ \text{kPa}$ without leakage. Computer-controlled external solenoid valves allow actuation of multiplexors, which in turn allow complex addressing of a large number of microvalves.

Using two multiplexors as fluidic design elements, we designed a microfluidic memory storage device with 1000 independent compartments and 3574 microvalves, organized as an addressable 25×40 chamber microarray (Fig. 2A). The large multiplexor valve systems allow each chamber of the matrix to be individually addressed and isolated, and only 22 outside control interconnects are needed. Fluid can be

loaded into the device through a single input port, after which control layer valves then act as gates to compartmentalize the array into chambers with a volume of $250\ \text{pL}$ ($2.5 \times 10^{-4}\ \mu\text{L}$). Individual chamber addressing is accomplished through flow channels that run parallel to the sample chambers and use pressurized liquid under the control of the row and column multiplexors to flush the chamber contents to the output (Fig. 2B).

This device adds a level of complexity to

previous microfluidic plumbing, in that there are two successive levels of control—the multiplexors actuate valve control lines, which in turn actuate the valves themselves. The design and mechanics of the microfluidic array are similar to random-access memory (RAM). Each set of multiplexors is analogous to a memory address register, mapping to a specific row or column in the matrix. Like dynamic RAM, the row and column multiplexors have unique functions. The row multiplexor is used for fluid

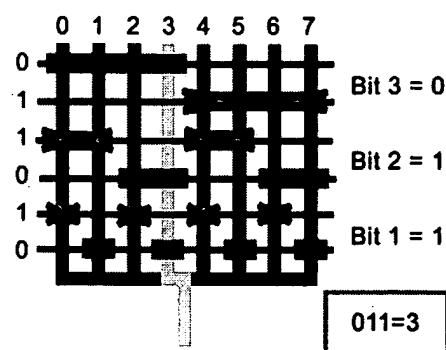


Fig. 1. Microfluidic multiplexor operational diagram. The blue lines represent flow channels containing the fluid of interest; the red lines represent control lines that can be hydraulically actuated. Valves are formed at the intersection of the wide part of a control channel with a flow channel. The actuation pressure is chosen so that only the wide membranes are fully deflected. Each combination of open and closed valves in the multiplexor selects for a single channel, so that n flow channels can be addressed with only $2 \log_2 n$ control channels. The pattern illustrated here has all channels closed except the cyan channel.

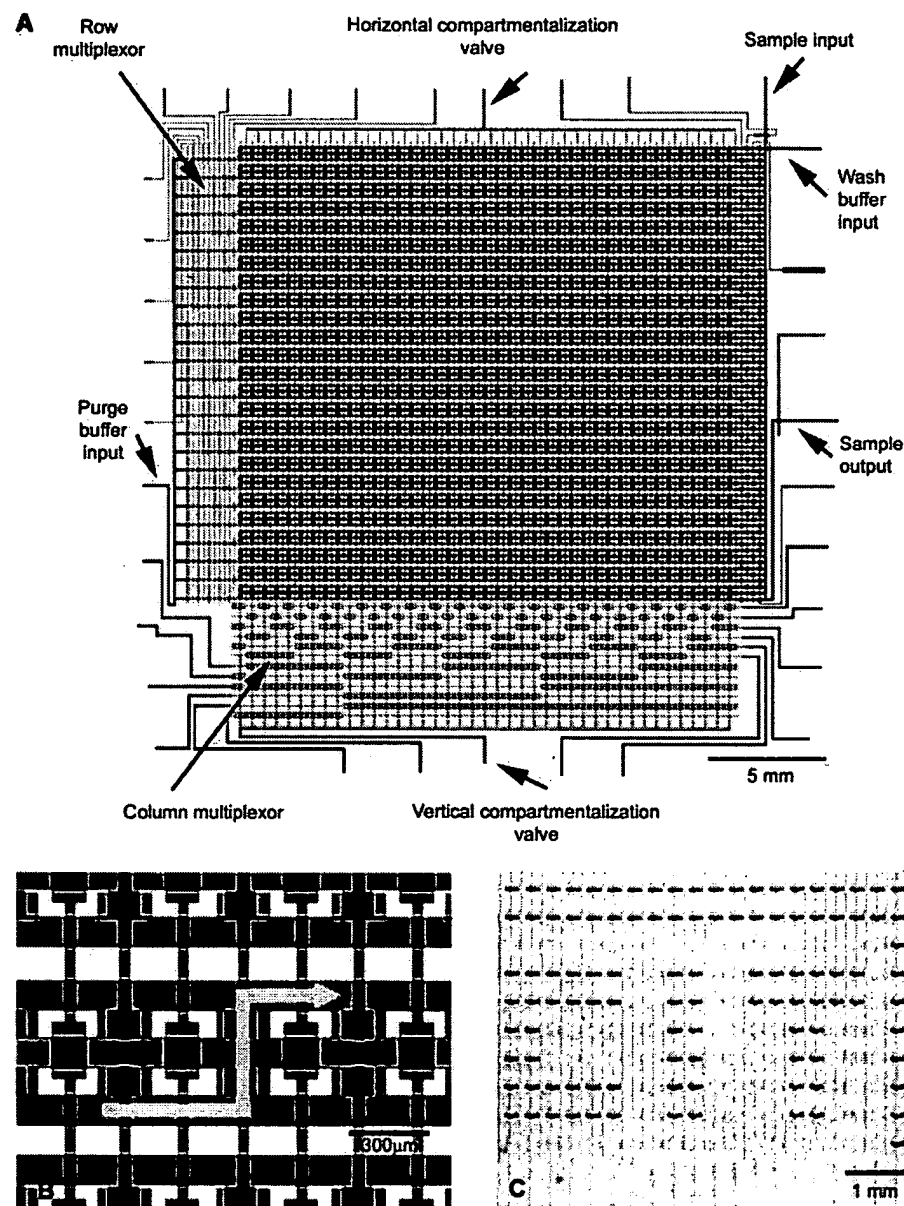


Fig. 2. (A) Mask design for the microfluidic memory storage device. The chip contains an array of 25×40 chambers, each of which has a volume of $\sim 250\ \text{pL}$. Each chamber can be individually addressed using the column and row multiplexors. The contents of each memory location can be selectively programmed to be either blue dye (sample input) or water (wash buffer input). (B) Purging mechanics for a single chamber within a selected row of the chip. Each row contains three parallel microchannels. A specific chamber is purged as follows: (i) Pressurized fluid is introduced in the purge buffer input. (ii) The row multiplexor directs the fluid to the lower channel of the selected row. (iii) The column multiplexor releases the vertical valves of the chamber, allowing the pressurized fluid to flow through the chamber and purge its contents. (C) Demonstration of microfluidic memory display: Individual chambers are selectively purged to spell out "C I T".

REPORTS

trafficking; it directs the fluid responsible for purging individual compartments within a row and refreshes the central compartments (memory elements) within a row, analogous to a RAM word line. The column multiplexor acts in a fundamentally different manner, controlling the vertical input-output valves for specific central compartments in each row. The column multiplexor, located on the flow layer, begins to operate when the vertical containment valve on the control layer is pressurized to close off the

entire array. It is activated with its valves deflected upward into the control layer to trap the pressurized liquid in the entire vertical containment valve array. A single column is then selected by the multiplexor, and the pressure on the vertical containment valve is released to open the specified column, allowing it to be rapidly purged by pressurized liquid in a selected row.

To demonstrate the functionality of the microfluidic memory storage device, we loaded

the central memory storage chambers of each row with dye (2.4 mM bromophenol blue in sodium citrate buffer, pH 7.2) and proceeded to purge individual chambers with water to spell out "C I T". Because the readout is optical, this memory device also essentially functions as a fluidic display monitor (Fig. 2C). A key advantage of the plumbing display is that once the picture is set, the device consumes very little power.

We designed a second device containing 2056 microvalves (Fig. 3A), which is capable of performing more complex fluidic manipulations. In this case, two different reagents can be separately loaded, mixed pairwise, and selectively recovered, making it possible to perform distinct assays in 256 subnanoliter reaction chambers and then recover a particularly interesting reagent. The microchannel layout consists of four central columns in the flow layer consisting of 64 chambers per column, with each chamber containing ~750 pL of liquid after compartmentalization and mixing. Liquid is loaded into these columns through two separate inputs under low external pressure (~20 kPa), filling up the array in a serpentine fashion. Barrier valves on the control layer function to isolate the sample fluids from each other and from channel networks on the flow layer used to recover the contents of each individual chamber. These networks function under the control of a multiplexor and several other control valves (13). The elastomeric valves are analogous to electronic switches, serving as high-impedance barriers for fluidic trafficking. To demonstrate the device plumbing, we filled the fluid input lines with two dyes to illustrate the process of loading, compartmentalization, mixing, and purging of the contents of a single chamber within a column (Fig. 3B). Each of the 256 chambers on the chip can be individually addressed and its respective contents recovered for future analysis using only 18 connections to the outside world, illustrating the integrated nature of the microfluidic circuit.

We used this chip as a microfluidic comparator to test for the expression of a particular enzyme. A population of bacteria is loaded into the device, and a fluorogenic substrate system provides an amplified output signal in the form of a fluorescent product. An electronic comparator circuit is designed to provide a large output signal when the input signal exceeds a reference threshold value. An operational amplifier amplifies the input signal relative to the reference, forcing it to be high or low. In our microfluidic comparator, the nonfluorescent resorufin derivative Amplex Red functions as the reference signal. The input signal consists of a suspension of *Escherichia coli* expressing recombinant cytochrome c peroxidase (CCP); the enzyme serves as a chemical amplifier in the circuit (Fig. 4A). The cells and substrate are loaded into separate input channels with the central mixing barrier closed in each column and com-

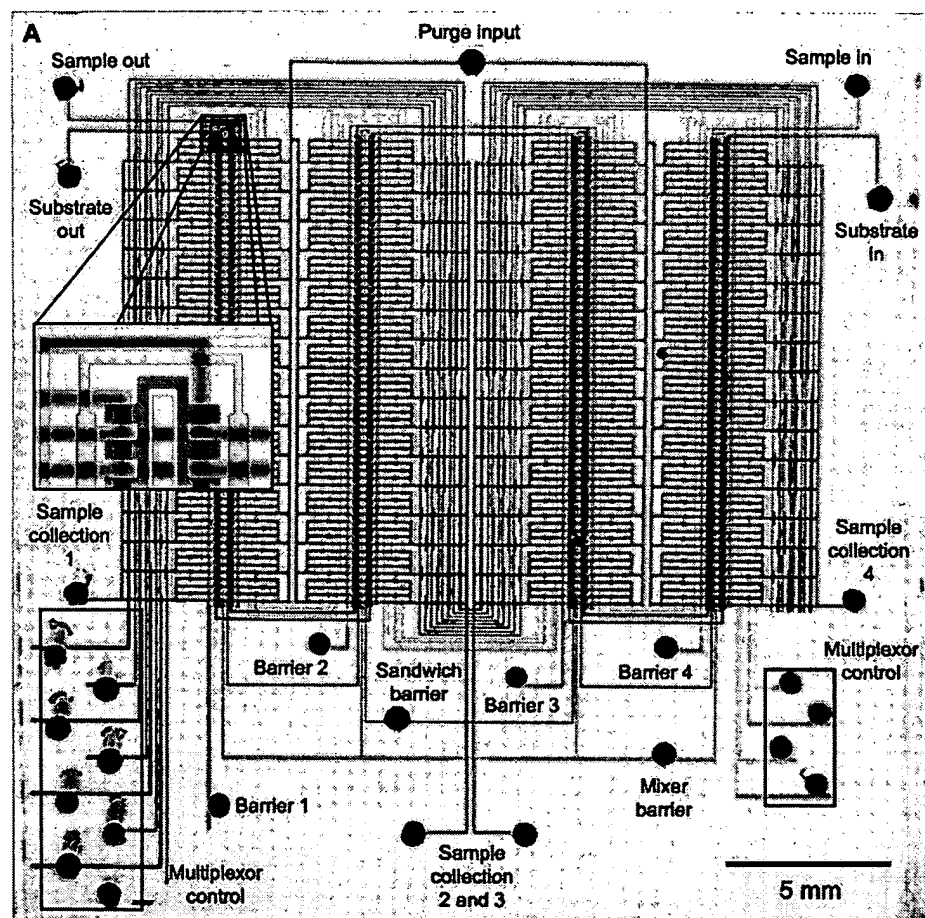


Fig. 3. (A) Optical micrograph of the microfluidic comparator chip. The various inputs have been loaded with food dyes to visualize the channels and sub-elements of the fluidic logic. **(B)** Set of optical micrographs showing a portion of the comparator in action. A subset of the chambers in a single column is imaged. Elastomeric microvalves enable each of the 256 chambers on the chip to be independently compartmentalized, mixed pairwise, and selectively purged with the blue and yellow solutions.

partmentalized exactly like the procedure illustrated for the blue and orange dyes. The cell dilution (1:1000 of confluent culture) creates a median distribution of ~0.2 cells per compartment, as verified by fluorescence microscopy. The barrier between the substrate and cell sub-compartments is opened for a few minutes to allow substrate to diffuse into the compartments containing the cell mixture. The barrier is then closed to reduce the reaction volume and improve the signal/noise ratio for the reaction. After a 1-hour incubation at room temperature, the chip is scanned (excitation wavelength λ_{ex} = 532 nm, emission filter centered at λ_{em} = 590 nm with a 40-nm bandwidth) with a modified DNA microarray scanner (GenePix 4000B, Axon Instruments, Union City, CA). The presence of one or more CCP-expressing cells in an individual chamber produces a strong amplified output signal, because Amplex Red is converted to the fluorescent compound resorufin while the signal in the compartments with no cells remains low (Fig. 4B). To verify that the output signal is a function of CCP activity, we performed a similar experiment using a heterogeneous mixture of *E. coli* expressing either CCP or enhanced green fluorescent protein (eGFP). The amplified output signal was only dependent on the number of CCP-expressing cells in an individual chamber (Fig. 4C).

Recovery from the chip can be accomplished by selecting a single chamber and then purging the contents to a collection output. Each column in the chip has a separate output, enabling a chamber from each column to be collected without cross-contamination. To illustrate the efficacy of the collection process, we loaded a dilute phosphate-buffered saline (PBS) solution of *E. coli* expressing eGFP into the chip. After compartmentalization, approximately every second chamber contained a bacterium. Using an inverted light microscope (Olympus IX50) equipped with a mercury lamp and GFP filter set, single eGFP cells were identified with a 20 \times objective and their respective chambers were purged. The purged cells were collected from the outputs with polyetheretherketone (PEEK) tubing, which has low cell adhesion properties. Isolations of single eGFP-expressing bacteria were confirmed by visualization of the collected liquid samples under a 40 \times oil immersion lens (using the fluorescence filter set) and by observations of single colony growth on Luria-Bertani broth (LB) plates inoculated with the recovered bacteria. Because single molecules of DNA can be effectively manipulated in elastomeric microfluidic devices (14), it is possible that in future applications individual molecules or molecular clusters will be selected or manipulated in this fashion.

The performance of an electronic comparator is not ideal—for example, there is a finite noise floor, there are absolute voltage and cur-

rent limitations, there are leakage currents at the inputs, and so forth. Some of these limits result from intrinsic properties of the materials used for the devices, whereas others depend on fabrication tolerances or design limitations. The performance of integrated fluidic circuits suffers from similar imperfections. Fluidic circuits fabricated from PDMS will not be compatible with all organic solvents—in particular, many of the nonpolar solvents present a problem. This issue can be addressed by the use of chemically resistant elastomers. Cross-contamination in microfluidic circuits is analogous to leakage currents in an electronic circuit and is a complex phenomenon. A certain amount of contamination will occur as a result of diffusion of small molecules through the elastomer itself. This effect is not an impediment with the organic dyes and other small molecules used in the examples in this work, but at some level and performance requirement it may become limiting. There are also surface effects due to non-specific adhesion of molecules to the channel walls; these can be minimized by either passive (15, 16) or chemical (17, 18) modifications to the PDMS surface. Cross-contamination is also a design issue whose effects can be mitigated by the design of any particular circuit. In the 256-well comparator chip, we introduced a compensation scheme by which each of the

four columns has a separate output in order to prevent cross-contamination during the recovery operation. As fluidic circuit complexity increases, similar design rules will evolve that will yield high performance despite the limitations of the particular material and fabrication technology being used.

The computational power of the memory and comparator chips is derived from the ability to integrate and control many fluidic elements on a single chip. For example, the multiplexor component allows specific addressing of an exponentially large number of independent chambers. This permits selective manipulation or recovery of individual samples, an important requirement for high-throughput screening and other enrichment applications. It may also be a useful tool for chemical applications involving combinatorial synthesis, where the number of products also grows exponentially. Another example of computational power is the ability to segment a complex or heterogeneous sample into manageable subsamples, which can be analyzed independently (as shown in the comparator chip) and can be used in other applications to subdivide a homogeneous sample into aliquots that can be analyzed separately with independent chemical methods. On the basis of the utility of these examples, we believe that other concepts developed for electronic inte-

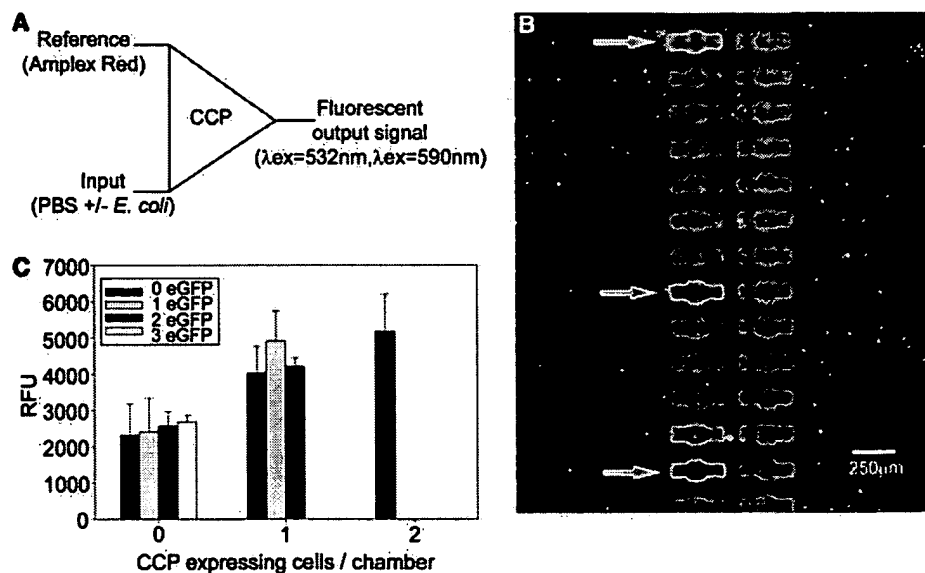


Fig. 4. (A) Schematic diagram of the microfluidic comparator logic using an enzyme and fluorogenic substrate. When an input signal chamber contains cells expressing the enzyme CCP, nonfluorescent Amplex Red is converted to the fluorescent product, resorufin. In the absence of CCP, the output signal remains low. (B) Scanned fluorescence image of the chip in comparator mode. Left side: Dilute solution of CCP-expressing *E. coli* in sterile PBS (137 mM NaCl, 2.68 mM KCl, 10.1 mM Na_2HPO_4 , and 1.76 mM KH_2PO_4 , pH 7.4) after mixing reaction with Amplex Red. Arrows indicate chambers containing single cells. Chambers without cells show low fluorescence. The converted product (resorufin) is clearly visible as green signal. Right side: Uncatalyzed Amplex Red substrate. (C) A micro-high-throughput screening comparator: Effect of heterogeneous mixture of eGFP-expressing control cells and CCP-expressing cells on output signal. The resorufin fluorescence measurement (λ_{ex} = 532 nm, λ_{em} = 590 nm) was made in individual comparator chambers containing *E. coli* cells expressing either eGFP or CCP. There is a strong increase in signal only when CCP-expressing cells are present, with little effect on the signal from eGFP-expressing cells. The vertical axis is relative fluorescence units (RFU); error bars represent one standard deviation from the median RFU.

grated circuits can be usefully transferred to chemical and biochemical analysis and processing in microfluidic devices.

The two devices presented here illustrate that complex fluidic circuits with nearly arbitrary complexity can be fabricated using microfluidic LSI. The rapid, simple fabrication procedure combined with the powerful valve multiplexing can be used to design chips for many applications, ranging from high-throughput screening applications to the design of new liquid display technology. The scalability of the process makes it possible to design robust microfluidic devices with even higher densities of functional valve elements, so that the ultimate complexity and application are limited only by one's imagination.

References and Notes

1. T. R. Reid, *The Chip: How Two Americans Invented the Microchip and Launched a Revolution* (Simon & Schuster, New York, 1984).
2. A. G. Hadd, S. C. Jacobson, J. M. Ramsey, *Anal. Chem.* **71**, 5206 (1999).
3. D. J. Harrison *et al.*, *Science* **261**, 895 (1993).
4. P. C. H. Li, D. J. Harrison, *Anal. Chem.* **69**, 1564 (1997).
5. A. G. Hadd, D. E. Raymond, J. W. Haliwell, S. C. Jacobson, S. C. Ramsey, *Anal. Chem.* **69**, 3407 (1997).
6. E. T. Lagally, I. Medintz, R. A. Mathies, *Anal. Chem.* **73**, 565 (2001).
7. J. Khandurina *et al.*, *Anal. Chem.* **72**, 2995 (2000).
8. E. Eteshola, D. Leckband, *Sens. Actua. B* **72**, 129 (2001).
9. J. Wang, A. Ibanez, M. P. Chatrathi, A. Escarpa, *Anal. Chem.* **73**, 5323 (2001).
10. M. A. Unger, H.-P. Chou, T. Thorsen, A. Scherer, S. R. Quake, *Science* **288**, 113 (2000).
11. Master molds for the microfluidic channels are made by spin-coating positive photoresist (Shipley SJR 5740) on silicon (9 μm high) and patterning them with high-resolution (3386 dpi) transparency masks. The channels on the photoresist molds are rounded at 120°C for 20 min to create a geometry that allows full valve closure. The devices were fabricated by bonding together two layers of two-part cure silicone (Dow Corning Sylgard 184) cast from the photoresist molds. The bottom layer of the device, containing the flow channels, is spin-coated with 20:1 part A:B Sylgard at 2500 rpm for 1 min. The resulting silicone layer is $\sim 30\ \mu\text{m}$ thick. The top layer of the device, containing the control channels, is cast as a thick layer ($\sim 0.5\ \text{cm}$ thick) with 5:1 part A:B Sylgard using a separate mold. The two layers are initially cured for 30 min at 80°C. Control channel interconnect holes are then punched through the thick layer (released from the mold), after which it is sealed, channel side down, on the thin layer, aligning the respective channel networks. Bonding between the assembled layers is accomplished by curing the devices for an additional 45 to 60 min at 80°C. The resulting multilayer devices are cut to size and mounted on RCA cleaned No. 1, 25 mm square glass coverslips, or onto coverslips spin-coated with 5:1 part A:B Sylgard at 5000 rpm, and cured at 80°C for 30 min, followed by incubation at 80°C overnight.
12. L. Buchallot, E. Farnault, M. Hoummady, H. Fujita, *Jpn. J. Appl. Phys.* **2**, 36, L794 (1997).
13. The control channels are dead end-filled with water before actuation with pneumatic pressure; the compressed air at the ends of the channels is forced into the bulk porous silicone. This procedure eliminates gas transfer into the flow layer upon valve actuation, as well as evaporation of the liquid contained in the flow layer.
14. H. P. Chou, C. S. Spence, A. Scherer, S. R. Quake, *Proc. Natl. Acad. Sci. U.S.A.* **96**, 11 (1999).
15. V. Linder, E. Verpoorte, W. Thormann, N. F. de Rooij, H. Sigrist, *Anal. Chem.* **73**, 4181 (2001).
16. T. Yang, S. Jung, H. Mao, P. S. Cremer, *Anal. Chem.* **73**, 165 (2001).
17. D. C. Duffy, J. C. MacDonald, O. J. A. Schueller, G. M. Whitesides, *Anal. Chem.* **70**, 4974 (1998).
18. B. A. Grzybowski, R. Haag, N. Bowden, G. M. Whitesides, *Anal. Chem.* **70**, 4645 (1998).
19. We thank M. Enzelberger, C. Hansen, M. Adams, and

M. Unger for helpful discussions. Supported in part by Army Research Office grant DAAD19-00-1-0392 and by the DARPA Bioflips program.

5 August 2002; accepted 17 September 2002

Published online 26 September 2002;

10.1126/science.1076996

Include this information when citing this paper.

Self-Assembly of Highly Phosphorylated Silaffins and Their Function in Biosilica Morphogenesis

Nils Kröger,¹ Sonja Lorenz,² Eike Brunner,² Manfred Sumper^{1*}

Silaffins are uniquely modified peptides that have been implicated in the biogenesis of diatom biosilica. A method that avoids the harsh anhydrous hydrogen fluoride treatment commonly used to dissolve biosilica allows the extraction of silaffins in their native state. The native silaffins carry further posttranslational modifications in addition to their polyamine moieties. Each serine residue was phosphorylated, and this high level of phosphorylation is essential for biological activity. The zwitterionic structure of native silaffins enables the formation of supramolecular assemblies. Time-resolved analysis of silica morphogenesis in vitro detected a plastic silaffin-silica phase, which may represent a building material for diatom biosilica.

Diatoms are unicellular, eukaryotic algae that produce a wide variety of nanopatterned silica structures in a genetically controlled manner (1). Biosilica morphogenesis is an extremely rapid process that is accomplished under mild physiological conditions, thus exceeding the capabilities of present-day materials engineering. Elucidating the molecular mechanisms of biosilica formation is therefore expected to help researchers devise new synthetic routes to nanostructured silica materials (2, 3).

Recently, silaffins and long-chain polyamines have been identified as constituents of biosilica and shown to accelerate silica formation from a monosilicic acid solution in vitro (4, 5). On the basis of the physicochemical properties of polyamines, a phase separation model has been proposed that is able to explain the nanopatterning of biosilica (6). Silaffins are peptides that carry numerous posttranslational modifications. The silaffins from *Cylindrotheca fusiformis* contain lysine residues that are linked by their ϵ -amino groups to long-chain polyamines (7). It is due to this modification that silaffin peptides can precipitate silica nanospheres at mildly acidic pH conditions (4), which likely represent the physiologically relevant pH range (8).

Previously, the extraction and purification of silaffins has been achieved by the treatment of diatom shells with anhydrous hydrogen fluoride

(HF), a treatment known to cleave O-glycosidic and phosphate ester bonds (9). However, silaffins contain a high percentage of hydroxyamino acids, candidates for posttranslational modifications. Therefore, the silaffins extracted to date may have lost functional modifications of hydroxyamino acids. To address this concern and to be able to study silica precipitation activities of native silaffins, we developed a gentler method for silaffin extraction. We found that native silaffins carry additional modifications that proved to be essential for biosilica formation.

It has previously been shown that an acidic aqueous solution of ammonium fluoride is capable of dissolving diatom biosilica (10) by converting silica into soluble ammonium hexafluorosilicate. When *C. fusiformis* cell walls are treated with an aqueous solution of ammonium fluoride at pH = 5, the complete set of silaffins and long-chain polyamines is solubilized. The apparent molecular masses of all silaffin species present in the aqueous ammonium fluoride extract are shifted toward higher molecular masses, indicating the existence of HF-labile modifications (11). An abundant peptide (apparent molecular mass of 6.5 kD) was purified from the ammonium fluoride extract (Fig. 1, lane 1) (12). After an additional treatment with anhydrous HF, this peptide exhibited a much higher electrophoretic mobility and comigrated in SDS-polyacrylamide gel electrophoresis (SDS-PAGE) with silaffin-1A (Fig. 1, lanes 2, 3), which has previously been characterized from HF-extracted cell walls (4). NH_2 -terminal amino acid sequencing of this material resulted in the sequence SSXXSGSYSGS (G, Gly; S, Ser; Y, Tyr; X, modified lysine residue)

¹Lehrstuhl Biochemie I, ²Institut für Biophysik und Physikalische Biochemie, Universität Regensburg, 93053 Regensburg, Germany.

*To whom correspondence should be addressed. E-mail: manfred.sumper@vkl.uni-regensburg.de

EXHIBIT C

Information Storage and Retrieval using Macromolecules as Storage Media

M. Mansuripur[†], P.K. Khulbe[†], S.M. Kuebler[‡], J.W. Perry^{††}, M.S. Giridhar[†],
J. Kevin Erwin[†], Kibyoung Seong[†], Seth Marder^{††}, and N. Peyghambarian[†]

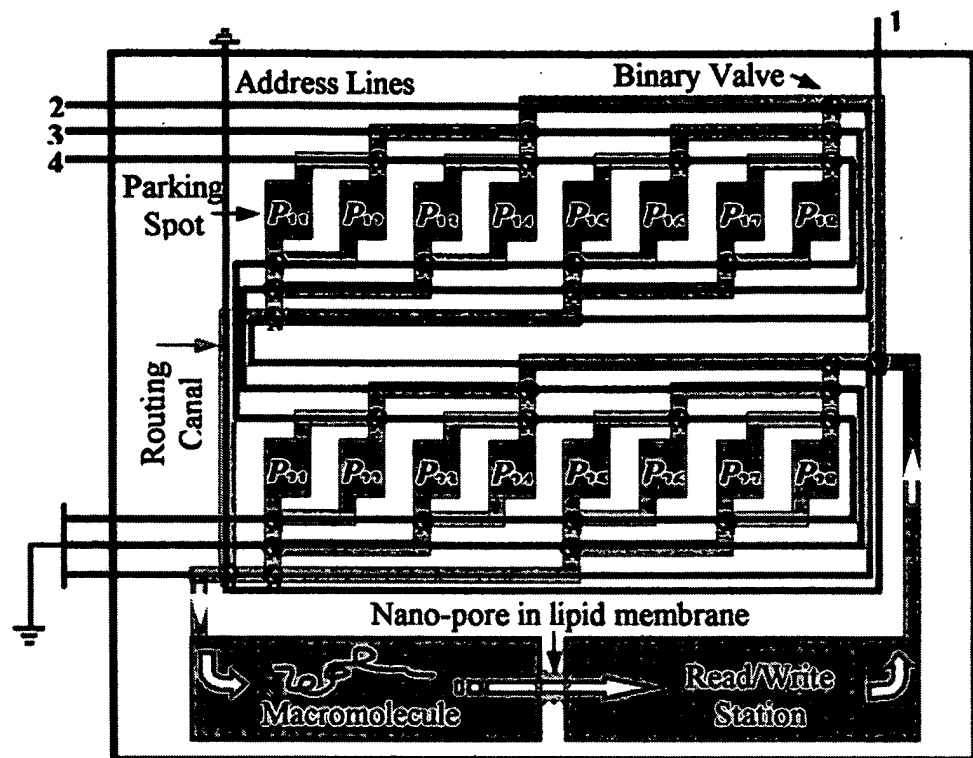
[†]Optical Sciences Center and [‡]Department of Chemistry, University of Arizona,
Tucson, Arizona, 85721 <masud@u.arizona.edu>

Introduction. To store information at extremely high-density and data-rate, we propose to adapt, integrate, and extend the techniques developed by chemists and molecular biologists for the purpose of manipulating biological and other macromolecules. In principle, volumetric densities in excess of 10^{21} bits/cm³ can be achieved when individual molecules having dimensions below a nanometer or so are used to encode the 0's and 1's of a binary string of data. In practice, however, given the limitations of electron-beam lithography, thin film deposition and patterning technologies, molecular manipulation in submicron dimensions, etc., we believe that volumetric storage densities on the order of 10^{16} bits/cm³ (i.e., petabytes per cubic centimeter) should be readily attainable, leaving plenty of room for future growth. The unique feature of the proposed new approach is its focus on the feasibility of storing bits of information in individual molecules, each only a few angstroms in size. Nature provides proof of principle for this type of data storage through the ubiquitous existence of DNA and RNA molecules, which encode the blueprint of life in four nucleic acids: Adenine, Guanine, Cytosine, and Thymine/Uracil.¹ These macromolecules are created on an individual basis by enzymes and protein-based machinery of biological cells, are stable over a fairly wide range of temperatures, are read and decoded by ribosomes (for the purpose of manufacturing proteins), and can be readily copied and stored under normal conditions.

Advances in molecular biology over the past decades have made it possible to create (i.e., write) artificial molecules of arbitrary base-sequence, and also to decode (i.e., read) such sequences. These techniques can now be adapted and extended in the service of a new generation of ultra-high-density data storage devices. Macromolecular strings (representing blocks of data several megabytes long) can be created on-demand, then stored in secure locations (parking spots) on a chip. These data blocks can then be retrieved by physically moving them to decoding stations (also located on the same chip), subjecting them to a "read" process, then returning them to their secure parking spots until the next request for readout is issued, or until there is a call for their removal and destruction (i.e., erasure).

System architecture. The required parking lots as well as the read, write, and erase stations for data encoding/decoding can be fabricated in integrated fashion on the surface of a glass substrate using lithography or other surface patterning techniques. Transfer of the molecular data blocks between the parking lots and the various read/write/erase stations may be achieved via controlled electric-field gradients, optical tweezers, micro-fluidic pumps, opto-electronic micro-motors, etc. Schemes for high-resolution reading and writing of data blocks utilizing electro-photo-chemical processes will be described in the following sections. As for achievable data rates, although the individual read/write stations envisioned in this paper may not be able to handle data rates in excess of a few megabits per second, the possibility of using multiple parallel read/write stations should enable the proposed scheme to compete with the projected data-transfer-rates in conventional optical and magnetic storage technologies.

Fig. 1. Diagram showing the patterned surface of the proposed data storage chip. Once a parking spot is selected, its macromolecular content will be transferred to the read/write station under the influence of an applied electric voltage (i.e., electro-phoretic transfer). Following the completion of the read/write operation, the macromolecule is returned to its designated spot.



A possible implementation of the proposed storage device, depicted schematically in Fig. 1, shows a specific arrangement of 16 parking spots in conjunction with a single read/write station on a chip surface. Various canals are etched on this surface to connect the parking spots to the read/write chamber. Binary valves placed at the cross-sections of these canals control the flow direction (a possible design of a binary μ -valve appears in Fig. 2). Controlling the valves is accomplished by means of electrical signals on four separate lines.

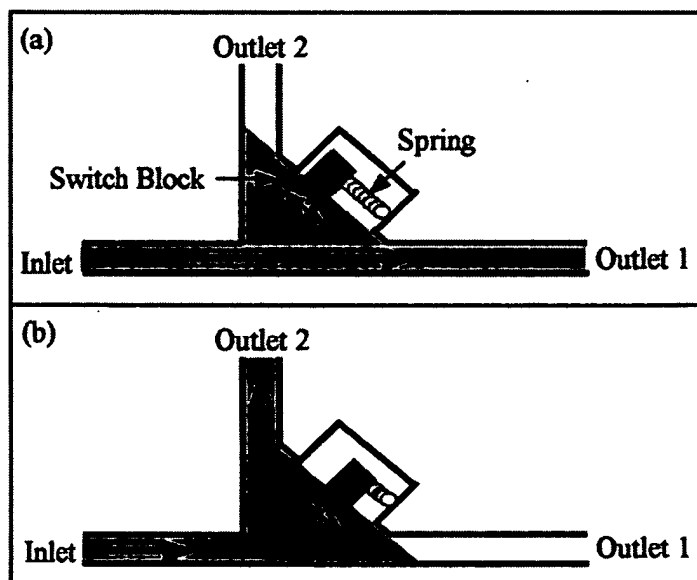


Fig. 2. Binary valve channels the flow of incoming liquid toward either of outlets 1 or 2. An electronic command signal is required to compress the spring and pull the switch block to the lower position. When the command signal is removed, the spring relaxes to its initial state, thus redirecting the flow toward outlet 1.

The aforementioned binary scheme of grouping the parking spots results in a number of address lines that is the base-2 logarithm of the number of spots. One can thus address over a million parking spots on the surface of a chip with only 20 lines. If each parking spot, for example, occupies a

$10 \times 10 \mu\text{m}^2$ area, one million such spots will cover a square centimeter of the chip surface. With the macromolecule stored in each parking spot corresponding to a mega-byte block of user data, the areal density of storage on the chip will approach 1 TeraBytes/ cm^2 . Moreover, if

the parking spots (and associated read/write/erase stations) are stacked in 10 μm -thick layers, the volumetric capacity of the envisioned device will easily reach 1 PetaBytes/cm³.

Macromolecular readout by translocation through a nano-pore. The diagrams in Fig. 3 depict a method of readout by translocation through a nano-pore.² As different nucleotides pass through the pore, they hamper the flow of the ionic current differently. Fluctuations in current blockage are due to differences in the size and/or charge of the various nucleotides. Given a sufficient SNR, one should be able to uniquely identify the base sequence of the translocated DNA molecule by analyzing the electrolytic current waveform.

Fig. 3. (a) Nano-pore created in a lipid membrane by α -hemolysin proteins. The bilayer separates two sections of a buffer solution. With 100 mV applied across the bilayer, ~ 120 pA of ionic current flows through the nano-pore. (b) DNA strand passing through the nano-pore partially blocks the ionic current.

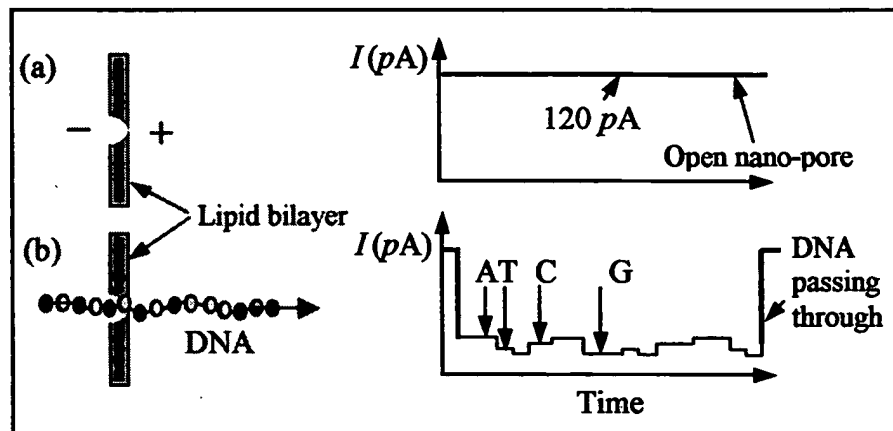


Figure 4 is a schematic diagram of a setup for conducting DNA translocation experiments in our laboratory. The system consists of two $\sim 150\mu\text{L}$ wells, machined in a teflon block and connected by a U-shaped tube. One end of the U-tube has a sleeve of teflon tubing, which is rapidly tapered to provide a $\sim 40\mu\text{m}$ diameter aperture. Ag-AgCl electrodes are inserted into both wells. To form a lipid bilayer at the $40\mu\text{m}$ aperture, one must first prime the aperture by applying $5\mu\text{L}$ of a $200\mu\text{g/mL}$ solution of lipid (diphytanoyl phosphatidylcholine) dissolved in spectroscopic-grade hexane. The primer is then allowed to evaporate in a mild stream of nitrogen gas. The wells on both sides of the aperture are subsequently filled with a buffer solution (1.0M KCl + 10 mM HEPES/KOH, pH = 8.0). At this point, a relatively large ionic current passes through the aperture (several hundred nA at 120mV applied voltage). To form a lipid bilayer, a single bristle of a fine brush is dipped in a $\sim 3\text{mg/mL}$ lipid solution (dissolved in spectroscopic-grade hexadecane), then brushed across the aperture. Formation of the bilayer is indicated by the blockage of the ionic current (several hundred G Ω resistance between the Ag-AgCl electrodes).

Once a stable bilayer has been created, 80 ng of α -hemolysin in $2\mu\text{L}$ buffer solution is added to the well that contains the aperture and, subsequently, a 120mV potential is applied to the electrodes. Typically, a single ion-channel consisting of seven α -hemolysin molecules self-assembles in a time span of 5-20 minutes; successful self-assembly is indicated by an abrupt increase of the electrolytic current to 120pA. To avoid formation of multiple ion-channels, the excess α -hemolysin is removed by perfusion with $\sim 20\text{mL}$ of fresh buffer. (In our experiments, individual ion-channels were stable for up to six hours.) With an ion-channel formed stably within the lipid bilayer, we add single-stranded DNA molecules (ssDNA) to the cis (i.e.,

grounded) side of the bilayer. Ionic current through the α -hemolysin channel is then monitored using a HEKA EPC-9 patch-clamp amplifier in voltage clamp mode. Data were acquired at 5 μ s intervals and filtered with a low-pass Bessel filter (bandwidth = 5, 20, or 100 kHz). The passage of DNA strands through the ion-channel is indicated by transient blockage events in the ionic current. Several hundred blockage events were recorded and analyzed for poly-A, poly-C, and poly-AC samples.

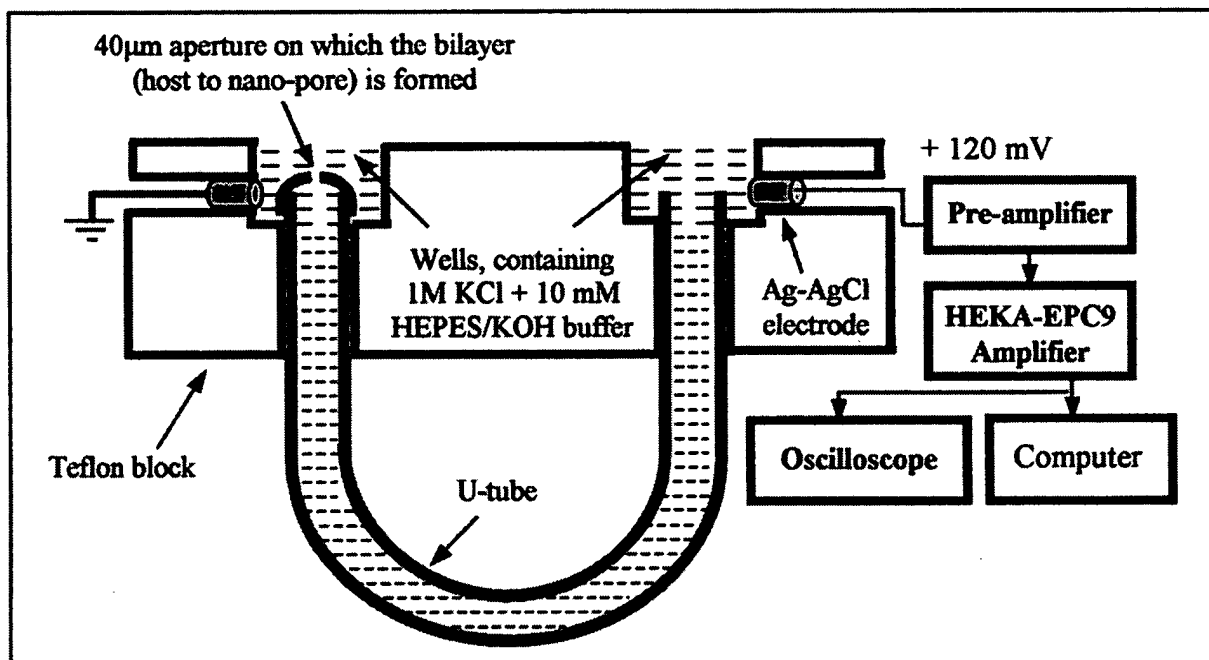


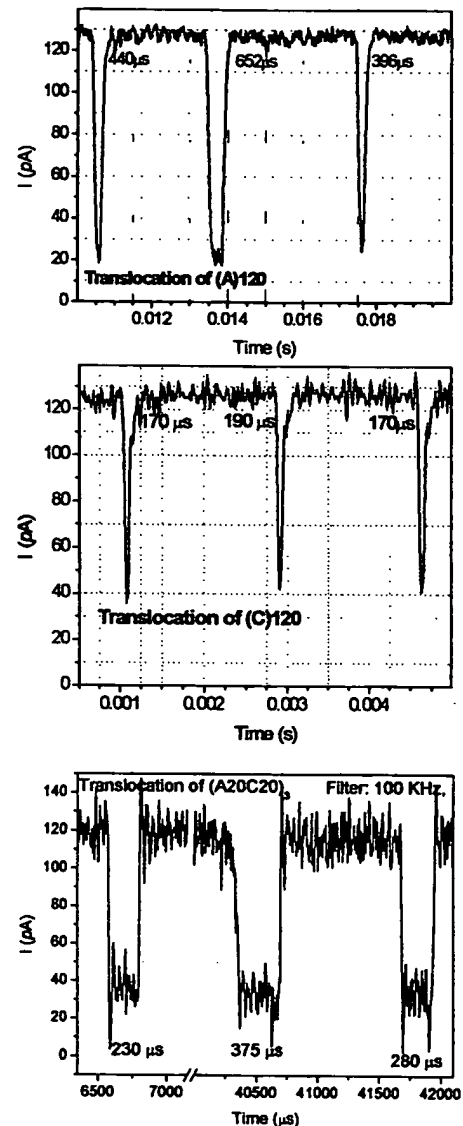
Figure 4. Experimental setup for translocation studies. Two 150 μ L wells are machined in a teflon block and connected via a U-shaped teflon tube (inner diameter \sim 1.6 mm). The electrodes, which have a silver core with AgCl coating, are connected to a constant voltage source.

Translocation experiments conducted with poly-A, poly-C, and poly-AC. Size-purified ssDNA samples were purchased from *Midland Certified Reagents* (Midland, TX). In a typical experiment these DNA samples were added to the cis chamber (concentration \sim 200 nM/mL). About one hundred translocation events were recorded separately for each type of DNA sample. Figure 5(a) shows three typical translocation events of a ssDNA molecule having 120 continuous adenine bases (A-120). Similarly, Fig. 5(b) shows translocation events associated with DNA molecules having 120 cytosine bases (C-120). A comparison of these events reveals that adenine bases block the ionic current more than the cytosine bases. During translocation of A-120, the ionic current drops from 130 pA to 20 pA, whereas in the case of C-120 the current drops from 128 pA to 40 pA. The experiments also reveal that cytosine bases translocate faster than the adenine bases. The translocation speed for C-120 is \sim 1.5 μ s/base, while that for A-120 is either \sim 3.3 μ s/base or \sim 5.4 μ s/base, depending on the direction of translocation (5' \rightarrow 3' or 3' \rightarrow 5'). It is thus seen that 120-base poly-A and poly-C molecules of ssDNA can be readily distinguished from each other by measuring the magnitude and/or duration of the current blockage.

To determine whether smaller segments of A-bases can be distinguished from similar segments of C-bases, we conducted experiments with a 120-base sample having the periodic sequence 20A-20C-20A-20C-20A-20C. The results, depicted in Fig. 5(c), indicate that alternate 20A and 20C segments cannot be distinguished via current blockage measurements. This is because the length of the α -hemolysin ion-channel in the translocation direction is $\sim 10\text{nm}$, while each DNA base is only 0.34nm long. At any given time, therefore, there are roughly 30 bases in the channel, which explains why 20-base-long sequences are irresolvable with this particular ion-channel.

For a single DNA base, the transit time through the ion-channel can be as short as $1.5\mu\text{s}$ (poly-C). To resolve alternate segments, each consisting of ~ 30 identical bases, one should monitor the ionic current with a fairly wide-band amplifier. (The highest bandwidth presently available to us is 100kHz .) One must also try to substantially reduce the noise, whose magnitude, as present measurements indicate, rises in proportion to the area of the lipid bilayer. Reduction of the buffer volume (by reducing the chamber size) should also be an effective way of reducing the noise.

Figure 5. Three typical current blockade events during translocation of purified, 120-base-long ssDNA molecules. (a) With poly-A strands, the ionic current drops from $\sim 130\text{ pA}$ to $\sim 20\text{ pA}$, with a blockade duration of either $\sim 400\mu\text{s}$ or $\sim 650\mu\text{s}$, depending on the direction of travel of the molecule. (b) With poly-C strands, the current drops from $\sim 128\text{ pA}$ to $\sim 40\text{ pA}$; the blockade duration per cytosine base is $\sim 1.5\mu\text{s}$. (c) With ssDNA having 20 bases of adenine alternating with 20 bases of cytosine the current drops from $\sim 120\text{ pA}$ to $\sim 35\text{ pA}$ during translocation. (The poly-AC data is recorded at a larger amplifier bandwidth, which results in a higher noise level compared to the poly-A and poly-C data.)



Micro-chamber fabrication. To realize high storage density and high data-rate, the system architecture requires miniaturized parking lots for storing macromolecular strings (i.e., data blocks) as well as integrated read/write/erase stations for data encoding and decoding. We have fabricated a prototype read station on a microscope slide using 2-photon-initiated polymerization of certain resins.³ A $150\mu\text{m}$ -thick photo-polymerizable resin is coated on a glass slide, upon which the desired pattern is written by tracing a highly focused laser beam. The localized photo-excitation cross-links the resin, thereby reducing the solubility of the exposed material, and the desired 3D structure is obtained by washing away the unexposed resin. Our read station made by this method consists of two adjacent chambers, $150 \times 150 \times 150\mu\text{m}^3$, separated by a partition wall, as shown in Fig. 6. The partition wall has a $20\mu\text{m}$ diameter hole at its center, upon which a lipid bilayer must be formed to host the nano-pore.

This and similar structures will be used for DNA translocation experiments in the next phase of our program. Figure 7 shows the water-filling and subsequent drying of the chambers. The first frame of Fig. 7 shows a micro-pipette, in contact with the partition wall, injecting water into one of the chambers. The third frame shows the over-filled section of the chamber with a convex surface (water meniscus). As the water evaporates, the meniscus first becomes flat at $t = 14\text{s}$, then concave at $t = 22\text{s}$. The chamber eventually dries up at $t = 31\text{s}$.

Figure 6. (Top) Two views of the micro-chamber fabricated by 2-photon lithography. Each chamber is approximately $150\mu\text{m}$ on the side, and about $150\mu\text{m}$ deep. (Bottom) Two views of the μ -hole in the wall separating the two chambers. The μ -hole is $\sim 20\mu\text{m}$ in diameter and is located $\sim 20\mu\text{m}$ above the chambers' floor.

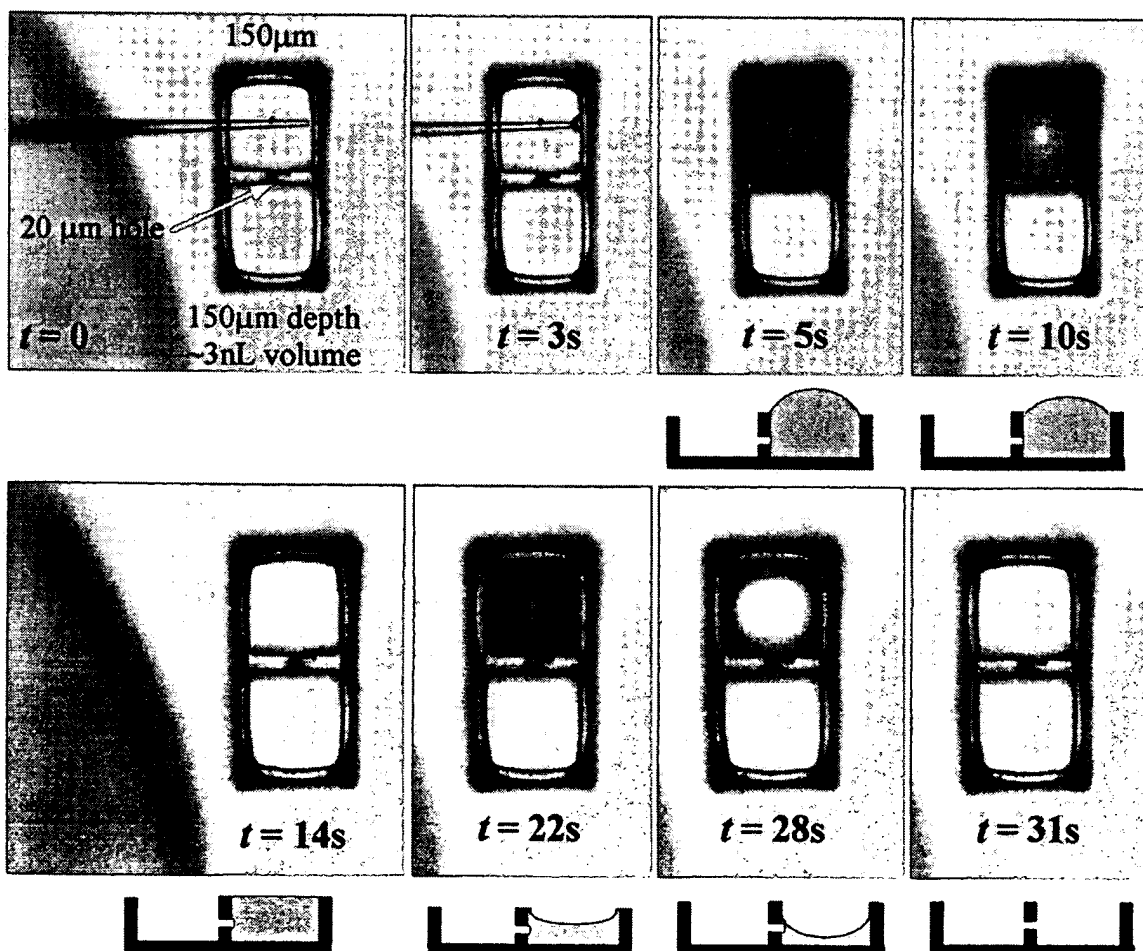
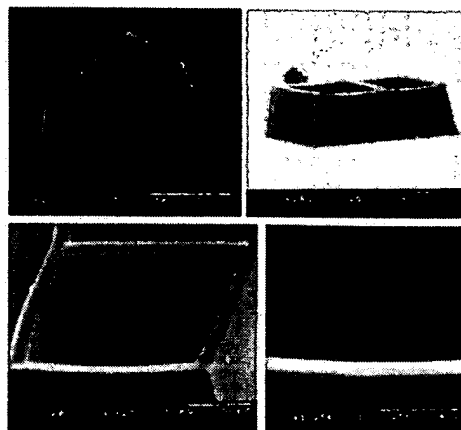
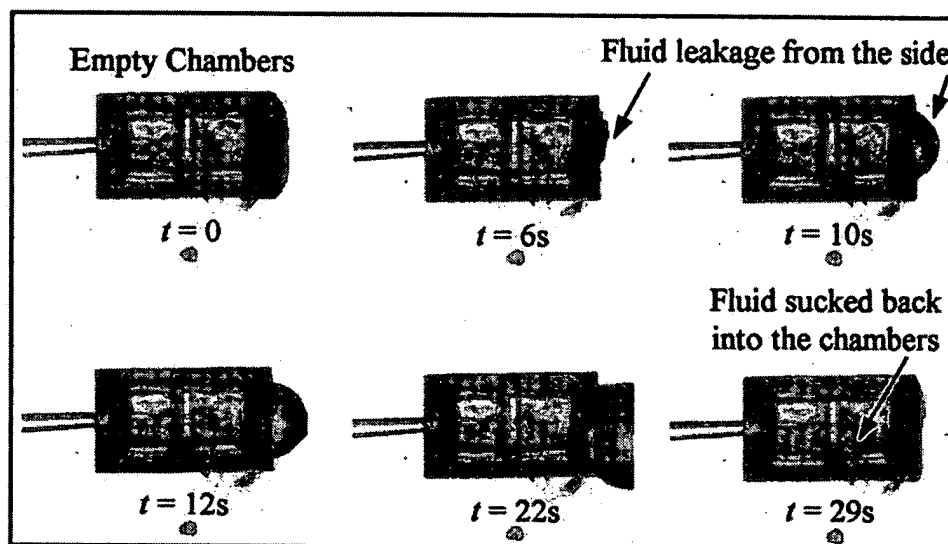


Figure 7. Water filling sequence of a μ -chamber. A μ -pipette (inner diameter $\sim 10\mu\text{m}$) is brought in contact with a side-wall to release its content. Each μ -chamber can hold $\sim 3\text{nL}$ of water, which completely evaporates in less than 30 seconds at the room temperature under normal conditions.

To prevent evaporation, we fabricated covered (i.e., roofed) chambers having access holes on the end walls to enable μ -pipette insertion. One such device is shown in Fig. 8, where the μ -pipette is seen to be inserted through the wall on the left-hand side. The injected liquid goes through the central hole and starts leaking out of the hole on the right-hand wall. (The water continues to leak until the pressure inside the pipette falls to the atmospheric level.) The leaked droplets can be sucked back into the chambers, as shown in the last frame of Fig. 8.

The above μ -chambers' shortcomings for use as DNA read stations include: (i) high evaporation rates, (ii) structural fragility that renders them unusable after only a few experiments, and (iii) difficulty of attaching electrodes, performing perfusion, or accessing the central hole to paint the lipid bilayer and/or to inject the nano-pore proteins.

Figure 8. Filling a covered μ -chamber with water via a μ -pipette inserted through a hole on a side-wall. The last frame at $t = 29\text{s}$ shows the liquid being sucked back into the chambers.



Device fabrication using polydimethylsiloxane (PDMS). To integrate the read station with the parking spots, to reduce the noise level during readout (which noise arises in part from the large chamber size as well as the large surface area of the lipid membrane), and in order to overcome the aforementioned shortcomings of the 2-photon micro-fabrication method, we attempted to miniaturize the read station of Fig. 1 using several alternative techniques. In one such attempt, we built a device by molding a PDMS block, as can be seen in Fig. 9. The liquid PDMS precursor was poured into a cup, and thin tungsten wires were placed in the liquid at locations where it was desired to create channels, chambers, and access ports. The cup was then heated to $\sim 50^\circ\text{C}$, where it was kept for two to three hours until the PDMS solidified. Subsequently the tungsten wires were removed, the device was fitted with Ag-AgCl electrodes, and the chambers were filled with a buffer solution via μ -pipettes. In Fig. 9 the read station has two cylindrical chambers connected by a tapered aperture (diameter $\sim 150\mu\text{m}$) over which a lipid bilayer will be formed. There are two ports for Ag-AgCl electrodes, and a perfusion line to flush out the excess α -hemolysin after ion-channel formation. The inset to Fig. 9 is a photograph showing the central section of the fabricated device.

Capillary pipettes used for filling and emptying the above chambers were made by a commercial pipette-puller (Narishige Scientific Instruments), which has a circular filament that heats the center of a glass capillary to the glass softening temperature. Both ends of the

capillary are held by iron rods and pulled by an adjustable magnetic force. The length of the pipette taper is controlled by adjusting the filament current (heating) and the magnetic force. The capillaries used in the above experiments have an inner tip diameter in the range of 10 to 50 μm ; the taper length is in the 1-2cm range.

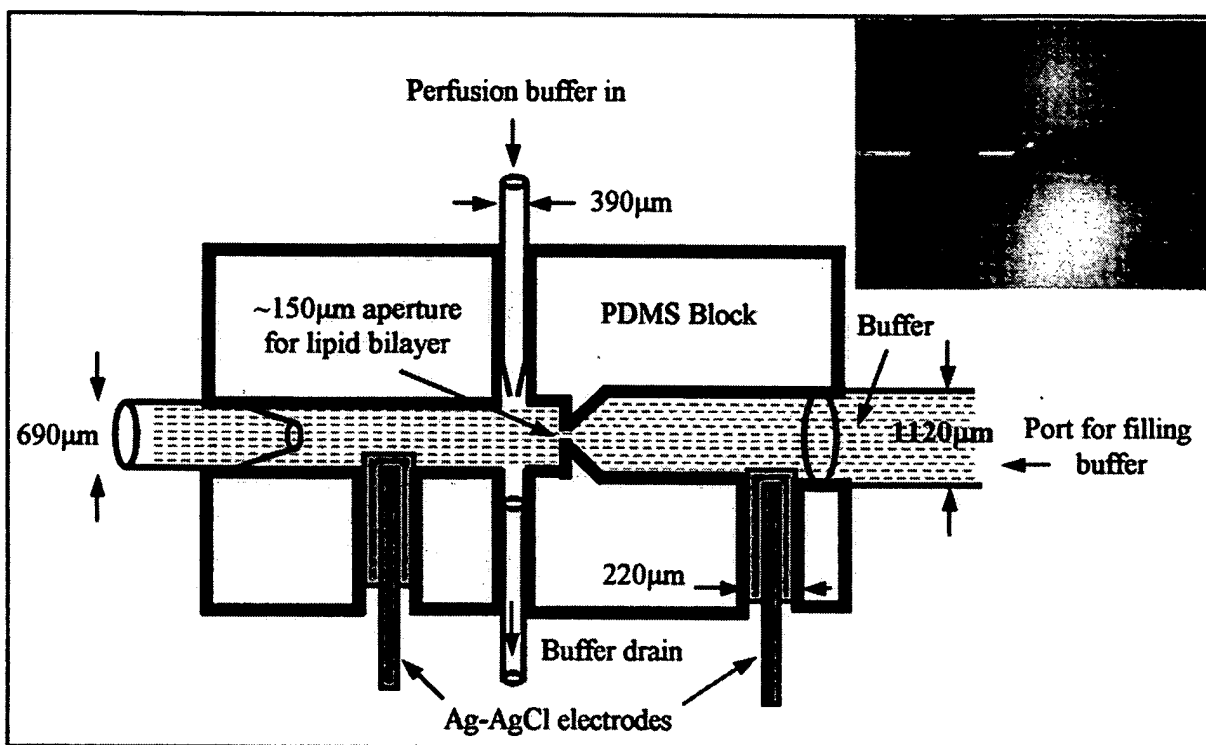


Figure 9. Miniature DNA read station made by molding a PDMS block. The inset is a photograph of the central region of the fabricated read station.

Femto-second pulse laser micro-machining of a glass substrate. An alternative method of fabricating the μ -channels and μ -chambers of the read station is based on femto-second pulse laser micro-machining of a glass substrate. Figure 10 shows scanning electron micrographs of a polished glass slide on which three chambers, each $\sim 180 \times 180 \times 100 \mu\text{m}^3$, have been written. One of these chambers is used for calibration purposes, while the other two are connected via a μ -hole at the center of the partition wall. The micro-machining was done with a (time-averaged) laser power of 18mW, wavelength = 1.66 μm , pulse width = 150 fs, repetition rate = 1 kHz, focusing lens NA = 0.25. For the chambers the scanning speed was 50 $\mu\text{m/s}$, with 4 μm steps in the XY -plane and 15 μm steps in the depth direction Z . The conical hole at the center of the partition wall has a diameter $\sim 40 \mu\text{m}$ on the front side and $\sim 10 \mu\text{m}$ on the rear side. The hole was created by focusing the laser beam through the edge of the glass slide onto the partition wall that separates the chambers. Creating the hole required a scanning speed in the range of 1-5 $\mu\text{m/s}$, with 2 μm steps in the X , Y , and Z -directions. In practice, these μ -chambers must be covered with a solid PDMS layer to prevent the evaporation of liquids.

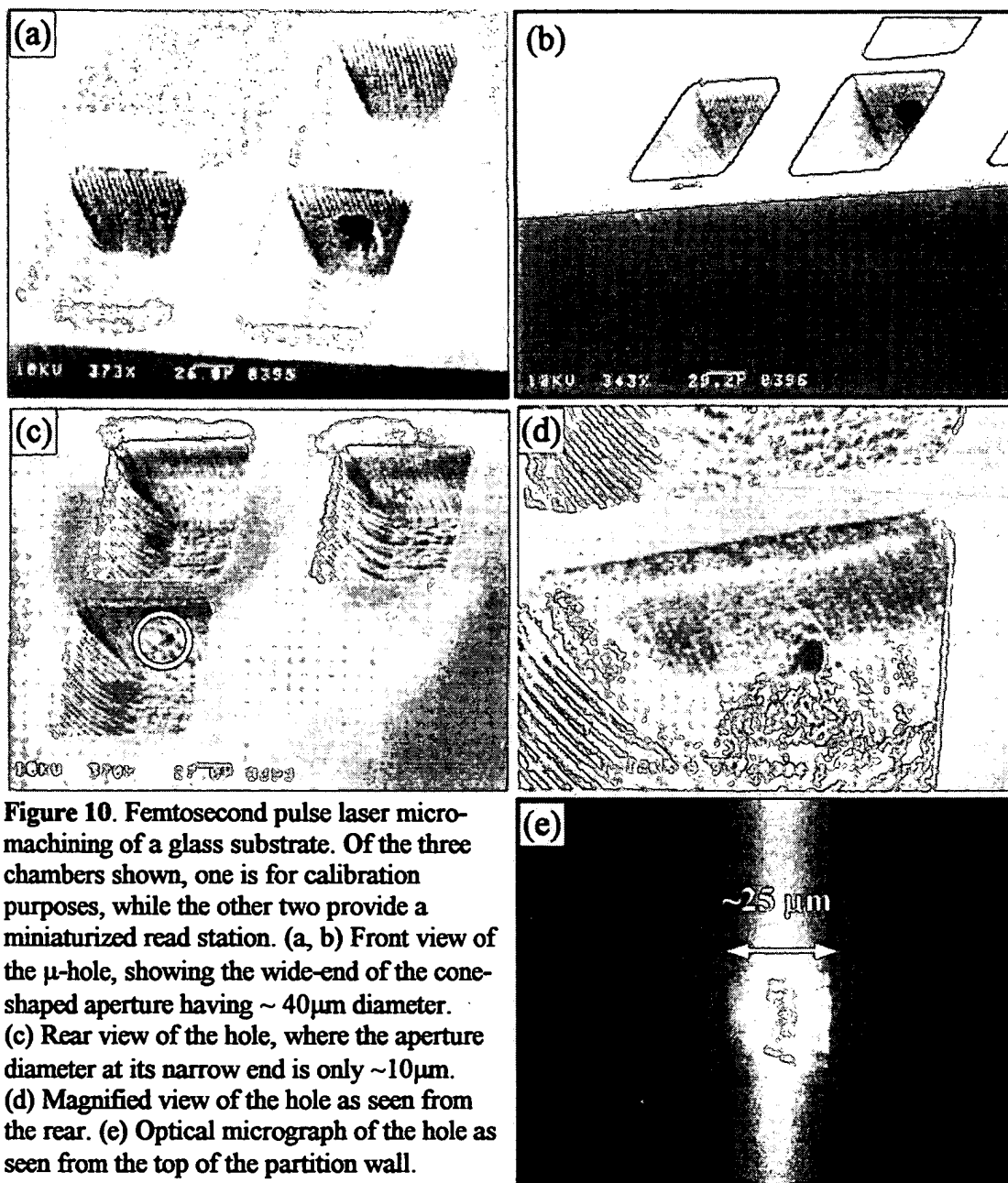
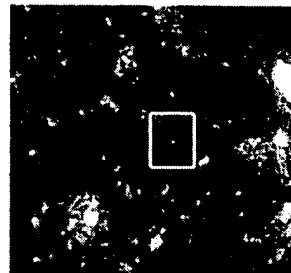


Figure 10. Femtosecond pulse laser micro-machining of a glass substrate. Of the three chambers shown, one is for calibration purposes, while the other two provide a miniaturized read station. (a, b) Front view of the μ -hole, showing the wide-end of the cone-shaped aperture having $\sim 40\mu\text{m}$ diameter. (c) Rear view of the hole, where the aperture diameter at its narrow end is only $\sim 10\mu\text{m}$. (d) Magnified view of the hole as seen from the rear. (e) Optical micrograph of the hole as seen from the top of the partition wall.

Micro-pump action using a focused, circularly-polarized laser beam. Fluid circulation by means of a micro-pump is one of the envisioned methods of transporting macro-molecular data blocks between the parking spots and the read/write stations. Anticipating the need for such micro-pumps, we have investigated methods of circulating micro-fluids under focused laser beams. The ultimate goal is to fabricate these micro-pumps in an integrated fashion around the periphery of the chip, where they can be accessed and controlled by external laser beams focused through transparent side-windows. Figure 11 shows a birefringent particle submerged in water and rotating under a focused, circularly-polarized beam of light. Birefringent particles, ranging in size from $1\mu\text{m}$ to $10\mu\text{m}$, were produced by grinding a half-wave plate. The particles were suspended in a $150\mu\text{m}$ -thick layer of water, and circularly-

polarized laser light ($\lambda = 635\text{nm}$) was focused onto individual particles via a 0.6NA microscope objective lens. The observed rotation of the particles was due to the transfer of angular momentum from circularly-polarized photons. On varying the laser power in the range from 3.0 mW to 9.0 mW, we observed uniform rotation of the particles with rotational frequencies ranging from 0.8 Hz to 5.0 Hz. These particles could be rotated in both clockwise and counterclockwise directions, depending on whether the focused beam was right- or left-circularly polarized. We believe the combination of micro-fluidic techniques with remote pump control via an external laser beam is a powerful tool for macro-molecular transport within a micro-fluidic chip.

Figure 11. Birefringent particle (diameter $\sim 5\mu\text{m}$) rotates under a focused, circularly-polarized laser beam. The photograph shows a large number of particles (obtained by grinding a half-wave plate) suspended in water and observed through an optical microscope within its field of view. The microscope objective (NA=0.6) is used to focus a red laser beam ($\lambda = 635\text{nm}$) onto the particle seen here near the center of the frame. Laser beam scattering from the spinning particle creates a rotating beacon that is readily visible to the naked eye.



Writing individual macromolecules. A method of writing macromolecules of arbitrary base sequence is shown in Fig. 12. This is essentially a miniaturized and automated version of the photo-chemical technique used in Gene-Chip manufacture.⁴ A short strand of a precursor molecule is needed to initiate the recording process, whereby individual bases are sequentially added to the free end of the precursor. The precursor is anchored at the center of the write station to prevent its drift. The write station is illuminated by a focused laser beam for the purpose of removing the blocking molecule attached to the growing end of the macromolecule. The various bases (i.e., A, C, G, T in the case of deoxyribonucleic acids) are kept within specific reservoirs and blocked by a chemical group that prevents the growth of the molecule beyond a single base during each visit to the reservoir. The reservoirs are connected to the main chamber of the write station through a nano-pore; opening each nano-pore (e.g., by applying a proper voltage between the reservoir and the main chamber) causes the free-floating end of the macromolecule to enter the selected reservoir. Within the reservoir a single base attaches itself to the free end of the growing macromolecule, but further growth will be prevented by the presence of the blocking group. The macromolecule is subsequently returned to the main chamber, where the laser beam removes its blocking group in preparation for entry into the next reservoir. This writing scheme, although probably too slow for practical purposes, has the advantage that its chemistry is well understood and, therefore, can provide a proof of principle for the proposed method of molecular data storage.

Alternative writing scheme based on widely-separated active molecules. Another possible writing mechanism is depicted in Fig. 13. In (a) a long precursor strand consisting of relatively long, inert segments separating individual active molecules, which are identical in their native (or ground) state, is exposed to an activator. The inert segments simply act as spacers to create a reasonable distance between adjacent active molecules. The activator may be a tightly focused laser beam, a localized electric field, a tunneling electrode, an anchored enzyme, etc. The strand in Fig. 13(a) is being pulled under the activator by a micro-machine (not shown); for instance, optical tweezers may be dragging the strand from right to left.

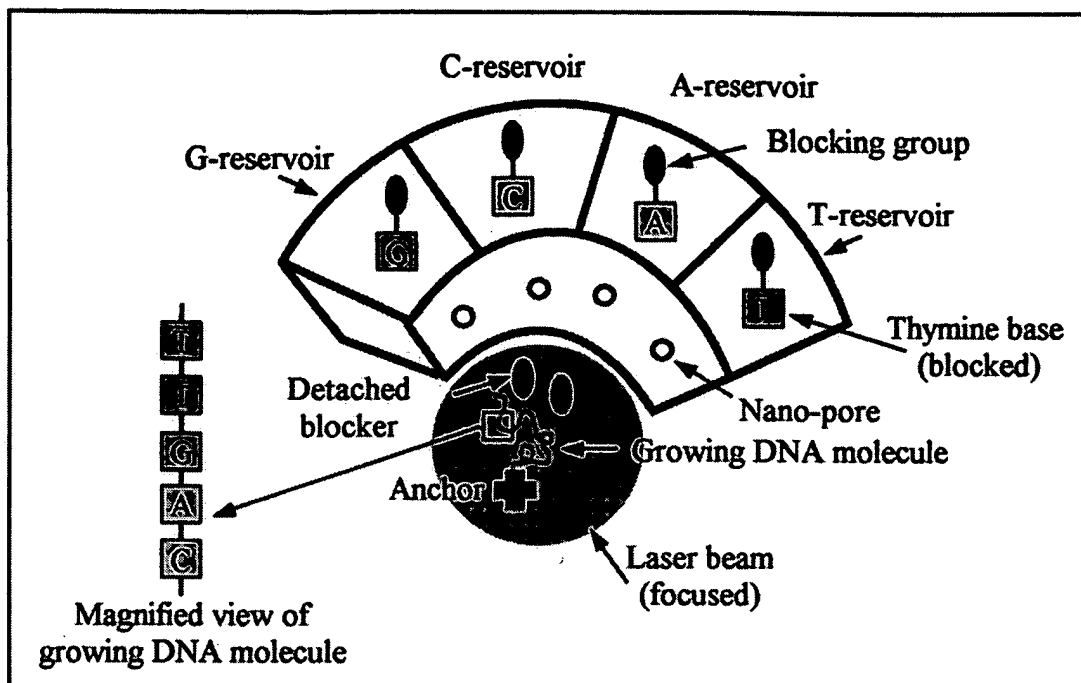


Fig. 12. Write station for creating DNA molecules of arbitrary base sequence. Four isolated chambers act as reservoirs for the four deoxyribonucleic acid bases; all base molecules stored in these reservoirs are blocked by a chemical group to ensure the attachment of a single base to the growing DNA strand at each stage of the process. Each reservoir is connected through a nano-pore to the main chamber, where a growing DNA molecule is anchored at one end but is free to float otherwise. When the growing DNA strand enters a reservoir through its nano-pore, it adds the desired base to its growing end, then returns to the main chamber. A photo-activation process in the main chamber (initiated by the focused laser beam) removes the blocker from the growing end of the strand. Upon completion of recording, the DNA molecule is detached from the anchor and transferred to a designated parking spot.

Whenever the activator is energized, the exposed active molecule is transformed from its native state to a (physically or chemically) different “excited” state. In Fig. 13(b) the two states of the active molecule are shown as differently colored. The native (ground) state and the transformed (excited) state of the active molecule must be stable; they must also be distinguishable from each other through the mechanism employed in the read station. (Once the entire strand is written, that is, when the active molecules are selectively converted from the ground state to the excited state, one may excise and remove the inert spacers while splicing the active molecules together without changing their sequential order.) The recorded strand thus created represents a binary sequence, whereby the ground state of the active molecule represents the binary digit “zero”, and the excited state represents “one,” or vice versa. If active molecules having more than two stable states are embedded in the precursor strand, non-binary (e.g., ternary, quaternary) recording will be possible as well.

The recorded strands will be “erasable” if the excited state(s) of the active molecule can somehow be reversed; otherwise the recorded strand will be an example of a write-once storage medium. In the latter case, however, erasable or rewritable data storage will still be possible in the following sense: any recorded strand that is no longer needed will be removed from its parking spot and destroyed (or abandoned), and a new precursor strand is written with fresh data, and stored in the same physical location (i.e., parking spot) from which the abandoned strand had been removed.

In this proposed scheme, the inert spacer molecules are needed only if the dimensions of the activator (i.e., the write head) are greater than those of the active molecule. In the case of an ultra-violet (UV) activator of wavelength $\lambda = 200\text{nm}$, for instance, if far-field optics are used to focus the beam, the diameter of the focused spot cannot be much smaller than 100nm . Since typical active molecules have dimensions on the order of 1nm , the required spacer molecules must be at least 100nm long. With near-field optics, it is possible to confine the optical activators to sub-wavelength dimensions, thereby reducing the required length of the spacer molecules. Electric-field or tunneling-tip activators may require even shorter spacers.

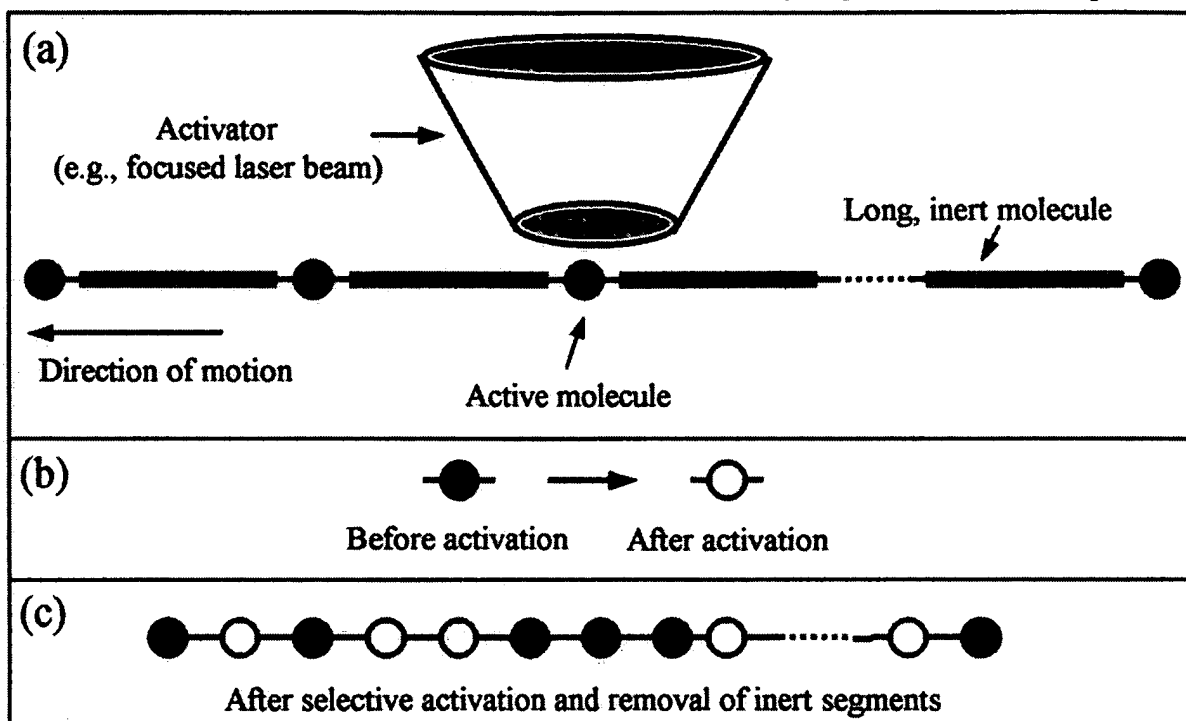


Figure 13. (a) A precursor strand consisting of long, inert segments separating active molecules in their native (or ground) state, is exposed to an activator. The strand is being pulled under the activator by a nano-actuator. (b) When the activator is energized, the active molecules are transformed from their native (ground) state to an excited state. If the activator is turned off, however, the active molecules remain in their ground state. (c) Once the entire precursor strand is written (i.e., its active molecules selectively placed in the excited state), the inert spacer molecules may be removed, and the active molecules spliced together in the same order in which they were arranged by the activator.

Access Time. An important characteristic of our data storage system, known as *access time*, is the average time it takes a macromolecular data block to travel from its parking spot to the read/write station. To simplify the analysis, let us assume that the macromolecule is bundled up in the form of a sphere of radius $r_o = 0.5\mu\text{m} = 5 \times 10^{-7}\text{m}$, moving at $V = 10\text{m/s}$ through water. At $T = 20^\circ\text{C}$, water has density $\rho = 10^3\text{kg/m}^3$ and viscosity $\eta = 10^{-3}\text{Newtons}\cdot\text{sec/m}^2$. The Reynolds number for the spherical particle moving through water would thus be $R = 2\rho Vr_o/\eta \approx 10$, which is fairly small.⁵ This means that the flow of the liquid past the micron-sized sphere will be steady and laminar.

The drag force on the surface of the sphere will be $F = 6\pi\eta r_o V = 10^{-7}\text{Newtons}$.⁵ Suppose the applied voltage across a 1cm -wide chip is 10V , so the electric field acting on the spherical

particle will be $E = 10^3$ V/m. Since $F = qE$, the particle must have a charge of $q = 10^{-10}$ C in order to move at the desired velocity under the applied field. Since a single-stranded DNA molecule has (on average) 2.5 electrons per base (i.e., 4×10^{-19} C per base), the macromolecule must have $\sim 2.5 \times 10^8$ nucleic acid bases. (This corresponds to a 60 Mbyte block of data associated with each molecule.) Since each base occupies roughly 1 nm^3 , a 2.5×10^8 -base molecule should fit in a micron-sized sphere, in agreement with our earlier assumptions.

The conclusion is that, if a polymer consisting of 10^8 – 10^9 building blocks (monomers) is used to encode each data block, and if each monomer happens to have a few unpaired electrons, then the molecule can be transferred between its parking spot and the read/write station in a matter of milliseconds under the influence of a reasonable electric field (e.g., 10 Volts across a $1 \times 1 \text{ cm}^2$ chip). We are aware, of course, that a charged polymer as assumed cannot be bundled up into a compact sphere, and a more realistic analysis needs to be undertaken in order to estimate the actual access time of the proposed system. Experimental data from gel electrophoresis indicate that the travel time of macromolecules under the above conditions should be on the order of a few seconds (rather than milliseconds). We plan to investigate this question further and, if necessary, consider alternative techniques for transporting our molecular data blocks. For instance, it is possible to neutralize the charge on a single-stranded DNA molecule by pairing it with its complement (i.e., creating double-stranded DNA), then place the uncharged molecule in a small lipid vesicle (similar to those used in biological systems) and move the vesicle across the system using either an electromagnetic field or a flow field created by the action of a micro-pump.

Concluding remarks. The objective of our research program is to build a data storage device using macromolecules, in general, and DNA molecules, in particular, as the storage medium. We use micro-fluidic techniques for transporting the molecules through various chambers (i.e., read, write, erase, and storage chambers) within a small, integrated chip. To date we have succeeded in building several micro-chambers, conducted DNA translocation experiments in different-sized chambers, and also demonstrated the principle of optical pumping in these devices. Future work includes fabrication of nano-pores in μ -chambers, conducting translocation experiments within these μ -chambers, and investigating various schemes of macromolecular writing and transportation.

Acknowledgement. The authors are grateful to Professors Raphael Gruener and Michael Hogan of the University of Arizona for illuminating discussions. The paper is based upon work supported in part by the *National Science Foundation* STC Program, under Agreement No. DMR-0120967.

1. M. Mansuripur, "DNA, Human Memory, and the Storage Technology of the 21st Century," keynote address at the 2001 *Optical Data Storage Conference* (Santa Fe, New Mexico, April 2001). Published in *SPIE Proceedings* 4342, 1-29 (2001).
2. A. Meller, L. Nivon, and D. Branton, "Voltage-driven DNA translocations through a nano-pore," *Phys. Rev. Lett.* **86**, 3435-3438 (2001); A. Meller, L. Nivon, E. Brandin, J. Golovchenko, and D. Branton, "Rapid nanopore discrimination between single polynucleotide molecules," *PNAS*, Vol. **97**, 1079-1084 (2000).
3. B. K. Cumpston et al. "Two-photon polymerization initiators for three-dimensional optical data storage and microfabrication," *Nature* **398**, 51 (1999).
4. S. Fodor et al, "Light-directed, spatially addressable parallel chemical synthesis," *Science* **251**, 767-773 (1991); A. Pease et al, "Light-generated oligonucleotide arrays for rapid DNA sequence analysis," *Proc. Natl. Acad. Sci.* **91**, 5022-5026 (1994); E. Southern, K. Mir, and M. Shchepinov, "Molecular interactions on microarrays," *Nature Genet.* **21**, Supplement, pp 1-5.
5. R.P. Feynman, R.B. Leighton, M. Sands, *The Feynman Lectures on Physics*, Vol. II, Chap. 41.

EXHIBIT D

Biocompatible Writing of Data into DNA

Gary M. Skinner^{1,*}, Koen Visscher^{1,2,3}, and Masud Mansuripur³

¹The Department of Physics, The University of Arizona, Tucson, Arizona 85721, USA

²The Department of Molecular and Cellular Biology, The University of Arizona, Tucson, Arizona 85721, USA

³College of Optical Sciences, The University of Arizona, Tucson, Arizona 85721, USA

A simple DNA-based data storage scheme is demonstrated in which information is written using “addressing” oligonucleotides. In contrast to other methods that allow arbitrary code to be stored, the resulting DNA is suitable for downstream enzymatic and biological processing. This capability is crucial for DNA computers and may allow for a diverse array of computational operations to be carried out using this DNA. Although here we use gel-based methods for information read-out, we also propose more advanced methods involving protein/DNA complexes and atomic force microscopy/nanopore schemes for data readout.

Keywords:

1. INTRODUCTION

DNA is attractive for storing digital information, partly due to its potentially ultrahigh density;¹ in theory 1 g of DNA is capable of storing about the same amount of data as 10¹² CD-ROMs.² DNA also offers the possibility of creating extremely durable information archives, e.g., by introducing the DNA into a reproducing organism, such as bacteria tolerant to radioactivity.³ As the organism replicates its genome, the information is carried into the next generation. In combination with some form of selection pressure to reduce mutation rates, such information could be secured for thousands, perhaps millions, of years. Under appropriate conditions, even *in vitro* storage of DNA could be secure for hundreds of years. Another key attraction of DNA as a memory storage device is the novel forms of computational problems that can be addressed using it. For example, in his seminal paper, Adleman demonstrated that DNA could be used to solve an instance of the Hamiltonian path or “Traveling Salesman” problem.⁴ Such problems require large amounts of conventional computing time, even for problems of modest complexity. By making use of DNA’s ability to rapidly search a large information space in parallel, DNA computing offers the possibility of solving these problems on a practical timescale. The DNA memory scheme presented here might further enable DNA computation, by allowing the DNA computer to be “programmed” in a faster, more efficient manner. This could save enormous time and expense over synthesizing each unique molecule one by one.

Previous groups have encoded meaningful information in DNA directly as a sequence of base pairs.^{3,5} However, chemical DNA synthesis is slow and expensive, and a new molecule must be created each time new data is to be written. To overcome this limitation, methods have been developed that take advantage of the formation of complementary base pairs in DNA to generate molecules representing information. Notably, a 3-bit system has been developed by Shin and Pierce that allows for the encoding of up to eight distinct states in a DNA molecule, which is even rewritable.⁶ This method has some important limitations, however, which may hinder its development into a fully fledged DNA memory device. It was not possible to unambiguously read out the information using simple gel-based methods, in this case only the total number of memory bits that were “1” or “0” could be determined.⁶ To resolve the ambiguities, a fluorescence-based system was included, using the quenching of different fluorophores at each memory location to determine the precise data content. However, this method is not practical for large capacity devices; a new fluorophore would be required for each new memory location, quickly exhausting all distinct fluorophore excitation/emission combinations available. A further limitation of this approach is that the resulting DNA construct is not easily manipulated by enzymatic or biological processes. Such a capability is critical, as the promise of DNA computers relies upon such manipulation of the encoded data to perform operations.⁴ Specifically, Shin and Pierce’s DNA construct is not linear but resembles “frayed wires”⁶ and, if introduced into a living organism, will not be faithfully replicated, and furthermore, it cannot be amplified using the polymerase chain reaction, as has been

*Author to whom correspondence should be addressed.

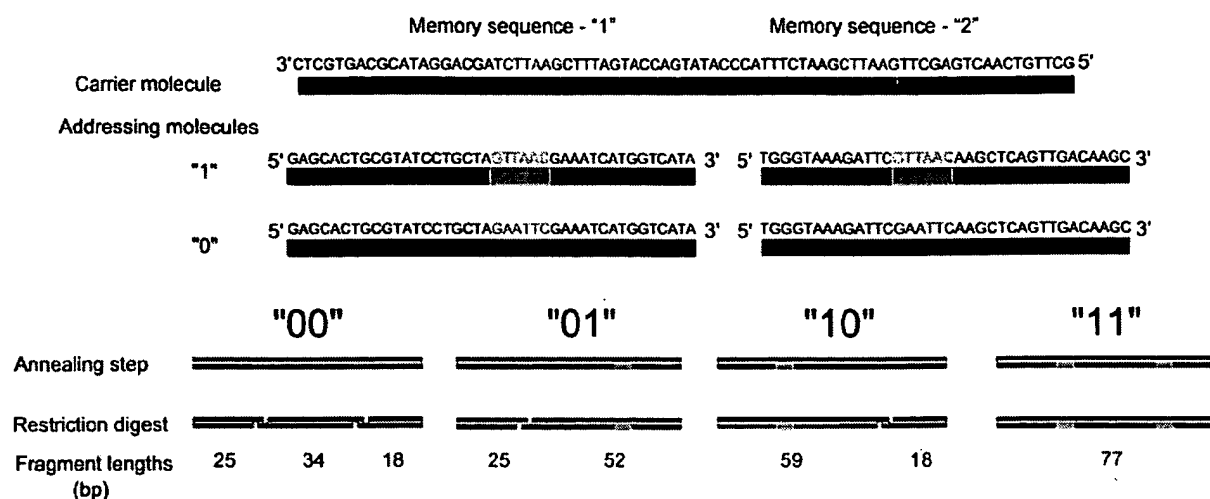


Fig. 1. Memory sequences used are shown at the top, with the EcoRI sites (blue), and the addressing sequences for memory sequence 1 (magenta) and memory sequence 2 (red). In the addressing molecules, the binary digit "1" is represented by a partially mismatched EcoRI site (green), while the binary digit "0" has the full complement to the EcoRI site (blue). Shown are 2-bit sequences (00, 01, 10, 11) written into the DNA. Prior to annealing, the carrier and specific addressing molecules are added to the reaction to achieve the desired data sequence after annealing. Shown are the expected DNA fragments resulting from EcoRI digestion of the encoded DNA products.

important in previous DNA computation demonstrations.⁴ Although we do not claim that our method could be used directly in DNA computing, we hope that such ideas may be useful to those engaged in these endeavors.

In order to address the limitations of pre-existing DNA memory devices, we have developed an alternative DNA based memory that requires only simple methods to write information into DNA. Since the resulting molecules are linear double-stranded DNA, in principle this memory is compatible with a broad range of enzymatic and biological methods. Our method takes advantage of DNA recognition enzymes in order to distinguish between the "1" and "0" memory states. For this purpose we have chosen to use the restriction endonuclease EcoRI,⁷ an enzyme that binds to the palindrome sequence G^AAATTC, cutting both DNA strands at the site marked "A". We chose this enzyme as it is well-known to possess high stringency for its cognate recognition site.⁷ By engineering the memory states "0" and "1" so that in one state the enzyme can recognize the DNA, while in the other it cannot, we can unambiguously determine the information content by a simple EcoRI digestion procedure. Similar methods for distinguishing DNA molecules have been routinely used for "DNA fingerprinting" and have been applied to solve certain criminal cases.⁸ This approach is also somewhat similar to the method developed for the DNA "finite automaton,"⁹ developed by Benenson et al., in that a recognition enzyme is used to differentiate certain states of the system. An intriguing unidirectional motor has also been constructed from DNA using a sequence-recognizing nicking enzyme.¹⁰ However, our device is different from these approaches in that we merely wish to create a generic memory device, enabling the easier encoding of a linear sequence of information directly into DNA.

Our device operates on the principle of using linear DNA as a "carrier" to specify a one-dimensional array of writeable memory sequences (see Figs. 1 and 3). Each of these sequences is unique and the address space is large. For example, by using 24 bases for the address, there are potentially 4²⁴ unique address sequences. One *memory* sequence on a carrier strand consists of two logical parts partitioned into three physical parts: two *addressing* sequences that flank one writeable *data* sequence. The writeable data sequence is composed of the recognition sequence (GAATTC) for the restriction endonuclease, EcoRI.⁷ To write to a memory sequence, one oligonucleotide spanning the entire memory sequence and fully complementary to the address sequences is used. To write a "0" the oligonucleotide is further also fully complementary to the data sequence, whereas in the case of writing a "1" the oligonucleotide contains a 4-nucleotide mismatch (GTTAAC) with the data sequence. Read-out of the memory now is based upon the ability of EcoRI to recognize, bind, and cleave at its restriction site, the data sequence. In the case of a "1," however, the DNA structure is locally melted due to the mismatch, prohibiting EcoRI recognition, binding, and cleavage. Only in the case when a "0" is written is the restriction site intact, i.e., double-stranded, and cleavable by EcoRI. The data sequence is flanked by two addressing sequences to reduce steric hindrance and allow sufficient physical space for EcoRI enzymes to bind. Here we demonstrate that DNA cleavage by the EcoRI enzyme provides a means to read out information from our memory device.

2. METHODS

In order to create a 2-bit capacity DNA based device with four distinct states (00, 01, 10, and 11), five chemically

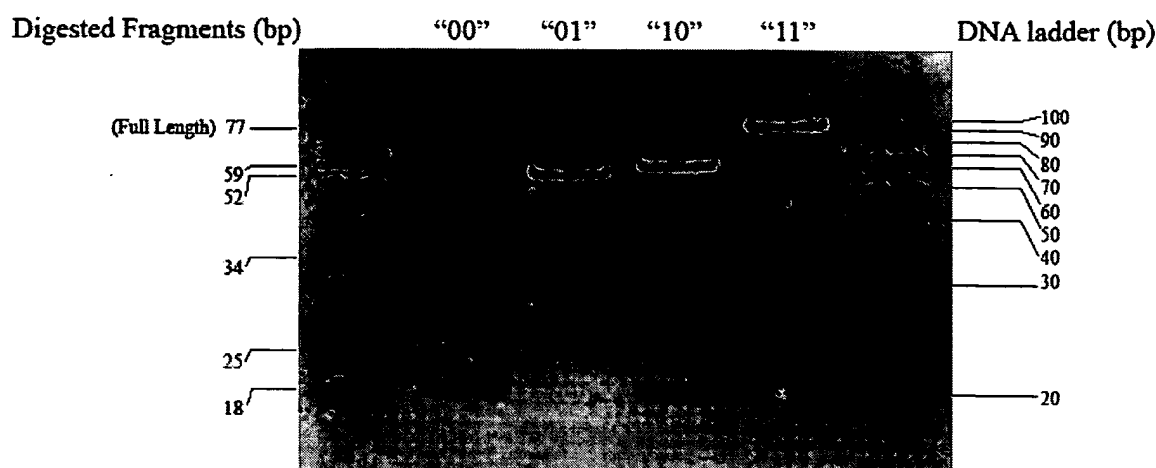


Fig. 2. Restriction digest with EcoRI enzyme yields a distinct pattern of DNA fragments, which depends upon the specific EcoRI sites that have been protected. In this way the four states of the 2-bit device, 00, 01, 10, and 11, can unambiguously be determined.

synthesized ssDNA oligonucleotides were ordered from Integrated DNA Technologies (see Fig. 1 for sequences). The carrier molecule consists of 77 bases and contains two memory sequences. For each memory sequence on the carrier, two shorter ssDNA oligonucleotides complementary to the addressing sequences and encoding either a “0” or a “1” were synthesized. The “0” molecules contain the complement to the EcoRI sites as the data sequence, whereas the “1” molecules have four mismatched bases within this field (GAATTC → *GTTAAC*).

To store information using these molecules, one need only mix together the carrier molecule with either of the addressing molecules for each memory sequence, depending on whether a “0” or a “1” is desired. In practice, this was done by setting up a 50 μ l annealing reaction in 1 \times NEB buffer #2 (10 mM Tris-HCl pH 7.9 @ 25 $^{\circ}$ C, 50 mM NaCl, 10 mM MgCl₂, 1 mM dithiothreitol), with each ssDNA molecule present at a concentration of 3 μ M. The reaction was incubated at 95 $^{\circ}$ C to melt all base-pair interactions and then slowly cooled to room temperature over several hours. Following this step, the information was then stored within the molecules.

Subsequent readout of the stored digital information was achieved by performing a restriction digest with the enzyme EcoRI (New England Biolabs). If a “0” was written at any given memory sequence, a completely base-paired cognate EcoRI site is formed that can be recognized and cleaved by the enzyme. However, if a “1” was written, the four mismatched bases prevent the EcoRI from recognizing and cleaving the DNA. By subsequent gel electrophoresis of the digestion products, it is now possible to unambiguously determine the information encoded. In practice, 10 μ l of the encoded product DNA was added to 40 μ l of NEB buffer #2 plus 40 units of EcoRI. These reactions were incubated for 48 h at 37 $^{\circ}$ C to ensure complete digestion of all EcoRI sites. The reaction products were then analyzed by polyacrylamide gel electrophoresis

(PAGE) in Tris-borate EDTA buffer at 10 V/cm, stained with ethidium bromide, and imaged by using an ultraviolet light source. A 10 bp DNA stepladder was run alongside the samples in order to determine fragment lengths on the gel (Fig. 2).

3. RESULTS

The molecules used in this demonstration were engineered so that the EcoRI sites were not spaced evenly along the DNA molecule. This was done so that “01” could be distinguished from “10,” as cutting at one or other of these sites produced differently sized fragments. The expected DNA fragment lengths for each state of the device are as follows (Fig. 1). “00”: Since both data sequences are represented by fully base-paired cognate EcoRI, complete digestion yields three fragments, 18, 25, and 34 base-pairs in length. “01”: Only one site is cleavable yielding two fragments 25 and 52 base pairs in length. “10”: Again, only one site is cleavable, but due to the spacing of EcoRI sites, the fragments are now 18 and 59 base pairs long. “11”: Since both EcoRI sites are mismatched, no digestion can occur and the full-length 77 base-pair molecule is expected.

Following EcoRI digestion, the resulting products were analyzed using a native polyacrylamide gel; see Figure 2. As can be seen, each state of the DNA memory device is easily distinguished from the other three and the expected DNA fragments are present as described above. Each of the four states “00,” “01,” “10,” and “11” has been faithfully recorded into the DNA and can be unambiguously read using EcoRI, as expected.

4. DISCUSSION

The presented DNA memory device is easily scaled to much larger capacities, one need only increase the overall

length of the carrier molecule to include additional memory sequences and synthesize the corresponding addressing molecules for them. It should be noted that these molecules must be made, in the first instance, by chemical synthesis. However, following these initial investments, any arbitrary data can be stored without the need for synthesis of further molecules, and further stocks of the carrier molecule could then be prepared by amplification using the PCR reaction, followed by conversion to ssDNA using established methods.¹¹ In this way, our DNA memory device is a truly generic storage media. We note that current DNA synthesis methods are limited to around 10000 bases (e.g., gene synthesis by such companies as GenScript, <http://www.genscript.com>). However, we anticipate that longer sequences could be made by ligation of several synthetic genes, and perhaps even longer constructs will be possible as DNA synthesis technologies improve.

In this prototype device, the EcoRI sites were engineered so as to yield differently sized fragments upon digestion, e.g., to distinguish "01" from "10." As the capacity of such a memory device increases, this method for removing ambiguity will become increasingly impractical. In a larger device, the sites should be equally spaced along the molecule and the data stored as a palindrome within the DNA, i.e., all memory sequences duplicated and reflected around the center of the molecule (Fig. 3(a)). With such a construct, all states will yield a unique pattern of digestion products. This has the added advantage of introducing redundancy into the memory, while decreasing the information density by only a factor of 2.

The resulting DNA memory is ready for use in further enzymatic manipulations; the fact that EcoRI is able to digest the product efficiently already shows that it is a suitable substrate for at least this class of DNA processing

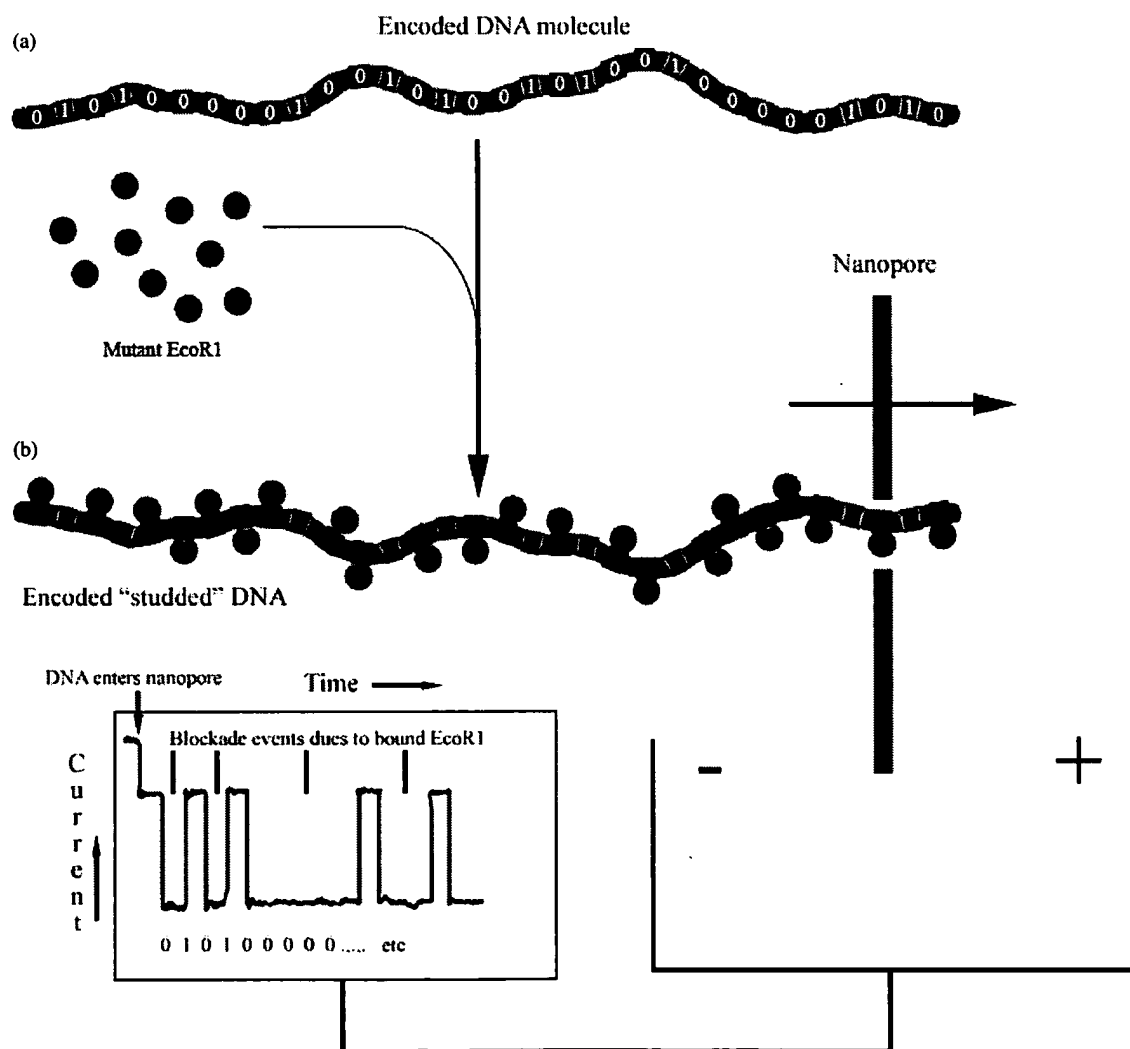


Fig. 3. Advanced readout system. (a) The encoded DNA molecule is incubated with the mutant form of EcoRI that is able to bind tightly to its correct DNA site but is not able to cleave the DNA.⁸ (b) The resulting "studded" DNA is then fed through a solid-state nanopore, driven by an applied voltage. The current through the nanopore is measured as a function of time and discrete additional blockade events would be observed (simulated here) each time an EcoRI/DNA complex passes through the nanopore. This current versus time data could then be used to determine the digital sequence of the encoded DNA.

enzymes. By sealing the single-stranded “nicks” in the DNA between adjacent memory locations, using ligase, it should be possible to amplify such DNA by PCR and potentially to introduce it into living systems; such steps have been shown to be crucial for successful DNA information technology applications.^{3–5} It would be true that only 50% of the PCR amplified DNA would be of the sequence desired, but by molecular cloning of these sequences into single-copy plasmids (e.g., Novagen’s pETcoco-1), the clones could be screened and only the desired sequence selected from resulting transformants.

We do not expect that restriction digestion and gel analysis will be the method of choice for read-out of the data in a practical application, especially when the capacity is increased. The gel method used here has two distinct limitations, first, it is slow, and very long gels would have to be run to resolve the digestion fragments in larger devices. Furthermore, as the data are read in this fashion, the information is destroyed. However, we propose an alternative read-out strategy that would overcome these limitations. A mutant version of EcoRI exists that has the ability to bind tightly to the cognate DNA site but is unable to cut the molecule.¹² It simply remains bound, forming a protein “stud” on the DNA; such mutant EcoRI/DNA complexes studded along a length of λ -DNA have been imaged by using atomic force microscopy (AFM).¹² It should be possible to use a similar method to decorate our memory device with EcoRI. A protein would bind to the cognate sites located at the “0” positions, while leaving gaps where the EcoRI is unable to bind the mismatched sites that represent “1.” The readout could be performed by using AFM and subsequent image analysis, as was done with EcoRI on λ -DNA.¹² However, a more exciting prospect is to feed the protein/DNA complex through a solid-state nanopore¹³ forming a “nanoscale digital tape drive” (Fig. 3(b)). We have previously shown that, using the α -hemolysin protein pore, structural landmarks on ssDNA can be distinguished and potentially used to store information.¹ The pore diameter would be engineered to yield a large current blockade differential when EcoRI/DNA complexes pass through, as opposed to when naked DNA strands pass

through. The palindrome nature of the encoded data means that there is no need to control the orientation of the DNA molecule as it enters the nanopore. Thus, the data could be read as a sequence of blockade events, and the intact protein/DNA complex could then be returned to a storage area to be accessed later.

By having a robust, simple means to encode a sequence of digital information into DNA in a form that is suitable for a wide range of further manipulations, the goal of practical, large-scale DNA data storage may be a step closer to reality.

Acknowledgments: This work is supported by the Office of Naval Research MURI grant No. N00014-03-1-0793. G. M. S. is a fellow of the University of Arizona BIO5 Institute and also thanks the Jane Coffin Childs Memorial Fund for Medical Research (www.jccfund.org) for support.

References and Notes

1. P. K. Khulbe, M. Mansuripur, and R. Gruner, *J. Appl. Phys.* 97, 104 317 (2005).
2. S. Kashiwamura, M. Yamamoto, A. Kameda, T. Shiba, and A. Ohuchi, *Biosystems* 80, 99 (2005).
3. P. C. Wong, K. K. Wong, and H. Foote, *Commun. Acn* 46, 95 (2003).
4. L. M. Adleman, *Science* 266, 1021 (1994).
5. C. T. Clelland, V. Risco, and C. Bancroft, *Nature* 399, 533 (1999).
6. J. S. Shin and N. A. Pierce, *Nano Lett.* 4, 905 (2004).
7. J. A. McClarin, N. A. Frederick, B. C. Wang, P. Greene, H. W. Boyer, J. Grable, and J. M. Rosenberg, *Science* 234, 1526 (1986).
8. A. C. Goes, D. A. Silva, C. S. Domingues, J. M. Sobrinho, E. F. Carvalho, *Sao Paulo Med. J.* 120, 77 (2002).
9. Y. Benenson, R. Adar, T. Paz-Elizur, Z. Livneh, and E. Shapiro, *PNAS* 100, 2191 (2003).
10. J. Bath, S. J. Green, and A. J. Turberfield, *Angew. Chem. Int. Ed.* 44, 4358 (2005).
11. L. G. Mitchell and C. R. Merrill, *Anal. Biochem.* 178, 239 (1989).
12. D. P. Allison, P. S. Kerper, M. J. Doktycz, J. A. Spain, P. Modrich, F. W. Larimer, T. Thundat, and R. J. Warmack, *PNAS* 93, 8826 (1996).
13. A. J. Storm, C. Storm, J. Chen, H. Zandbergen, J. F. Joanny, and C. Dekker, *Nano Lett.* 5, 1193 (2005).

Received: xx Xxxx xxxx. Revised/Accepted: xx Xxxx xxxx.

EXHIBIT E

Macro-molecular data storage with petabyte/cm³ density, highly parallel read/write operations, and genuine 3D storage capability

Masud Mansuripur and Pramod Khulbe

Optical Sciences Center, University of Arizona, Tucson, Arizona 85721, masud@u.arizona.edu

Abstract. Digital information can be encoded in the building-block sequence of macromolecules, such as RNA and single-stranded DNA. Methods of “writing” and “reading” macromolecular strands are currently available, but they are slow and expensive. In an ideal molecular data storage system, routine operations such as write, read, erase, store, and transfer must be done reliably and at high speed within an integrated chip. As a first step toward demonstrating the feasibility of this concept, we report preliminary results of DNA readout experiments conducted in miniaturized chambers that are scalable to even smaller dimensions. We show that translocation of a single-stranded DNA molecule (consisting of 50 adenosine bases followed by 100 cytosine bases) through an ion-channel yields a characteristic signal that is attributable to the 2-segment structure of the molecule. We also examine the dependence of the rate and speed of molecular translocation on the adjustable parameters of the experiment.

1. Introduction. Many of the traditional problems in disk and tape data storage can be overcome if data-blocks were to be released from the confines of a disk (or tape) and allowed to float freely between read/write stations (i.e., heads) and permanent “parking spots.” The heads and parking spots thus become fixed structures within an integrated chip, while the macro-molecular data blocks themselves become the (mobile) storage media. In this scheme, a large number of read/write heads could operate in parallel, the heads and parking spots would be constructed (layer upon layer) in a truly 3-dimensional fashion, and individual nanometer-sized molecules—strung together in a flexible macromolecular chain—would be used to represent the 0's and 1's of binary information. In this paper we discuss the potential advantages of this alternative scheme for (secondary) data storage and, to demonstrate the feasibility of the concept, we present results of experiments based on DNA molecules that travel within micro-fluidic chambers.

In principle, the four nucleotides of DNA can be used to represent a 2-bit sequence (A = 00, C = 01, G = 10, T = 11), although practical considerations may impose certain restrictions on the specific sequences that can be used to encode the information. A data storage device built around this concept must have the ability to (i) create macromolecules with any desired sequence of building blocks, i.e., *write* or encode the digital information into macromolecular strands; (ii) analyze and decode the sequence of a previously created macromolecule, i.e., *read* the recorded information; (iii) provide an automated and reliable mechanism for transferring the macromolecules between the read station, the write station, and designated locations (parking spots) for storing each such macromolecule. Although methods of writing and reading macromolecular strands are currently available (e.g., arbitrary sequences of oligonucleotides can be synthesized, and DNA sequences can be deciphered), these methods require large machines and are slow and expensive. In an ideal molecular data storage system, routine operations such as write, read, erase, store, and transfer must be carried out within an integrated chip, reliably and at high speed.

2. Device architecture. As a possible alternative to present-day mass data storage devices (e.g., magnetic and optical disks and tapes), we envision a system in which data blocks are encoded into macromolecules constructed from two or more distinct bases, say, x and y ; the bases can be strung together in arbitrary order such as $xyxyxyxy...xyx$ to represent binary sequences of user-data ($x = 0, y = 1$).^{1,2} The macromolecular data blocks must be created in a *write station*, transferred to *parking spots* for temporary storage, and brought to a *read station* for decoding and readout. The *erase* operation is as simple as discarding a data block and allocating its parking spot to another macromolecule. (In principle, discarded molecules can be recycled after being broken down to their constituent elements.) The parking spots and read/write stations depicted in Fig. 1, for example, are μ -fluidic chambers connected via μ -channels and μ -valves (not shown) that enable automatic access through an electronic addressing scheme.² With the dimensions of the various chambers indicated in Fig. 1, one can readily incorporate, on a 1.0 cm^2 surface area, a total of 10^6 parking spots ($\sim 0.25\text{ cm}^2$), 1000 read/write stations ($\sim 0.1\text{ cm}^2$), and necessary plumbing (e.g., $1\mu\text{m}$ -wide connecting routes, $1 \times 1\mu\text{m}^2$ binary valves or switches), which would occupy an area $\sim 0.65\text{ cm}^2$. Assuming megabyte-long data-blocks, the storage capacity of the 10^6 parking spots in this scheme will be 10^{12} bytes/ cm^2 . In a three-dimensional design based on $10\mu\text{m}$ -thick layers, the capacity of the proposed molecular storage system would exceed 10^{15} bytes/ cm^3 . For a comparison with a current state-of-the-art technology, note that storing 10^{15} bytes of data on Digital Versatile Disks requires a 128 meter-tall stack of 12cm-diameter DVD platters.

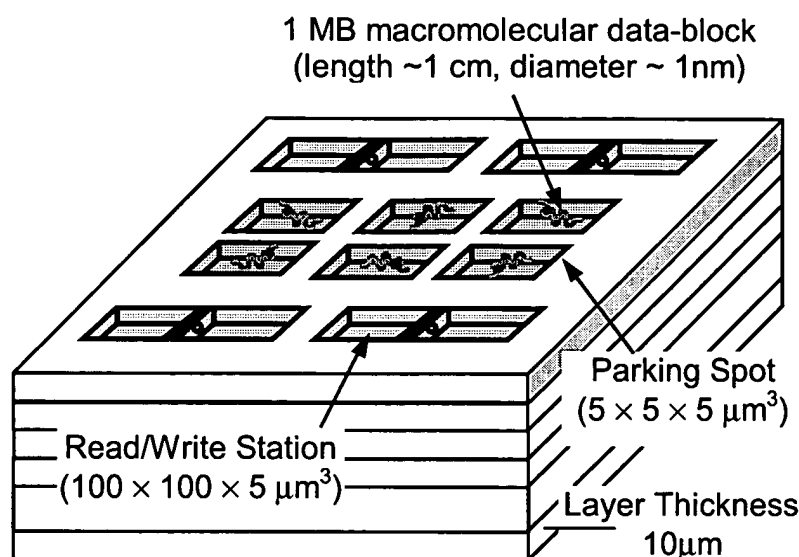


Fig. 1. Chip surface utilization. The same arrangement of read, write stations and parking spots is repeated in stacked layers.

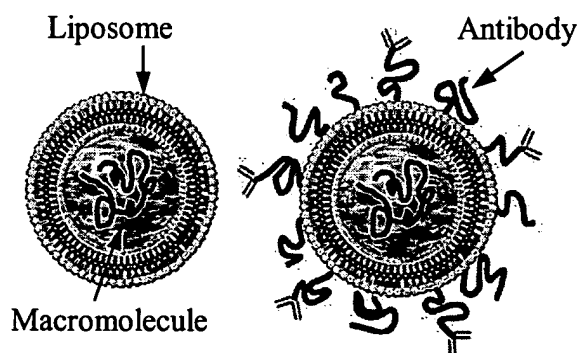


Fig. 2. Liposomes are microscopic spherical vesicles that form when phospholipids are hydrated. When mixed in water under low shear conditions, the phospholipids arrange themselves in sheets, the molecules aligning side by side with heads up and tails down. The sheets then join tails-to-tails to form a bilayer membrane. Phospholipid bilayer spheres enclosing water and one or more macromolecules can be produced with uniform size (diameter $\sim 200\text{ nm}$ or smaller). Antibodies inserted in the outer surface of the liposome can target specific locations within the device tagged with antibody-specific antigens.

One may also envision packaging the molecular data blocks in microscopic spherical vesicles known as liposomes (see Fig. 2). This would provide a robust environment for the transfer of data blocks between the parking spots and the read/write stations. Moreover, by planting specific antibody molecules on the vesicle surfaces, it becomes possible to direct these "addressed" packages to desired locations tagged with antibody-specific antigens (i.e., receptors).

In an effort to demonstrate the feasibility of the proposed molecular storage scheme, we have built miniaturized read stations for DNA strands.^{2,3} The idea is to translocate single-stranded DNA molecules through a nano-pore while monitoring the variations of the electrolytic current through the pore, as has been described elsewhere in the context of gene analysis and sequencing.⁴⁻¹¹ Whereas in decoding a genome the DNA sequence could be arbitrary, in the proposed data storage application it is possible to tailor the sequence to the characteristics of the read station. For instance, if the electrical signals corresponding to individual bases turn out to be indistinguishable (due to insufficient signal-to-noise ratio, SNR, or because the ion-channel is too long compared to the dimensions of single nucleotides), one might instead associate the information bits with strings of identical bases; for example, a string of 20 adenosines can be used to represent a 0, while a string of 30 cytosines could represent a 1.

3. Conventional modes of mass storage and their limitations. The hallmarks of traditional secondary (i.e., disk, tape) data storage may be summarized as follows: (i) mechanical motion of the storage medium; (ii) mechanical motion of the read/write head; (iii) confinement of data to two-dimensional surfaces; (iv) data organization in sectors or blocks (as opposed to words); (v) difficulty of achieving parallel access to multiple sectors; (vi) dependence of achievable data density on the read/write/servo mechanism (as opposed to the physical properties of the storage medium). By releasing the data-blocks from the confines of the storage medium and giving them an independent physical identity, as depicted in Fig. 3, one could solve many of the traditional problems associated with disk/tape data storage. The released data sectors must still represent large blocks of data (item iv above); they also continue to require mechanical motion for moving around the storage device (item i above). However, the free-floating data blocks can now operate with *stationary* read/write heads, and will no longer be confined to a two-dimensional surface. The read/write heads will be permanently fixed within the storage system (i.e., no need for flying heads, track-following, auto-focusing, or scanning the storage medium to access various sectors). Therefore, the number of read/write stations that can be integrated into the storage system can increase dramatically compared to what is achievable in present-day devices. Parallel access to data thus becomes a natural mode of operation for a system that has hundreds or thousands of independent read/write stations.

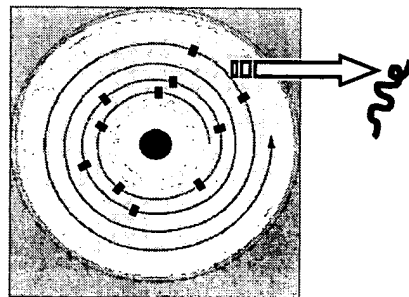
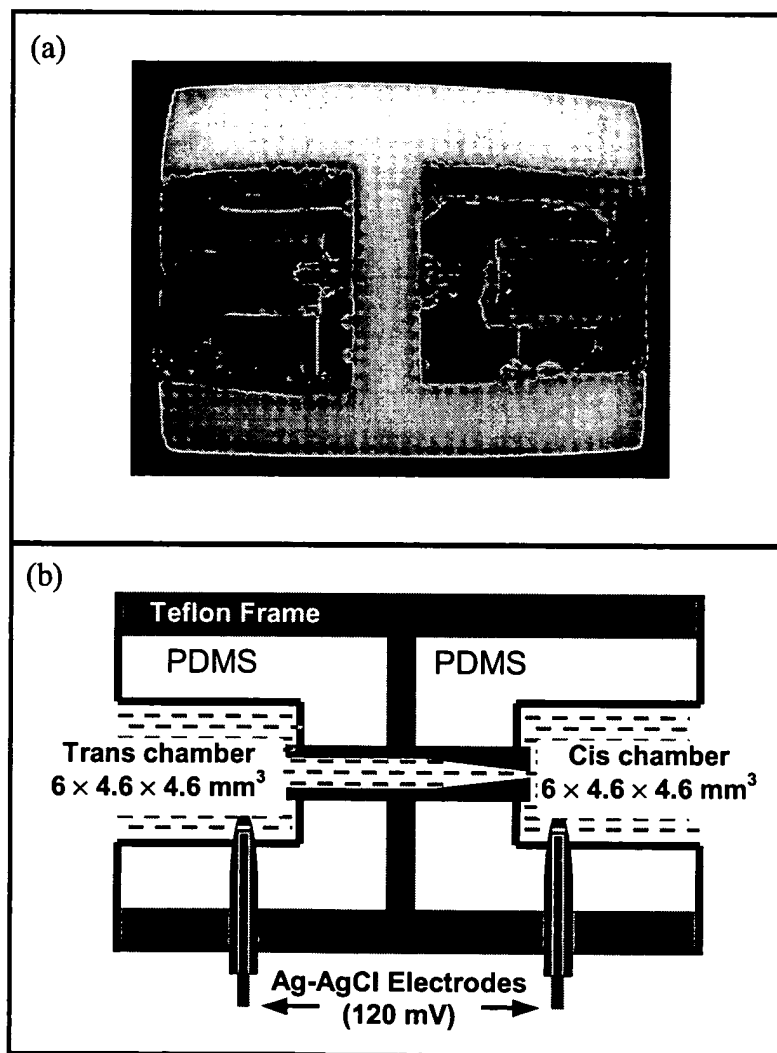


Fig. 3. Releasing the data blocks from the storage medium can, in principle, solve many of the problems associated with conventional data storage schemes.

4. Miniature read station. In previous publications we have described a method of reading molecular data blocks by translocation through nano-pores.² We have also reported methods of fabrication of the requisite fluidic chambers.^{2,3} Our current research is focused on miniaturizing the read/write stations and integrating them with parking spots, μ -fluidic channels, and μ -valves. Our read stations, complete with electrodes and access ports, were molded from polydimethylsiloxane (PDMS), cast in a machined Teflon block. This design, which is scalable to even smaller dimensions, allows easy integration with multiple parking spots on the same chip. In the read station depicted in Fig. 4, the needle-like end of the tube that connects the *cis* and *trans* chambers was covered with a Teflon cap (aperture diameter $\sim 20\mu\text{m}$) to promote the formation of a lipid membrane over the aperture. The nano-pore, self-assembled in the lipid membrane from seven subunits of α -haemolysin (αHL) protein, is a 10 nm-long ion-channel, whose cap (length $\sim 5\text{ nm}$) resides in the *cis* chamber, while its 5nm-long stem spans the lipid membrane. The ion-channel has an opening diameter of 2.6 nm at the entrance to the cap, 1.5 nm in the constricted region in the middle, and 2.2 nm at the far end of the stem located in the *trans* chamber.^{4,5}

Fig. 4. (a) Photograph and (b) diagram of a read station built inside a 10mm-thick H-shaped Teflon frame. A Teflon tube, shrunk at one end to a $20\mu\text{m}$ diameter aperture, goes through the central wall and forms a tight seal between the *cis* and *trans* chambers. The 6mm-long, 4.6mm diameter cylindrical chambers are large enough to hold the buffer solution for several hours; evaporation reduces the buffer by 50% in 24 hours. The chambers are connected to an Axopatch 200B amplifier via Ag-AgCl electrodes. The $20\mu\text{m}$ diameter aperture holds a (vertical) lipid bilayer, into which one or more αHL ion-channels are implanted. Single-stranded DNA molecules are driven through the channel by an applied voltage in the range 90-210mV, positive at the *trans* side.



In the read station of Fig. 4, the *cis* chamber is accessed (under microscope control) with a micro-pipette from the right-hand side, and the *trans* chamber from the left-hand side. The micro-pipette is used for filling the chambers with buffer, adding αHL or DNA to the *cis* chamber, and removing the additives by perfusion. At $50\mu\text{L}$ volume (partial filling), the chambers are small enough to yield a low-noise electrolytic current signal, yet large enough to avoid problems associated with the

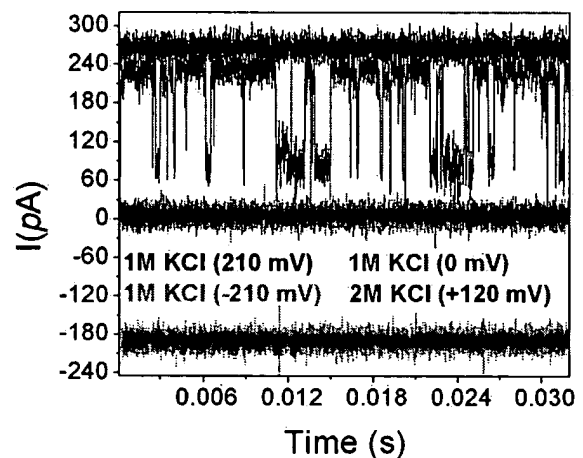
evaporation of the liquids. If the device dimensions were to shrink further, both chambers would have to be capped to prevent evaporation.

Our goal was to improve the signal-to-noise ratio (SNR) of readout by increasing *both* the KCl concentration in the buffer and the applied voltage. The increased salt concentration, however, resulted in ion-channel gating, which is unacceptable behavior for observation of DNA translocation events. The higher voltage, on the other hand, helped raise the SNR by enhancing the signal without causing much increase in the noise.

5. Gating behavior of α -haemolysin nano-pore at high KCl concentration. The black (top), green (bottom), and red (middle) traces in Fig. 5 show the electrical current through a single nano-pore with 1 molar KCl concentration at applied voltage levels of +210mV, -210mV, and 0 mV, respectively. The channel is always open at this KCl concentration, and the forward current is just over 250pA, while the reverse current is about -200pA. The width of the trace in each case is a good measure of the noise level present during the measurement. (The KCl concentration was 1M on both *cis* and *trans* sides; in other words, there was no transmembrane gradient.)

When the KCl concentration is raised to 2M, the ion-channel exhibits a “gating” behavior, namely, it opens and closes randomly, as can be seen in the blue trace in Fig. 5. The applied voltage was reduced in this case to +120mV to make the forward current (in the open state of the ion-channel) nearly equal to the forward current in the case of 1M KCl concentration. (At 2M KCl, gating behavior was also observed at higher voltages, up to 200mV, and also when a reverse voltage, $V = -120$ mV, was applied.) Apparently, at some KCl concentration between 1M and 2M, the nano-pore exhibits gating, irrespective of the level or polarity of the applied voltage.

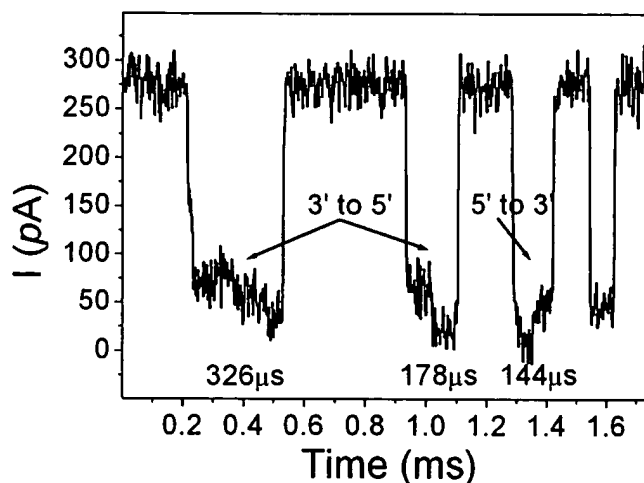
Fig. 5. Current traces obtained from an α HL channel incorporated into a bilayer. The red (middle) trace shows the channel in the non-conducting state, when there is no potential difference across the bilayer. The black (top) and green (bottom) traces show the channel in the conducting (open) state in response to a trans-bilayer applied voltage of +210 mV and -210 mV, respectively (in the presence of 1M KCl on both sides of the bilayer). Note the difference in the current level between the black and green traces, which indicates the channel's asymmetric response to a polarity reversal of the applied voltage. In the presence of 2M KCl, and in response to an applied voltage of +120 mV (blue, oscillating trace), the channel fluctuates spontaneously between open and closed states (gating).



6. Translocation of 5'A₅₀C₁₀₀3' single-stranded DNA. The ssDNA molecules traversed the ion-channel under $V = 210$ mV at 1M KCl buffer concentration, and were observed with the amplifier bandwidth set to 100 kHz. In one trial, of the 171 translocation events monitored, 49 events, or nearly 29%, showed bi-level behavior. (Not every event is expected to exhibit a bi-level signal, either due to the large fluctuations of the blockade current, or because of incomplete translocation, in which the molecule is trapped in the vestibular region of the α HL cap for a certain length of time,

then returned to the *cis* chamber without traversing the ion-channel.) The bi-level behavior is seen in three of the four events in Fig. 6. Translocation duration for the entire molecule is typically $\sim 150\mu\text{s}$. In some instances, such as the first event in Fig. 6, the molecule appears to get stuck in the midst of translocation, which results in a longer-than-average transition time. The fourth event in Fig. 6 is typical of the remaining 71% of events in which either the molecule entered the pore but did not complete translocation, or the bi-level signal was not clearly visible due to a lack of sufficient SNR. It is worth mentioning that, in our experiments, bi-level signals were *not* observed for $V = 120\text{mV}$, 150mV , or 180mV ; the higher applied voltage of 210mV , was somehow necessary to obtain these signals. (Although a bi-level translocation signal from 2-segment RNA molecules has been reported in the literature,⁶ we are not aware of any such results in the published record for ssDNA.)

Fig. 6. Effect on current flow of ssDNA passage through an αHL channel. $5'\text{A}_{50}\text{C}_{100}3'$ ssDNA was introduced into the *cis* chamber (where the cap of the ion-channel is located). Buffer concentration = 1M KCl , applied voltage = $+210\text{ mV}$, amplifier bandwidth = 100 kHz . The channel's open state is interrupted by four brief closures (translocation events). The first and second events show two closure substates indicating the translocation of ssDNA from the $3'$ to the $5'$ end. The third event also shows two substates which, however, are reversed, indicating passage from the $5'$ to the $3'$ end. In the fourth event, the A_{50} and C_{100} sections of the molecule are indistinguishable



It has been shown by several research groups that, for a given polynucleotide, translocation events generally fall into two categories, with one group of events showing less current blockade than the other. This grouping has been suggested to arise from translocation of the molecule in either of two orientations, namely, $3' \rightarrow 5'$ or $5' \rightarrow 3'$, or it might represent the translocation of the polymer in one of two different structural conformations.⁵⁻⁹ An asymmetric interaction between the polynucleotide and the internal pore structure has been suggested as the cause of the observed grouping in those occasions where the entry of the molecule into the pore from its $5'$ end produces a larger current blockade than when the $3'$ end enters the pore first.¹²

In our $5'\text{A}_{50}\text{C}_{100}3'$ ssDNA sample, keeping in mind that the C-nucleotide is smaller than the A-nucleotide, the 100-base-long C-segment is expected to drop the ionic current somewhat less than the 50 base-long A-segment does. The order in which the high and low portions of the bi-level signal occur during each translocation event depends on whether the $3'$ - or the $5'$ -end of the molecule enters the nano-pore first. Of the 29% bi-level events observed in the aforementioned experiment, nearly three-quarters were associated with the C-segment entering first, during which events the average normalized current, $\langle I_{\text{blocked}}/I_{\text{open}} \rangle$, was 0.37 ± 0.09 for the C-segment and 0.17 ± 0.04 for the A-segment. In the remaining quarter of the bi-level events (associated with the A-segment entering first) the average normalized current was 0.20 ± 0.03 for the C- and 0.12 ± 0.04 for the A-segment. These results are consistent with the aforementioned suggestion that the entry of polynucleotides into the pore from the $5'$ -end causes a larger current blockage than entry from the $3'$ -end.

7. Effect of increased voltage. Both the capture rate of the DNA molecules and the translocation speed through a single ion-channel were found to be strong functions of the applied voltage V , as has been reported by other researchers as well.⁵ The three frames in Fig. 7 represent the translocation of 120-base-long 5'(AC)₆₀3' DNA molecules under the influence of three different voltages. At $V=150\text{mV}$, the average open-channel current is $\langle I_{\text{open}} \rangle \sim 160\text{pA}$, and many translocation events are seen to occur. At $V=120\text{mV}$ and $\langle I_{\text{open}} \rangle \sim 130\text{pA}$, the translocation rate has declined, and at $V=90\text{mV}$, $\langle I_{\text{open}} \rangle \sim 90\text{pA}$, the events are relatively rare.

The observed behavior may indicate that the increased voltage has somehow directed a large number of DNA molecules (that would otherwise drift away from the vicinity of the pore) toward the ion-channel. This, in turn, is a clue concerning the transport mechanism of DNA molecules toward the pore, namely, that the drift of the molecule is not entirely controlled by thermal diffusion, and that the chamber geometry and placement of the electrodes can influence (and perhaps even control) the motion of DNA strands toward the ion-channel. When considering this particular method of molecular readout in the context of data storage, it must be remembered that controlled molecular transport is of utmost significance, as individual macromolecules are required to travel between their parking spots and the read/write stations.

Fig. 7. Translocation of 120-base-long 5'(AC)₆₀3' DNA molecules under different applied voltages. At $V=150\text{mV}$, $\langle I_{\text{open}} \rangle \sim 160\text{pA}$ and translocation events are frequent. At $V=120\text{mV}$, $\langle I_{\text{open}} \rangle \sim 130\text{pA}$ and translocation rate has declined. At $V=90\text{mV}$, $\langle I_{\text{open}} \rangle \sim 90\text{pA}$ and translocation events are rare.

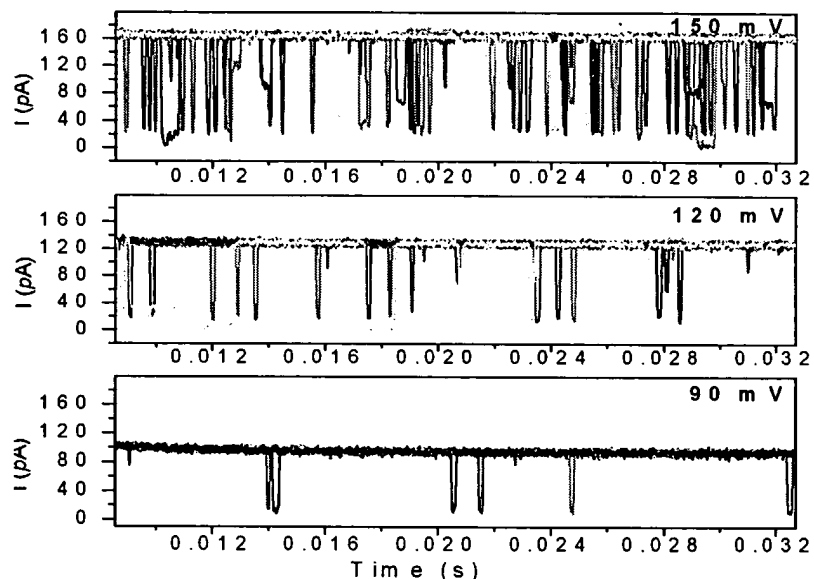


Figure 8 shows some statistics of the translocation experiment depicted in Fig. 7. Figure 8(a) shows that at lower applied voltages the ion-channel is open (i.e., not clogged by a passing molecule) for a larger fraction of time than at higher voltages. According to Fig. 8(b), the translocation rate (i.e., number of events per second), whether complete (■) or incomplete (●), is an increasing function of the applied voltage. The total translocation rate (▲), which is the sum of complete and incomplete translocations per second, increases nearly three-fold in going from $V=120\text{mV}$ to 150mV .

Figure 9 shows the distribution of the event duration ΔT versus the current blockage in the experiment of Fig. 7. These data indicate that, at higher applied voltages, there is less current blockage, perhaps because the molecules are likely to be linearized, thus presenting a smaller cross-section to the pore. Also, at higher applied voltages the translocation duration is reduced, meaning that the molecules travel faster through the ion-channel. The speed of the molecules passing through the nano-pore is seen to be roughly proportional to the applied voltage, as has been reported by other

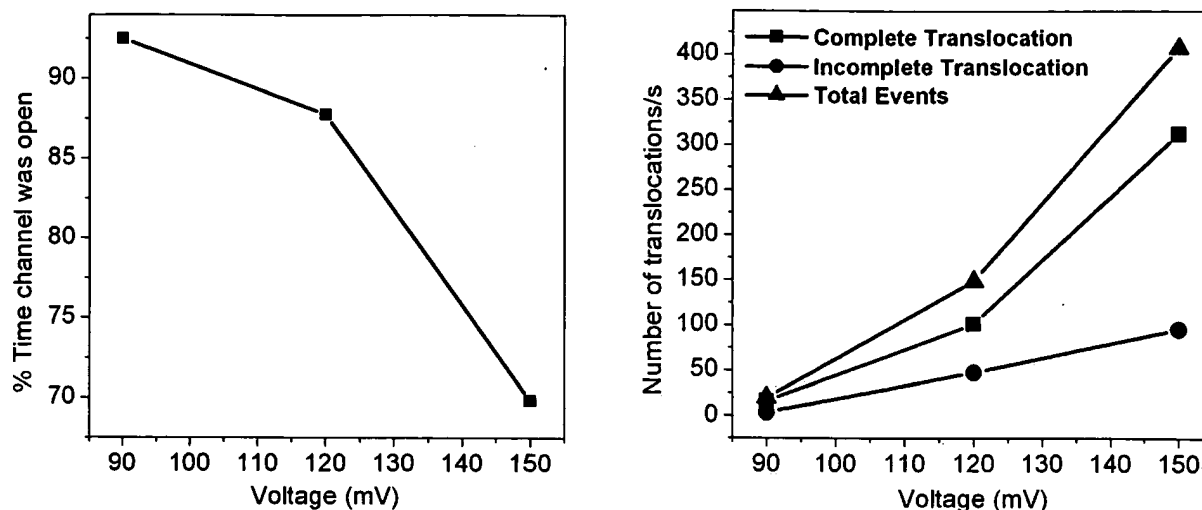
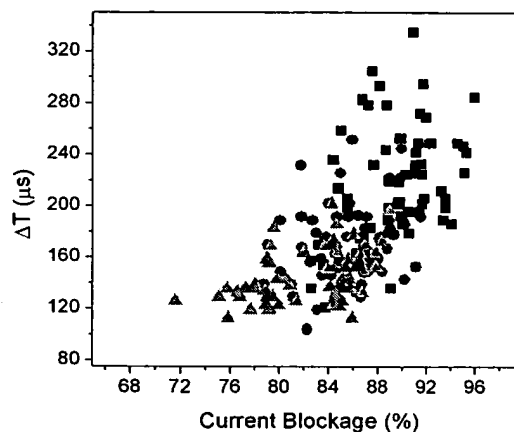


Fig. 8. Characteristics of translocation events in the experiment depicted in Fig. 7. (Left) Fraction of time during which the ion-channel is open (i.e., not clogged) as function of the applied voltage V . (Right) Translocation rate versus the applied voltage.

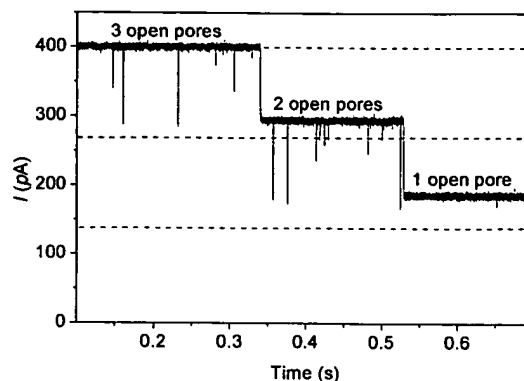
research groups.^{5,9} Faster translocation, of course, is desirable in data storage applications as it results in a greater data-transfer rate, so long as the SNR remains reasonably high at the correspondingly larger bandwidth.

Fig. 9. Translocation statistics in the experiment depicted in Fig. 7. The percentage current blockage is shown on the horizontal axis, while the event duration appears on the vertical axis. The cluster of triangles (\blacktriangle) represents the case of $V = 150\text{mV}$, circles (\bullet) correspond to $V = 120\text{mV}$, and squares (\blacksquare) represent the case of $V = 90\text{mV}$.



8. Experiments with multiple nano-pores. In a typical nano-pore experiment, αHL proteins are removed (by perfusion) from the *cis* chamber immediately after the formation of a single nano-pore. Given sufficient time, however, additional ion-channels reconstitute themselves in the same lipid membrane. In one experiment, the lipid bilayer had a diameter of $20\mu\text{m}$, resulting in a pair wise separation of at most $20\mu\text{m}$ between nano-pores. Figure 10 shows a typical trace of the electrolytic current across the membrane where, initially, the total current is $\sim 400\text{pA}$, indicating the presence of three open nano-pores. With all three channels open, the rate of capture and/or translocation is relatively high (31.8 events per second). When one of the pores is temporarily clogged, the current drops to $\sim 290\text{pA}$, and the rate of capture/translocation through the two remaining open pores drops to ~ 19.7 per second. Similarly, when two of the nano-pores are clogged, the current drops to $\sim 190\text{pA}$ and the event rate declines to ~ 10.3 per second. This data indicates that, for each nano-pore, the electrolytic current is $\sim 130\text{pA}$ in the open-channel state and $\sim 30\text{pA}$ in the clogged state. The observed capture and/or translocation rate ratio of nearly $3 : 2 : 1$ confirms that the three ion-channels operate independently of one another on drifting DNA molecules. We have observed the same behavior repeatedly: the event rate increased after reversing the applied voltage to clear the clogged channel(s), only to drop again with the next clogging.

Fig. 10. A typical trace of the electrolytic current obtained when three ion-channels (reconstituted in the same lipid membrane) operate simultaneously and independently of each other. When a DNA molecule is stuck in one of the nano-pores, the current drops to ~ 190 pA. With two nano-pores similarly clogged, the total current across the membrane is ~ 190 pA. The complete translocation events are found to have average rates of 12.6, 6.2, and 3.3 events per second, with zero, one, or two nano-pores clogged, respectively. The corresponding rate for partial events in these three cases are 19.2, 13.5, and 7.0 events/second, leading to total event rates of 31.8, 19.7 and 10.3 per second.



9. Concluding remarks. As a first step toward constructing a macromolecular data storage system, we have demonstrated the feasibility of conducting experiments with fairly short strands of DNA in a miniature read station. We showed that the A- and C-segments of a 5'A₅₀C₁₀₀3' ssDNA molecule can be distinguished during translocation through an α HL ion-channel. Needless to say, many hurdles must be overcome before this system can be implemented as an alternative to existing storage technologies.

The ultrahigh capacity is an obvious advantage of such molecular storage devices, but the data-rates require substantial improvement. If the 5'A₅₀C₁₀₀3' molecules, which represent 2-bit sequences of binary information, take ~ 150 μ s to pass through a nano-pore, the corresponding data-transfer rate of only 12 kbit/s would leave a lot to be desired. On the other hand, if the technology could improve to the point that individual bases could be detected during translocation (perhaps through a shorter, more robust, solid-state nano-pore),¹³ then the achievable rate of ~ 1 Mbit/s would not be out of bounds. Moreover, if thousands of read stations could be made to operate in parallel within the same chip, the overall data-transfer rate could approach the respectable value of several Gbits/s.

Access to data is another issue that requires extensive research. Our preliminary calculations show that a 1 Mbyte-long macromolecule, enclosed in a 200 nm diameter spherical shell (e.g., a liposome), can move electrophoretically across a 1.0 cm² chip in ~ 1.0 millisecond under a 10 V potential difference. Whether such molecules could be written and packaged on demand, within an integrated micro-chip, at high speed, and on a large scale, are questions to which only future research can provide satisfactory answers. Stability of the molecules over extended periods of time should obviously be a matter of concern. The lipid membrane and the proteinaceous ion-channel, both being of organic origin, are ill-suited for practical data storage systems; they must eventually be replaced with robust, solid-state equivalents.¹³ Despite all the difficulties, it is our hope that the proposed scheme will encourage debate in the pursuit of an alternative path to conventional approaches to data storage.

Acknowledgements. The authors are grateful to Professors Raphael Gruener, Michael Hogan, and Nasser Peyghambarian of the University of Arizona, and Joseph Perry and Seth Marder of the Georgia Institute of Technology, for many helpful discussions. This work has been supported by the *Office of Naval Research* MURI grant No. N00014-03-1-0793 and by the *National Science Foundation* STC Program, under Agreement No. DMR-0120967.

Appendix

Experimental conditions

The buffer used in our experiments was 1M KCl, 10mM HEPES (pH~8.0), pH balanced by KOH, and the lipid was diphytanoyl phosphatidycholine (DPC). The Ag-AgCl electrodes were made by dipping a silver wire in Clorox. The patch-clamp amplifier was Axon Instrument's Axopatch 200B. Two different oligodeoxynucleotide samples were used in our experiments: the 5'A₅₀C₁₀₀3', with a total of 150 base-units per molecule, was used in the experiment described in Fig. 6. All other experiments (reported in Figs. 7-10) used 5'(AC)₆₀3', with a total of 120 bases per molecule. Both custom-synthesized, PAGE (Poly Acrylic Gel Electrophoresis) grade samples were purchased from *Midland Certified Reagent Company* (Midland, Texas). The samples were suspended in TE buffer (10mM Tris/1mM EDTA) at pH 8.0, before being released into the cis chamber, where the final concentration of 5'A₅₀C₁₀₀3' was 7.15 nM/ml, while that of 5'(AC)₆₀3' was 14.3 nM/ml.

Prior to filling the chambers with buffer, 2μL of a lipid solution in hexane (1.5mg/mL) is released in the vicinity of the 20μm aperture between the *cis* and *trans* chambers. The chambers are then dried under a mild stream of nitrogen, thus allowing a thin layer of lipid to coat the surrounding walls without clogging the aperture. Care must be taken to completely evaporate the hexane, as even trace amounts in the aperture area can ruin the bilayer. We found the bilayer that must cover the aperture between the two chambers does not form properly when applied to a PDMS surface. Although PDMS is hydrophobic – a requirement for this application – its porosity ultimately destroys the lipid membrane a few minutes after the formation of a bilayer. In the read station depicted in Fig. 4, the needle-like end of the tube connecting *cis* and *trans* chambers had to be covered with a Teflon cap (aperture diameter~20μm) to promote the proper formation of a lipid membrane.

The *cis* and *trans* chambers (as well as the tube that connects them) are subsequently filled with buffer. We soaked 1.5 mg of lipid in 5 μL of hexadecane in a test tube for 60-90 seconds; the left-over hexadecane was then completely drained, leaving a viscous lipid at the bottom of the tube. A micro-capillary tube (length~1mm, inner diameter~300μm) was filled with this viscous lipid in such a way as to form a convex meniscus at the tip of the capillary. Using a micro-manipulator, this lipid meniscus was brushed across the 20μm aperture with a slight pressure. A 60 Hz, 5 mV square wave was then applied between the Ag-AgCl electrodes across the bilayer (the so-called seal test) to verify that the bilayer is adequate. The above procedure succeeds in creating a proper bilayer across the aperture in about 90% of the trials.

Once a stable bilayer was obtained, 40 ng of α-haemolysin (αHL) protein was dissolved in 2μL of buffer and added to the *cis* chamber. Applying a potential ($V = 120$ mV) across the bilayer enables one to observe the reconstitution of an ion-channel into the bilayer, an event which is indicated by an abrupt jump of the current from 0 to ~120pA. The observed voltage to current ratio of ~1.0 GΩ is consistent with the single-channel conductance of αHL nano-pores under similar conditions, as reported in the literature.⁵ Self-assembly of a single ion-channel within the lipid membrane typically takes 20-30 minutes, after which the excess αHL is removed by perfusion of 10 mL of fresh buffer.

References

1. M. Mansuripur, "DNA, human memory, and the storage technology of the 21st century," keynote address at the *Optical Data Storage Conference*, Santa Fe, New Mexico, April 2001; published in *SPIE Proceedings*, Vol. 4342, pp 1-29 (2001).
2. M. Mansuripur, P.K. Khulbe, S.M. Kuebler, J.W. Perry, M.S. Giridhar, and N. Peyghambarian, "Information Storage and Retrieval using Macromolecules as Storage Media," *Optical Data Storage Conference*, Vancouver, Canada, May 2003; published in *SPIE Proceedings*, Vol. 5069, pp 231-243 (2003).
3. M.S. Giridhar, K.B. Seong, A. Schülzgen, P.K. Khulbe, N. Peyghambarian, and M. Mansuripur, "Femtosecond pulsed laser micro-machining of glass substrates with application to microfluidic devices," to appear in *Applied Optics* (2004).
4. D. W. Deamer and D. Branton, "Characterization of nucleic acids by nanopore analysis," *Acc. Chem. Res.* **35**, 817-825 (2002).
5. A. Meller, "Dynamics of polynucleotide transport through nanometre-scale pores," *J. Phys. Condens. Matter* **15**, R581-R607 (2003).
6. M. Akeson, D. Branton, J. J. Kasianowicz, E. Brandin, and D. Deamer, "Microsecond time-scale discrimination among polycytidylic acid, polyadenylic acid, and polyuridylic acid as homopolymers or as segments within single RNA molecules," *Biophysical Journal* **77**, 3227-3233 (1999).
7. A. Meller, L. Nivon, E. Brandin, J. Golovchenko, and D. Branton, "Rapid nanopore discrimination between single polynucleotide molecules," *Proc. Natl. Acad. Sci.* **97** (3) 1079-1084 (February 1, 2000).
8. J. J. Kasianowicz, E. Brandin, D. Branton, and D. W. Deamer, "Characterization of individual polynucleotide molecules using a membrane channel," *Proc. Natl. Acad. Sci.* **93**, 13770-13773 (1996).
9. A. Meller, L. Nivon, and D. Branton, "Voltage-driven DNA translocations through a nanopore," *Phys. Rev. Lett.* **86**, 3435-3438 (2001).
10. S. Howorka, S. Cheley, and H. Bayley, "Sequence-specific detection of individual DNA strands using engineered nanopores," *Nature Biotechnology* **19**, 636-639 (2001).
11. H. Bayley and P.S. Cremer, "Stochastic sensors inspired by biology," *Nature* **413**, 226-230 (Sept. 2001).
12. T. A. Pologruto, private communication.
13. J. Li, M. Gershow, D. Stein, E. Brandin, and J. A. Golovchenko, "DNA molecules and configurations in a solid-state nanopore microscope," *Nature Materials* **2**, 611-615 (2003).

EXHIBIT F

DNA translocation through α -hemolysin nanopores with potential application to macromolecular data storage

EXHIBIT F

Pramod K. Khulbe^{a)} and Masud Mansuripur
Optical Sciences Center, University of Arizona, Tucson, Arizona 85721

Raphael Gruener
Department of Physiology, University of Arizona, Tucson, Arizona 85721

(Received 20 December 2004; accepted 17 March 2005; published online 6 May 2005)

Digital information can be encoded in the building-block sequence of macromolecules, such as RNA and single-stranded DNA. Methods of “writing” and “reading” macromolecular strands are currently available, but they are slow and expensive. In an ideal molecular data storage system, routine operations such as write, read, erase, store, and transfer must be done reliably and at high speed within an integrated chip. As a first step toward demonstrating the feasibility of this concept, we report preliminary results of DNA readout experiments conducted in miniaturized chambers that are scalable to even smaller dimensions. We show that translocation of a single-stranded DNA molecule (consisting of 50 adenosine bases followed by 100 cytosine bases) through an ion channel yields a characteristic signal that is attributable to the two-segment structure of the molecule. We also examine the dependence of the translocation rate and speed on the adjustable parameters of the experiment. © 2005 American Institute of Physics. [DOI: 10.1063/1.1905791]

I. INTRODUCTION

Digital information can be encoded in the building-block sequence of macromolecules, such as RNA and single-stranded DNA. In principle, the four nucleotides of DNA, for example, can be used to represent a 2-bit sequence (e.g., $A=00$, $C=01$, $G=10$, and $T=11$), although practical considerations may impose certain restrictions on the specific sequences that can be used to encode the information. A data storage device built around this concept must have the ability to (i) create macromolecules with any desired sequence of building blocks, i.e., write or encode the digital information into macromolecular strands; (ii) analyze and decode the sequence of a previously created macromolecule, i.e., read the recorded information; and (iii) provide an automated and reliable mechanism for transferring the macromolecules among the read station, the write station, and designated locations (parking spots) for storing each such macromolecule. Although methods of writing and reading macromolecular strands are currently available (e.g., arbitrary sequences of oligonucleotides can be synthesized, and DNA sequences can be deciphered), these methods require large machines and are slow and expensive. In an ideal molecular data storage system, routine operations such as write, read, erase, store, and transfer must be carried out within an integrated chip, reliably and at high speed.

As a possible alternative to present-day mass data storage devices (e.g., magnetic and optical disks and tapes), we envision a system in which data blocks are encoded into macromolecules constructed from two or more distinct bases, say, x and y ; the bases can be strung together in arbitrary

sequence such as $xyxyxyxy\cdots xyx$ to represent binary sequences of user data (e.g., $x=0$, $y=1$).^{1,2} The macromolecular data blocks must be created in a *write station*, transferred to *parking spots* for temporary storage, and brought to a *read station* for decoding and readout. The “erase” operation is as simple as discarding a data block and allocating its parking spot to another macromolecule. The parking spots and read/write stations depicted in Fig. 1, for example, are microfluidic chambers connected via microchannels and microvalves (not shown) that enable automatic access through an electronic addressing scheme.² With the dimensions of the various chambers indicated in Fig. 1, one can readily incorporate, on a 1.0-cm^2 surface area, a total of 10^6 parking spots ($\sim 0.25\text{ cm}^2$), 1000 read/write stations ($\sim 0.1\text{ cm}^2$), and the necessary plumbing (e.g., $1\text{-}\mu\text{m}$ -wide connecting routes and $1\times 1\text{-}\mu\text{m}^2$ binary valves or switches), which would occupy an area of $\sim 0.65\text{ cm}^2$. Assuming megabyte-long data blocks, the storage capacity of the 10^6 parking spots in this scheme will be 10^{12} bytes/ cm^2 . In a three-dimensional design based on $10\text{-}\mu\text{m}$ -thick layers, the capacity of the proposed molecu-

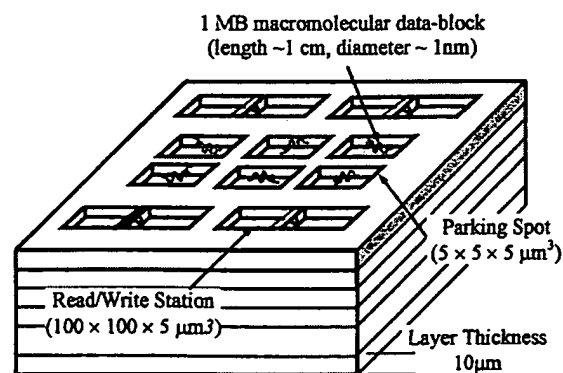


FIG. 1. Chip surface area utilization. The same arrangement of read/write stations and parking spots is repeated in stacked layers.

^{a)}Author to whom correspondence should be addressed; electronic mail: pkkhulbe@u.arizona.edu

lar storage system would exceed 10^{15} bytes/cm³.

Presently, secondary storage of data is the domain of magnetic hard disks, removable magnetic media (e.g., zip disk and magnetic tape), optical disk drives [e.g., compact disk-recordable (CD-R) and digital versatile disk-rewriteable (DVD-RW)], and magneto-optical media. All these storage technologies are inherently two dimensional in the sense that information is recorded on a thin layer at the surface of a disk or a tape medium. Considering possible advances in read/write heads and media technology, current methods of data storage can be (optimistically) pushed to densities in the range of 75–150 GB/cm². Going beyond this range, however, will be problematic owing to the fundamental physical limitations. The optical storage technology is exemplified by DVD-RW, a 12-cm-diameter platter having a capacity of 4.7 GB. The next-generation DVDs are expected to use blue lasers (wavelength ~ 400 nm) and have a capacity of ~ 25 GB per platter. Double layer disks with capacities of ~ 50 GB are also feasible. Beyond this, the optical drives planned for the year 2010 and beyond are expected to have capacities in excess of 100 GB, although several technical hurdles must be overcome before such devices can even be demonstrated in the laboratory. To summarize, both magnetic and optical recording technologies have the potential for terabyte capacity, but it is highly doubtful that these technologies can reach into the petabyte domain. The concept proposed in this paper has the potential to revolutionize information storage at extremely high density and rapid retrieval rates required for massive databases of the future. For a comparison with a current state-of-the-art technology, note that storing 10^{15} bytes of data on conventional DVDs requires a 128-m-tall stack of these 12-cm-diameter platters; the same amount of data that the 1-cm³ molecular data storage device of Fig. 1 is expected to be able to handle.

In an effort to demonstrate the feasibility of the proposed molecular storage scheme, we have built miniaturized read stations for DNA strands.^{2,3} The idea is to translocate single-stranded DNA molecules through a nanopore while monitoring the variations of the electrolytic current through the pore, as has been described elsewhere in the context of gene analysis and sequencing.^{4–11} Whereas in decoding a genome the DNA sequence could be arbitrary, in the proposed data storage application it is possible to tailor the sequence to the characteristics of the read station. For instance, if the electrical signals corresponding to individual bases turn out to be indistinguishable [due to insufficient signal-to-noise ratio (SNR) or because the ion channel is too long compared to the dimensions of single nucleotides], one might instead associate the information bits with strings of identical bases; for example, a string of 20 adenosines can be used to represent a 0, while a string of 30 cytosines could represent a 1.

II. MATERIALS AND METHODS

Our read stations, complete with electrodes and access ports, were molded from polydimethylsiloxane (PDMS), cast in a machined Teflon block. This design, which is scalable to even smaller dimensions, allows easy integration with mul-

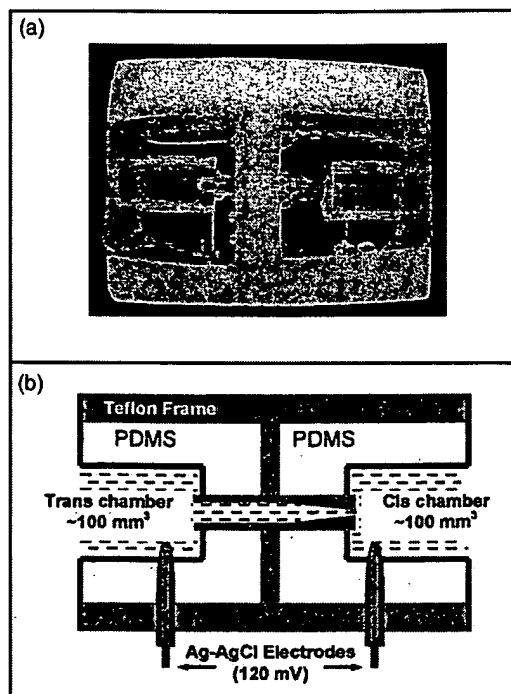


FIG. 2. (a) Photograph and (b) diagram of a read station built inside a 10-mm-thick H-shaped Teflon frame. A Teflon tube, shrunk at one end to a 20- μ m-diameter aperture, goes through the central wall and forms a tight seal between the *cis* and *trans* chambers. The 6-mm-long, 4.6-mm-diameter cylindrical chambers are large enough to hold the buffer solution for several hours; evaporation reduces the buffer by 50% in 24 h. The chambers are connected to an Axopatch 200B amplifier via Ag-AgCl electrodes. The 20- μ m-diameter aperture holds a (vertical) lipid bilayer, into which one or more α -HL ion channels are implanted. Single-stranded DNA molecules are driven through the channel by an applied voltage in the range of 90–210 mV, positive at the *trans* side.

tiple parking spots on the same chip. In the read station depicted in Fig. 2, the needlelike end of the tube that connects the *cis* and *trans* chambers was covered with a Teflon cap (aperture diameter ~ 20 μ m) to promote the formation of a lipid membrane over the aperture. The nanopore, self-assembled in the lipid membrane from seven subunits of α -hemolysin (α -HL) protein, is a 10-nm-long ion channel, whose cap (length ~ 5 nm) resides in the *cis* chamber, while its 5-nm-long stem spans the lipid membrane. The ion channel has an opening diameter of 2.6 nm at the entrance to the cap, 1.5 nm in the constricted region in the middle, and 2.2 nm at the far end of the stem located in the *trans* chamber.^{4,5}

In the read station of Fig. 2, the *cis* chamber is accessed (under microscope control) with a micropipette from the right-hand side, and the *trans* chamber from the left-hand side. The micropipette is used for filling the chambers with buffer, adding α -HL or DNA to the *cis* chamber, and removing the additives by perfusion. At 50- μ L volume (partial filling), the chambers are small enough to yield a low-noise electrolytic current signal, yet large enough to avoid problems associated with the evaporation of the liquids. If the device dimensions were to shrink further, both chambers would have to be capped to prevent evaporation.

The buffer used in our experiments was 1-M KCl, 10-mM 4-(2-Hydroxyethyl)piperazine-1-ethanesulfonic acid

(HEPES) (pH ~ 8.0), pH balanced by KOH, and the lipid was diphytanoyl phosphatidylcholine (DPC). The Ag–AgCl electrodes were made by dipping a silver wire in Clorox. The patch-clamp amplifier was Axon Instrument's Axopatch 200B.

Prior to filling the chambers with buffer, 2 μL of a lipid solution in hexane (1.5 mg/mL) is released in the vicinity of the 20- μm aperture between the *cis* and *trans* chambers. The chambers are then dried under a mild stream of nitrogen, thus allowing a thin layer of lipid to coat the surrounding walls without clogging the aperture. Care must be taken to completely evaporate the hexane, as even trace amounts in the aperture area can ultimately destroy the bilayer. We found that the lipid bilayer that must cover the aperture between the two chambers does not form properly when applied to a PDMS surface. Although PDMS is hydrophobic—a requirement for this application—its porosity ultimately destroys the lipid membrane a few minutes after the formation of a bilayer. In the read station depicted in Fig. 2, the needlelike end of the tube that connects the *cis* and *trans* chambers had to be covered with a Teflon cap (aperture diameter $\sim 20\ \mu\text{m}$) to form a stable lipid membrane.

The *cis* and *trans* chambers (as well as the tube that connects them) are subsequently filled with buffer. We soaked 1.5 mg of lipid in 5 μL of hexadecane in a test tube for 60–90 s; the leftover hexadecane was then completely drained, leaving a viscous lipid at the bottom of the tube. A microcapillary tube (inner diameter $\sim 300\ \mu\text{m}$) was filled to 1-mm height from its tip with this viscous lipid in such a way as to form a convex meniscus at the tip of the capillary. Using a micromanipulator, this lipid meniscus was brushed across the 20- μm aperture with a slight pressure. A 60 Hz, 5-mV square wave was then applied between the Ag–AgCl electrodes across the bilayer (the so-called seal test) to verify that the bilayer is adequate. The above procedure succeeds in creating a proper bilayer across the aperture in about 90% of the trials.

Once a stable bilayer was obtained, 40 ng of α -HL protein was dissolved in 2 μL of buffer and added to the *cis* chamber. Applying a 120-mV potential across the bilayer enables one to observe the reconstitution of an ion channel into the bilayer, an event which is indicated by an abrupt jump of the current from 0 to $\sim 120\ \text{pA}$. The observed voltage-to-current ratio of $\sim 1.0\ \text{G}\Omega$ is consistent with the single-channel conductance of α -HL nanopores under similar conditions, as reported in the literature.⁵ Self-assembly of a single-ion channel within the lipid membrane typically takes 20–30 min, after which the excess α -HL is removed by perfusion with 10 mL of fresh buffer.

Two different oligodeoxynucleotide samples were used in our experiments: the 5'*A*₅₀C₁₀₀3', with a total of 150 base units/molecule, was used in the experiment described in Fig. 4. All other experiments (reported in Figs. 5–10) used 5'(AC)₆₀3', with a total of 120 bases/molecule. Both custom-synthesized, polyacrylic gel electrophoresis (PAGE) grade samples were purchased from Midland Certified Reagent Company (Midland, Texas). The samples were sus-

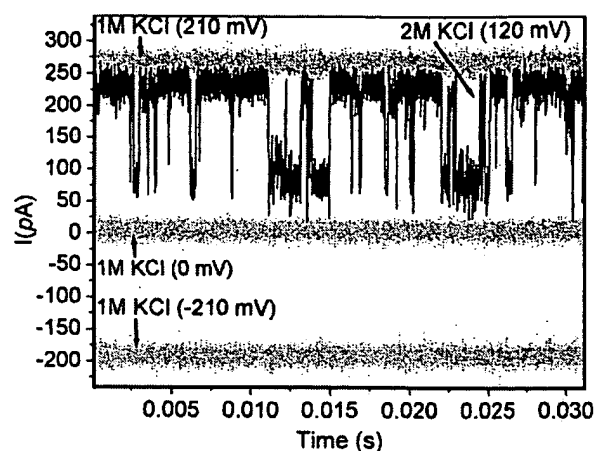


FIG. 3. Current traces obtained from a reconstituted α -HL channel incorporated into a bilayer. The gray traces show the channel in the nonconducting state (0 mV), forward conducting state (210 mV), and reverse-biased state ($-210\ \text{mV}$), in the presence of 1-M KCl on both sides of the bilayer. Note the difference in the current level between the $+210$ - and -210 -mV traces, which indicates the channel's asymmetric response to a polarity reversal of the applied voltage. In the presence of 2-M KCl, and in response to an applied voltage of $+120\ \text{mV}$ (black trace), the channel fluctuates spontaneously between the open and closed states—a behavior known as channel gating.

pending in TE buffer [10-mM tris/1-mM ethylenediamine tetraacetic acid (EDTA)] at pH 8.0, before being released into the *cis* chamber, where the final concentration of 5'*A*₅₀C₁₀₀3' was 7.15 nM/mL, while that of 5'(AC)₆₀3' was 14.3 nM/mL.

III. RESULTS

A. Gating behavior of α -hemolysin nanopore at high KCl concentration

One of our goals was to improve the SNR of readout by increasing both the KCl concentration in the buffer and the applied voltage. The increased salt concentration, however, resulted in ion-channel gating, which is an unacceptable behavior for the observation of DNA translocation events. The higher voltage, on the other hand, helped raise the SNR by enhancing the signal without causing much increase in the noise.

The gray traces in Fig. 3 show the electrical current through a single nanopore with 1-M KCl concentration at applied voltage levels of $+210$, -210 , and $0.0\ \text{mV}$, respectively. The channel is always open at this KCl concentration, and the forward current is just over 250 pA, while the reverse current is about $-200\ \text{pA}$. The width of the trace in each case is a good measure of the noise level present during the measurement. (The KCl concentration was 1 M on both *cis* and *trans* sides; in other words, there was no transmembrane gradient.)

When the KCl concentration is raised to 2 M, the ion channel exhibits a "gating" behavior, namely, it opens and closes randomly, as can be seen in the black trace in Fig. 3. The applied voltage was reduced in this case to $+120\ \text{mV}$ to make the forward current (in the open state of the ion channel) nearly equal to the forward current in the case of 1-M KCl concentration. (At 2-M KCl, a gating behavior was also observed at higher voltages, up to 200 mV, and also when a

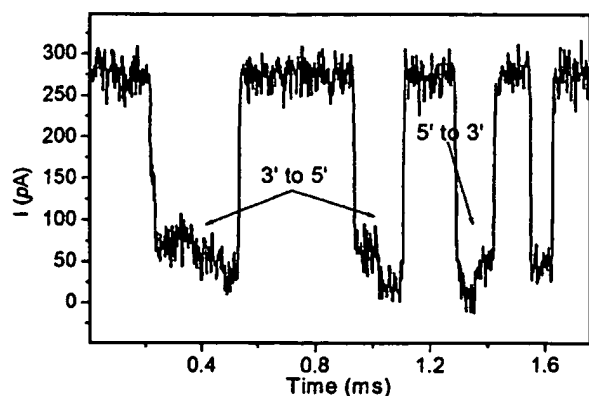


FIG. 4. Effects of ssDNA passage through the α -HL channel on current flow. Single-stranded DNA having a sequence of $5'A_{50}C_{100}3'$ was introduced into the *cis* chamber (where the cap of the reconstituted ion channel is located). The buffer concentration was 1-M KCl, the applied voltage was +210 mV, and the amplifier bandwidth was 100 kHz. The channel's open state is seen to be interrupted by four brief closures (i.e., translocation events). The first and second events show two closure substates indicating the translocation of ssDNA from the 3' end to the 5' end. The third event also shows two substates which, however, are reversed, indicating the passage of the ssDNA from the 5' end to the 3' end. The A_{50} and C_{100} sections of the molecule are not distinguishable in the fourth event.

reverse voltage, $V=-120$ mV, was applied.) Apparently, at some KCl concentration between 1 and 2 M, the nanopore exhibits gating, irrespective of the level or polarity of the applied voltage.

B. Translocation of $5'A_{50}C_{100}3'$ single-stranded DNA

The single-stranded DNA (ssDNA) molecules traversed the ion channel under $V=210$ mV at 1-M KCl buffer concentration, and were observed with the amplifier bandwidth set to 100 kHz. In one trial, of the 171 translocation events monitored, 49 events, or nearly 29%, showed a bilevel behavior. (Not every event is expected to exhibit a bilevel signal, either due to the large fluctuations of the blockade current or because of incomplete translocation, in which the molecule is trapped in the vestibular region of the α -HL cap for a certain length of time, then returned to the *cis* chamber without traversing the ion channel.) The bilevel behavior is seen in three of the four events shown in Fig. 4. Translocation duration for the entire molecule is typically ~ 150 μ s. In some instances, such as the first event in Fig. 4, the molecule appears to get stuck in the midst of translocation, which results in a longer-than-average transition time. The fourth event in Fig. 4 is typical of the remaining 71% of events in which either the molecule entered the pore but did not complete translocation or the bilevel signal was not clearly visible due to insufficient SNR. (It is worth mentioning that, in our experiments, the bilevel signals were *not* observed for $V=120$, 150, or 180 mV; the higher level of the applied voltage, $V=210$ mV, was necessary to obtain these signals.) Although bilevel translocation signals from two-segment RNA molecules have been reported in the literature,⁸ we are not aware of any such results in the published record for ssDNA.

It has been shown by several research groups that, for a given polynucleotide, translocation events generally fall into two categories, with one group of events showing less cur-

rent blockade than the other. This grouping has been suggested to arise from the translocation of the molecule in either of the two orientations, namely, $3' \rightarrow 5'$ or $5' \rightarrow 3'$, or it might represent the translocation of the polymer in one of the two different structural conformations.⁵⁻⁹ An asymmetric interaction between the polynucleotide and the internal pore structure has been suggested as the cause of the observed grouping in those occasions where the entry of the molecule into the pore from its 5' end produces a larger current blockade than when the 3' end enters the pore first.¹²

In our $5'A_{50}C_{100}3'$ ssDNA sample, keeping in mind the fact that the *C* nucleotide is smaller than the *A* nucleotide, the 100-base-long *C* segment is expected to drop the ionic current somewhat less than the 50-base-long *A* segment does. The order in which the high and low portions of the bilevel signal occur during each translocation event depends on whether the 3' end or the 5' end of the molecule enters the nanopore first. Of the 29% bilevel events observed in the aforementioned experiment, nearly three quarters were associated with the *C* segment entering first, during which events the average normalized current, $\langle I_{\text{blocked}}/I_{\text{open}} \rangle$, was 0.37 ± 0.09 for the *C* segment and 0.17 ± 0.04 for the *A* segment. In the remaining quarter of the bilevel events (associated with the *A* segment entering first) the average normalized current was 0.20 ± 0.03 for the *C* segment and 0.12 ± 0.04 for the *A* segment. These results are consistent with the aforementioned suggestion that the entry of polynucleotides into the pore from their 5' end causes a larger current blockage than entry from the 3' end.

The preceding statements based on only 49 complete threading events are admittedly inadequate, as such measurements are inevitably subject to large statistical variations. Our intent here has been a demonstration of the "possibility" of encoding and decoding bilevel signals using single-stranded DNA molecules. A detailed understanding of the processes involved obviously requires extensive measurements and detailed statistical analysis, which will require a separate study in its own right.

C. Effect of increased voltage

Both the capture rate of the DNA molecules and the translocation speed through a single-ion channel were found to be strong functions of the applied voltage V , as has been reported by other researchers as well.^{5,13} The three frames in Fig. 5 represent the translocation of 120-base-long $5'(AC)_{60}3'$ DNA molecules under the influence of three different voltages. At $V=150$ mV, the average open-channel current is $\langle I_{\text{open}} \rangle \sim 160$ pA, and many translocation events are seen to occur. At $V=120$ mV and $\langle I_{\text{open}} \rangle \sim 130$ pA, the translocation rate has declined, and at $V=90$ mV, $\langle I_{\text{open}} \rangle \sim 90$ pA, the events are relatively rare.

The observed behavior may indicate that the increased voltage has somehow directed a large number of DNA molecules (that would otherwise drift away from the vicinity of the pore) toward the ion channel. This, in turn, is a clue concerning the transport mechanism of DNA molecules toward the pore, namely, that the drift of the molecule is not entirely controlled by thermal diffusion, and that the cham-

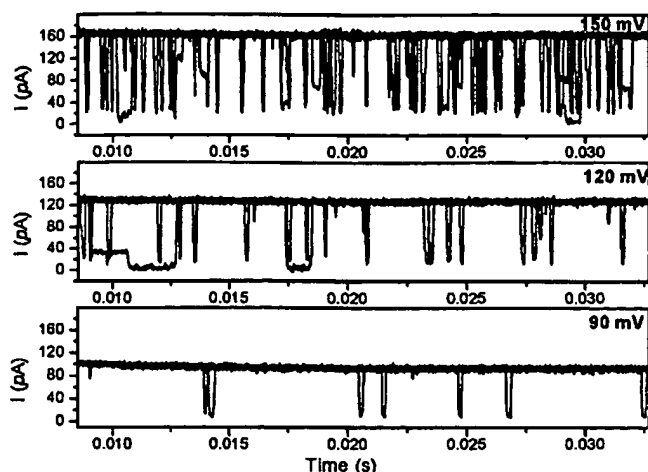


FIG. 5. Translocation of 120-base-long 5'(*AC*)₆₀3' DNA molecules under three different applied voltages. There are seven overlapping traces at each voltage corresponding to a total translocation time of 170 ms. At $V = 150$ mV, $\langle I_{\text{open}} \rangle \sim 160$ pA and translocation events are frequent. At $V = 120$ mV, $\langle I_{\text{open}} \rangle \sim 130$ pA and translocation rate has declined. At $V = 90$ mV, $\langle I_{\text{open}} \rangle \sim 90$ pA and the events are rare.

ber geometry and placement of the electrodes can influence (and perhaps even control) the motion of DNA strands toward the ion channel. When considering this particular method of molecular readout in the context of data storage, it must be remembered that, since individual macromolecules are required to travel between their parking spots and the read/write stations, controlled molecular transport is of utmost significance.

Figure 6 shows some of the statistics of the translocation experiment depicted in Fig. 5. Figure 6(top) shows that at lower applied voltages the ion channel is open (i.e., not clogged by a translocating molecule) for a larger fraction of time than at higher voltages. According to Fig. 6(bottom), the translocation rate (i.e., number of events per second), whether complete (■) or incomplete (●), is an increasing function of the applied voltage. The total translocation rate (▲), which is the sum of complete and incomplete translocations per second, increases nearly threefold between $V = 120$ mV and $V = 150$ mV.

Figure 7 shows the distribution of the event duration ΔT versus the current blockage in the experiment of Fig. 5. These data indicate that, at higher applied voltage, there is less current blockage, perhaps because the molecules are likely to be linearized, thus presenting a smaller cross section to the pore. Also, at higher applied voltage the translocation duration is reduced, meaning that the molecules travel faster through the ion channel. The speed of the molecules passing through the nanopore is seen to be roughly proportional to the applied voltage, as has been reported elsewhere.^{5,9} Faster translocation, of course, is desirable for the data storage application as it results in a greater data-transfer rate, so long as the SNR remains reasonably high at the correspondingly larger bandwidth.

D. Experiments with multiple nanopores

In a typical nanopore experiment, α -HL proteins are removed (by perfusion) from the *cis* chamber immediately af-

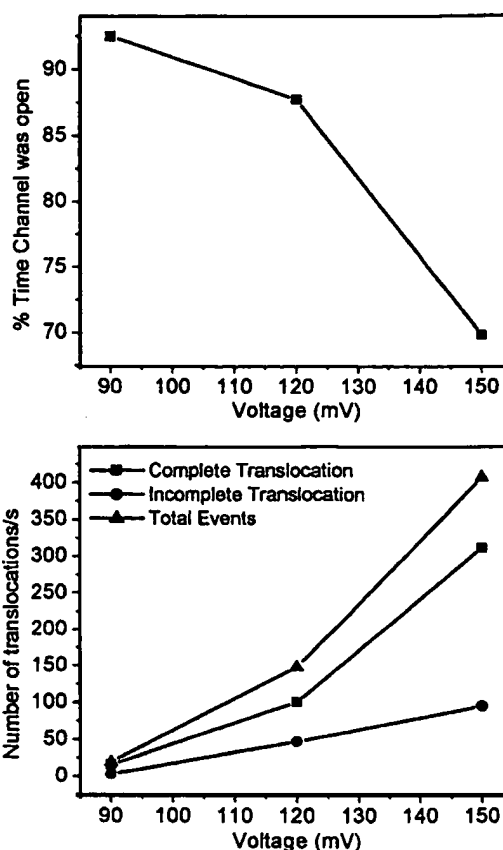


FIG. 6. Characteristics of translocation events in the experiment depicted in Fig. 5. (Top) Fraction of time during which the ion channel is open (i.e., not clogged) as function of the applied voltage V . (Bottom) Translocation rate vs applied voltage.

ter the formation of a single nanopore. Given sufficient time, however, additional ion channels reconstitute themselves in the same lipid membrane. In one experiment, the lipid bilayer had a diameter of $20 \mu\text{m}$, resulting in a pairwise sepa-

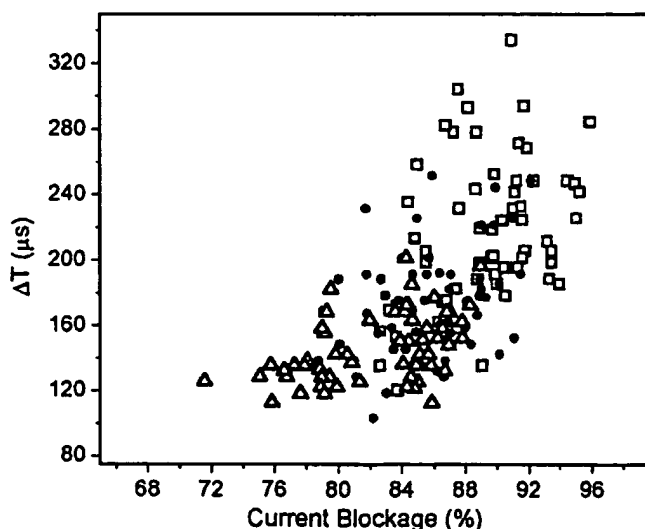


FIG. 7. Statistics of translocation events in the experiment depicted in Fig. 5. The percentage current blockage is shown on the horizontal axis, while the duration of the event appears on the vertical axis. The cluster of the open triangles represents the case of applied voltage $V = 150$ mV, the solid circles correspond to $V = 120$ mV, and the open squares represent the case of $V = 90$ mV.

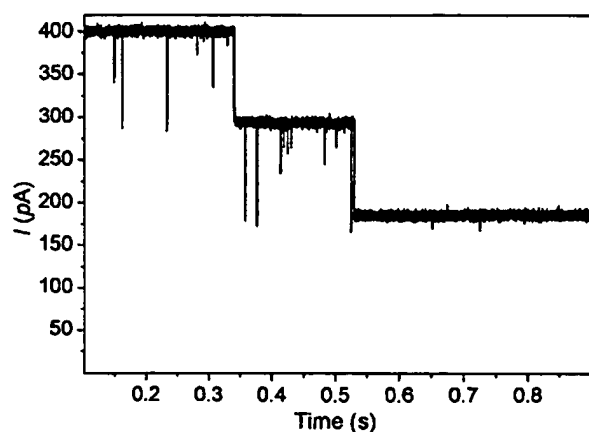


FIG. 8. A typical trace of the electrolytic current obtained when three ion channels (reconstituted in the same lipid membrane) operate simultaneously and independently of each other. When a DNA molecule is stuck in one of the nanopores, the current drops to ~ 290 pA. With two nanopores similarly clogged, the total current across the membrane is ~ 190 pA. The complete translocation events are found to have average rates of 12.6, 6.2, and 3.3 events/s, with zero, one, or two nanopores clogged, respectively. The corresponding rates for partial events in these three cases are 19.2, 13.5, and 7.0 events/s, leading to total event rates of 31.8, 19.7, and 10.3/s.

ration of at most $20\ \mu\text{m}$ between nanopores. Figure 8 shows a typical trace of the electrolytic current across the membrane where, initially, the total current is ~ 400 pA, indicating the presence of three open nanopores. With all three channels open, the rate of capture and/or translocation is relatively high (31.8 events/s). When one of the pores is temporarily clogged, the current drops to ~ 290 pA, and the rate of capture/translocation through the two remaining open pores drops to ~ 19.7 /s. Similarly, when two of the nanopores are clogged, the current drops to ~ 190 pA and the event rate declines to ~ 10.3 /s. These data indicate that, for each nanopore, the electrolytic current is ~ 130 pA in the open-channel state and ~ 30 pA in the clogged state. The observed capture and/or translocation rate ratio of nearly 3:2:1 confirms that the three ion channels operate independently of one another on drifting DNA molecules. We have observed the same behavior repeatedly: the event rate increased after reversing the applied voltage to clear the clogged channel(s), only to drop again with the next clogging.

In another multiple nanopore experiment, we constituted two forward nanopores as well as one reverse nanopore in the lipid membrane, then translocated DNA strands from the *cis* to the *trans* chamber and back again to the *cis* chamber. This experiment requires the addition of α -HL proteins to the *trans* chamber (to facilitate reverse nanopore formation), followed by perfusion removal of the excess α -HL. The presence of the long, narrow Teflon tube in the system of Fig. 2, however, makes it difficult to run the above protocol, since a sufficient number of α -HL molecules cannot easily diffuse through the tube (from the *trans* chamber to the lipid membrane) and also because, during perfusion, the excess α -HL cannot be readily removed from the vicinity of the membrane.

To overcome the above problems, we built the type of chamber shown in Fig. 9. In this device a $300\text{-}\mu\text{m}$ -thick Teflon sheet was perforated with a $40\text{-}\mu\text{m}$ -diameter aperture,

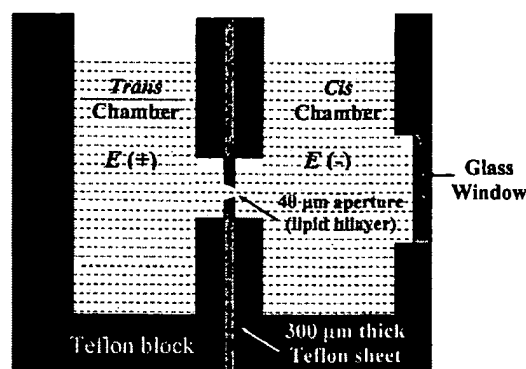


FIG. 9. Diagram of a read station designed to allow the study of back-to-back nanopores. A nanopore inserted from the *cis* side of the membrane translocates DNA molecules from the *cis* to the *trans* chamber, while a reverse nanopore (inserted from the *trans* side) returns the molecules back to the *cis* chamber on reversing the applied voltage. Two cylindrical wells (diameter= 3.8 mm, height= 7.0 mm, and volume $\sim 80\ \mu\text{L}$) drilled in Teflon blocks serve as *cis* and *trans* chambers. Each block has a 2.0 -mm-diameter hole on one of its sidewalls, wherein holes are subsequently aligned face to face. The Teflon blocks are screwed together, with a $300\text{-}\mu\text{m}$ -thick Teflon sheet (perforated with a $40\text{-}\mu\text{m}$ -diameter aperture) sandwiched in between. After filling both chambers with 1-M KCl/HEPES-KOH (pH ~ 8) buffer, a lipid bilayer is formed across the $40\text{-}\mu\text{m}$ aperture; membrane formation is monitored through the glass window of the *cis* chamber. Ag-AgCl electrodes denoted by $E(+)$ and $E(-)$ are inserted from the rear side into the *cis* and *trans* chambers, then connected to an Axopatch 200B amplifier.

then sandwiched between two Teflon blocks, each having a vertical chamber (diameter= 3.8 mm and height= 7.0 mm) and a 2.0 -mm hole on the sidewall. These holes, when properly aligned, provide access to the $40\text{-}\mu\text{m}$ aperture from both the *cis* and *trans* chambers. The chambers have rear-side ports (not shown) for inserting the electrodes E . The *cis* chamber is also provided with a glass window for viewing (through a microscope) the $40\text{-}\mu\text{m}$ aperture while applying the lipid bilayer. (The procedure for applying the lipid membrane is similar to that described earlier.) Once a stable bilayer had formed, we created a reverse nanopore by adding α -HL to the *trans* chamber, then removed the excess proteins by perfusion with fresh buffer. The forward nanopores were similarly constituted by adding α -HL to the *cis* chamber, followed by perfusion.

After forming two forward and one reverse nanopores, we added $5' A_{50}C_{100}3'$ ssDNA to the *cis* chamber and monitored the electrolytic current (bandwidth= 10 kHz) while a voltage pulse sequence was applied to the electrodes ($V = +120$ mV from $t=0$ to $257\ \mu\text{s}$, followed by $V = -120$ mV from $t=257$ to $850\ \mu\text{s}$). Out of hundreds of traces that contain forward translocations, Fig. 10 displays five traces that have at least one reverse translocation event. At $V = +120$ mV, the open state of the channels is seen to be interrupted by several brief closures, i.e., translocation events. (Also, every once in a while, one of the two forward channels gets clogged.) This behavior is similar to what was described previously. What is intriguing is that several translocation events are observed even when the applied voltage is reversed ($V = -120$ mV). Note that the number of ssDNA molecules initially introduced into the *cis* chamber is of the order of 10^{14} . After only a few hundred *cis* to *trans* translocations, we began to detect reverse translocation events. These are likely associated with those DNA molecules that,

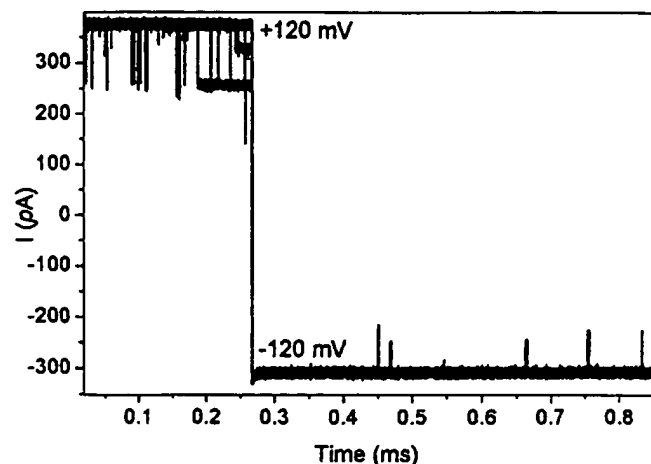


FIG. 10. Current traces obtained when two forward (*cis* to *trans*) and one backward (*trans* to *cis*) nanopores are constituted in the lipid membrane of the system of Fig. 9, then single-stranded DNA molecules are introduced into the *cis* chamber. The current was recorded when the voltage sequence $V = +120$ mV, $0 \leq t \leq 0.27$ ms; $V = -120$ mV, $0.27 \leq t \leq 0.85$ ms was applied to the electrodes. The buffer concentration was 1-M KCl, and the amplifier bandwidth was 10 kHz. When $V = +120$ mV, the open state of the channels is interrupted by several brief translocation events lasting a total of 1.35 ms (in five overlapping traces). When the voltage is switched to -120 mV, a few reverse translocations are observed (in five overlapping traces) during a 2.9-ms interval.

having been forward translocated, stay in the vicinity of the lipid membrane, then return through the reverse nanopore once the applied voltage is reversed.

The observation of reverse translocation in this experiment indicates that controlled transfer of individual molecules (e.g., from the parking lot to the read station) may be feasible, since it is the electric-field gradient, rather than random thermal drift, that is most likely responsible for the turning around (and return to the *cis* chamber) of our ssDNA molecules.

IV. CONCLUDING REMARKS

As a first step toward constructing a macromolecular data storage system, we have demonstrated the feasibility of conducting experiments with fairly short strands of DNA in a miniature read station. We showed that the *A* and *C* segments of a $5'A_{50}C_{100}3'$ ssDNA molecule can be distinguished during translocation through an α -HL ion channel. Needless to say, many hurdles must be overcome before this system can be implemented as an alternative to existing technologies.

The ultrahigh capacity is an obvious advantage of such molecular storage devices, but the data rates require substantial improvement. If the $5'A_{50}C_{100}3'$ molecules, which represent 2-bit sequences of binary information, take ~ 150 μ s to pass through a nanopore, the corresponding data-transfer rate of only 12 kbit/s would leave a lot to be desired. On the other hand, if the technology could improve to the point that individual bases could be detected during translocation, perhaps through a shorter, more robust, solid-state nanopore,^{13,14} then the achievable rate of ~ 1 Mbit/s would not be out of bounds. Moreover, if thousands of read stations could be made to operate in parallel within the same chip, the overall data-transfer rate could approach the respectable value of several Gbits/s.

Access to data is another issue that requires extensive research. Our preliminary calculations show that a 1-Mbyte-long macromolecule, enclosed in a 200-nm-diameter spherical shell (perhaps a liposome), can move electrophoretically across a 1.0-cm^2 chip in ~ 1.0 ms under a 10-V potential difference. Whether such molecules could be written and packaged on demand, within an integrated microchip, at high speed, and on a large scale, are questions to which only future research can provide satisfactory answers. Stability of the molecules over extended periods of time should obviously be a matter of concern. The lipid membrane and the proteinaceous ion channel, both being of organic origin, are ill suited for practical data storage systems; they must eventually be replaced with robust, solid-state equivalents.¹⁴

The proposed method overcomes the limitations of present-day data storage technology by creating a paradigm, thus side stepping the known obstacles to future growth in storage technology. One is no longer hampered by the superparamagnetic limit, the finite wavelength of light, the two-dimensional nature of surface recording, and other limitations of this kind. Our proposed approach also enables the creation of concepts and devices that have wide-ranging applications beyond the field of data storage. For example, rapid analysis of trace amounts of biological macromolecules, drug discovery and testing using micro-DNA synthesizer, machinery for single-chain molecular transport and manipulation, etc. Despite all the difficulties, it is our hope that this proposal will encourage debate in the pursuit of an alternative path to conventional approaches to data storage.

ACKNOWLEDGMENTS

The authors are grateful to Joseph Perry and Seth Marder of the Georgia Institute of Technology, and to Michael Hogan and Nasser Peyghambarian of the University of Arizona for many helpful discussions. This work has been supported by the Office of Naval Research MURI Grant No. N00014-03-1-0793 and by the National Science Foundation STC Program, under Agreement No. DMR-0120967.

¹M. Mansuripur, Proc. SPIE 4342, 1 (2001).

²M. Mansuripur, P. K. Khulbe, S. M. Kuebler, J. W. Perry, M. S. Giridhar, and N. Peyghambarian, Proc. SPIE 5069, 231 (2003).

³M. S. Giridhar, K. B. Seong, A. Schülzgen, P. K. Khulbe, N. Peyghambarian, and M. Mansuripur, Appl. Opt. 43, 4584 (2004).

⁴D. W. Deamer and D. Branton, Acc. Chem. Res. 35, 817 (2002).

⁵A. Meller, J. Phys.: Condens. Matter 15, R581 (2003).

⁶M. Akeson, D. Branton, J. J. Kasianowicz, E. Brandin, and D. Deamer, Biophys. J. 77, 3227 (1999).

⁷A. Meller, L. Nivon, E. Brandin, J. Golovchenko, and D. Branton, Proc. Natl. Acad. Sci. U.S.A. 97, 1079 (2000).

⁸J. J. Kasianowicz, E. Brandin, D. Branton, and D. W. Deamer, Proc. Natl. Acad. Sci. U.S.A. 93, 13770 (1996).

⁹A. Meller, L. Nivon, and D. Branton, Phys. Rev. Lett. 86, 3435 (2001).

¹⁰S. Howorka, S. Cheley, and H. Bayley, Nat. Biotechnol. 19, 636 (2001).

¹¹H. Bayley and P. S. Cremer, Nature (London) 413, 226 (2001).

¹²T. A. Pologruto (private communication).

¹³P. Chen, J. Gu, E. Brandin, Y. R. Kim, Q. Wang, and D. Branton, Nano Lett. 4, 2293 (2004).

¹⁴J. Li, M. Gershow, D. Stein, E. Brandin, and J. A. Golovchenko, Nat. Mater. 2, 611 (2003).